DOKUZ EYLÜL UNIVERSITY

GRADUATE SCHOOL OF NATURAL AND APPLIED SCIENCES

SWITCHING FREQUENCY TUNED CLASS-D AMPLIFIERS

by

Murat AYDEMİR

September, 2010

İZMİR

SWITCHING FREQUENCY TUNED CLASS-D AMPLIFIERS

A Thesis Submitted to the
Graduate School of Natural and Applied Sciences of Dokuz Eylül University
In Partial Fulfillment of the Requirements for the Degree of Master of Science
in Electrical and Electronics Engineering

by

Murat AYDEMİR

September, 2010
İZMİR

M.Sc THESIS EXAMINATION RESULT FORM

We have read the thesis entitled "**SWITCHING FREQUENCY TUNED CLASS-D AMPLIFIERS"** completed by **MURAT AYDEMİR** under supervision of **PROF. DR. HALDUN KARACA** and we certify that in our opinion it is fully adequate, in scope and in quality, as a thesis for the degree of Master of Science.

Prof. Dr. Haldun KARACA

Supervisor

(Jury Member)

(Jury Member)

Prof. Dr. Mustafa SABUNCU

Director

Graduate School of Natural and Applied Sciences

ACKNOWLEDGEMENTS

I express my deepest gratitude to my advisor Prof. Dr. Haldun KARACA for his guidance and support in every stage of my research. The technique background and the research experience I have gained under his care will be valuable asset to me in the future.

Also I would like to thank to Mustafa ÖZDEMİR for his support during my thesis research.

Finally, I am grateful to my wife and my parents for their patience and never ending support throughout my life.

Murat AYDEMİR

SWITCHING FREQUENCY TUNED CLASS-D AMPLIFIERS

ABSTRACT

The most important weakness of the switched-amplifiers is the residual ripple voltage on the load that remains in spite of filtering. It has been shown by examining the theoretical analysis and simulation results of the amplitudes of components comprising the Pulse Width Modulation(PWM) signal that the component having the highest amplitude is again the main component with the switching frequency for each value of modulation depth. A notch filter is proposed to suppress this component very effectively at the switching frequency. The characteristic of the filter is studied with theoretical, simulation and experimental results.

Switching frequency of the amplifier should trace notch frequency very precisely since the attenuation characteristic of the proposed filter is a sharp curve around the notch frequency. Otherwise, the filter performance would not be put forward. Because of this reason, an analog control circuit has been designed. Designed frequency control circuit generates a voltage that makes equal the switching frequency to the notch frequency by comparing the phases of the components of filter input and middle node voltages at the switching frequency. This voltage is connected to the leg of the chip that generates PWM signal determining the switching frequency through a series resistor. The performance of the method is studied with realized prototypes and simulation results. For the purpose of comparison, the filter has been transformed into the topology that is known as LC filter for switching amplifiers without changing the component values in the notch filter. Then the comparison of these two filters has been made with the help of experimental and simulation results.

Keywords: Switching amplifier, Class-D amplifier, notch filter, ripple steering, frequency tracking

ANAHTARLAMA FREKANSI AKORDLU D SINIFI YÜKSELTEÇLER

ÖZ

Anahtarlamalı yükselteçlerin en önemli zayıflığı, filtrelemeye rağmen yük üzerinde kalmış olan dalgacık (ripple) gerilimidir. Darbe Genişlik Modülasyonu (DGM) işaretini oluşturan bileşenlerin genlikleri kuramsal yoldan ve simulasyon sonuçları ile incelenerek modülasyon derinliğinin her değeri için en yüksek genlikli bileşenin yine anahtarlama frekanslı temel bileşen olduğu gösterilmiştir. Anahtarlama frekansındaki bu bileşenin çok etkin bir şekilde zayıflatılması için çentik karekteristiğinde bir filtre önerilmiştir. Önerilen filtrenin karekteristiği yine kuramsal, simulasyon ve ölçümler ile irdelenmiştir.

Önerilen filtrenin zayıflatma karekteristiğinin çentik frekansı etrafında çok keskin bir eğri olmasından dolayı yükseltecin anahtarlama frekansının çok doğru bir biçimde çentik frekansına eşit olması gerekir. Aksi takdirde filtre başarımı ortaya konmamış olacaktır. Bu neden ile analog bir kontrol devresi tasarlanmıştır. Tasarlanan frekans kontrol devresi filtre giriş ve ara düğümündeki anahtarlama frekansındaki bileşenlerin fazlarını karşılaştırarak anahtarlama frekansını çentik frekansına eşit olacak şekilde bir gerilim üretir. Bu gerilim de DGM üreten yonganın anahtarlama frekansını belirleyen ayağına seri bir direnç üzerinden bağlanmıştır. Gerçeklenen prototipler ve simulasyon sonuçlarından yöntemin başarımı irdelenmiştir. Karşılaştırma amacı ile çentik filtre içindeki elemanların değerleri değiştirilmeden filtre, anahtarlamalı yükselteçler için LC filtresi olarak bilinen topolojiye dönüştürülmüştür. Daha sonra bu iki filtrenin karşılaştırılması deneysel ve simulasyon sonuçlarından faydalanarak yapılmıştır.

Anahtar Sözcükler : Anahtarlamalı yükselteç, D sınıfı yükselteç, çentik filtre, ripple gerilimi, frekans izleme devresi

CONTENTS

Page

CHAPTER ONE
INTRODUCTION

Class-A and Class-B amplifiers are the most used types for applying to amplify analog signals. In this type of amplifiers, distortion on output signal can be reduced to small values with a good design. But in terms of power efficiency, calculated performance of this type of amplifiers are theoretically very limiting for today's applications.

Today as energy efficiency has gained more importance, efficiency in system design much more comes into prominence. As a result of improvement in the elements of this trend and power electronics, an amplifier type which will be more efficient to amplify analog signals has started to take more place.

Power efficiency of Switched Amplifiers based on Pulse Width Modulation (PWM) theoretically is calculated as 100% with ideal assumption of switches in amplifier. Common applications of PWM changing according to the signal modulating pulse width duty-cycle are seen in power electronics. Switched Mode Power Supplies and switched amplifiers are the most common applications of it.

In switched amplifiers, transistors (Bipolar, IGBT, MOSFET) situated on output stage function as switches. While current passing through them, voltage drop is quite low. While holding voltage in their terminals, currents are almost zero.

In application, the most important component which causes switch losses is losses occurring during switching process. It has been possible to decrease mentioned switching losses to smaller values with the development in semiconductor technology. Eventually, switched amplifiers whose theory was put forward 30-40 years ago have started to feature with their developing semiconductor technology. It's reported that switched amplifiers can reach power efficiency of about 85%, 90%. To be remembered, in Class-A amplifiers, the highest theorical efficiency is 25%, for Class-B, the same value is 78.5%(Walker, 2003).

As known in communication technique, the most important advantage provided by modulation is to reduce the band carrying signal information by carrying it to high frequency region to realizable values. Modulation in PWM enables the information included by an analogue signal to hide in a pulse shaped signal. Acquired pulse width is variable but pulse shaped signal can be amplified with a quite high efficiency with a circuit which contains transistors as switch. Signal which is re-modulating by filtering from amplified pulse signal is acquired as amplified. But this filtering has difficulties according to demodulation in communication systems. For example, in demodulation of FM radios, phonogram is filtered through the signal which also contains components of about 10.7 MHz and the multiples of it frequency (intermediate frequency).

Theoretically, carrier of switching frequency(f_s) of PWM as high, for example, there is no obstacle to choose 10 MHz. In application, switching isn't exactly possible with power semiconductor switches which can be found commercially. In addition, as f_s increases, efficiency of the process to amplify PWM signal decreases. Due to this factor which is caused by switching losses mentioned above, switching frequency is usually kept under a few hundreds kHz.

Amplifier output filter benefits from the topology of LC low-pass filter in many of applications. On the other hand, in recent years, there is a 2-3 Watt-powered product called "spread spectrum filterless Class-D amplifier" in the product range of most of famous chip producing companies (Tan, 2003). This chip is usually produced for hearing aids, MP3 player or similar low-power audio amplifier. Disappearing of output filter doesn't stem from used special modulation technique (spread spectrum). It's clear that a switched amplifier which doesn't need output filter isn't theoretically possible.

But almost all of the companies producing this type of products use similar descriptive (filterless Class-D amplifier) name. In fact, speaker inductance which will be connected to output of these chips provides filtering. It can be clearly

concluded that result from here. It's impossible to use mentioned chips with capacitive or resistive loads. It leaves from the thesis concept with this aspect of it.

Design of output filter of switched amplifier may not be so important in low-power audio applications. This has two reasons:

1) f_s can be chosen higher in amplifiers where semiconductor switches take place whose current and voltage carrying ability is poor. In other words, mentioned low-power switches usually work faster than high-power ones (Steigerwald, 2000). For this reason, by selecting f_s high, filtering can be improved.

2) As known, human ear can hear the voices in a band and upper limit frequency is about 20 kHz. Therefore for example, an MP3 player working at 100 kHz of switching frequency can be connected to headphones without filtering of audio amplifier output. High frequency component where inductance will pass in headphones, as it will weaken more or less according to its value and audio depends on this current, filter may not be necessary or for a better audio, the known LC low-pass filter may provide enough performance.

Output filter becomes more important if switching frequency is wanted to be kept at small values to increase amplifier efficiency. Efficiency is especially important when amplifier power is at the level of kW's in Magnetic Resonance Imaging application but minority of harmonic distortions in output signal is as important as it (Steigerwald, 2000). It's clear that the necessity for design of filter topology which weakens switching frequency and harmonics in higher proportion.

We can come across with switched amplifiers reaching the level of kW's in Ultrasonic Applications (Aggbossou, 2000) and powerful car audio systems which has become widespread in recent years. Filter topology suggested in this thesis will have important advantages over classic filter of switched amplifiers (LC low-pass

filter) in Magnetic Resonance Imaging and other mentioned applications. This advantage is provided by the weakness of the voltage appearing as ripple voltage in output signal.

CHAPTER TWO
SWITCHED AMPLIFIER TOPOLOGIES

2.1 Working Principle of Switched Amplifiers

The efficiency of circuits which will amplify the power of pulse shape signals can be designed in a way that can be higher than circuits which can be benefited to amplify analog signals. If a pulse shape signal on the output stage is amplified with a circuit in which semiconductor elements function as switch, loss energy that will be spent on switch elements is theoretically quite less according to analog operation of the same elements. It's possible to amplify analog signals benefiting from PWM and a power amplifier designed for pulse shape signals. The block diagram of a circuit providing this function is given in Figure 2.1. A triangular or sawtooth signal which has frequency above the signal which will be amplified and its bandwidth is applied to the inputs of PWM modulator. PWM Modulator can be an analog circuit. A comparator element can verify this modulation.

Pulse amplifier in Figure 2.1 is a power electronic circuit mostly in Half Bridge or Full Bridge topology.

After a low-pass filter, if PWM signal reinforced by pulse amplifier is connected to pole, modulating signal is connected to load ends as reinforced. Load is an element of the filter in switched amplifiers and usually there isn't any additional resistance element in filter as efficiency is important. Filter shown in block diagram is classic LC filter which usually takes place among switched amplifiers.

Feedback shown in block diagram of switched amplifier can provide a more linear amplification although it's not necessary in terms of basic working principle. Theoretically, there won't be distortion of being non-linear during demodulation provided by filter seen in block diagram and creating PWM. But, this feedback may be useful as elements verifying groups are not ideal. For example, to decrease the distortion caused by non-linearity of characteristics of magnetic cores of inductance

elements. Especially in 80’s, intensive studies have been made for the purpose of decreasing ripple effects of ripple voltages with network source of 50 Hz or 100 Hz frequency on voltage of pulse amplifier supple sources, which makes PWM mentioned feedback more powerful, on switched amplifier output signal.

These studies among switching power sources are based on modeling of source not to show oscillation behavior. It's quite under this type of feedback switching frequency. Benefiting from the Modeling Method named as State Space Averaging Model, model for design purposes has been suggested (Karaca, 1997). By taking this type of average formed models don't provide information related to ripple components repeating in switching frequency at the outputs of switched systems.

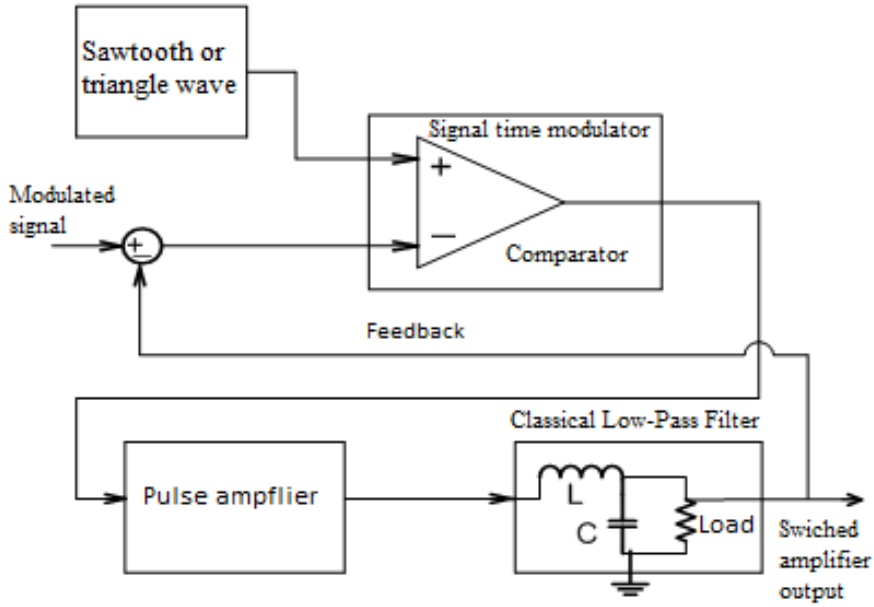

Figure 2.1. Block Diagram of Switched-Amplifier.

Typical signal shapes related to PWM modulation are seen in Figure 2.2. While A and B signals show the input of comparator, C shows the typical waveforms of output of comparator in this figure.

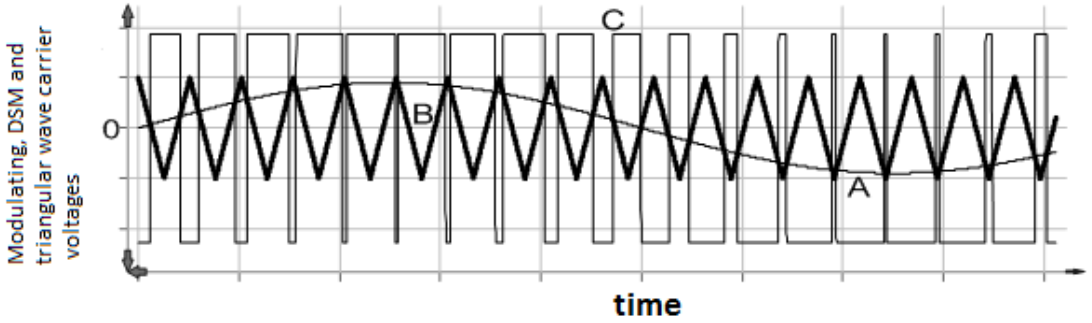

Figure 2.2. Sinusoidal signal (A) modulating PWM, Triangular carrier (B), PWM signal (C).

Input of switched amplifier, PWM and output signals are shown in Figure 2.3. There is ripple noise or distortion as a result of switching as seen in C waveform in this figure. Aim of this thesis is to search effective topologies and techniques which will decrease peak value of these ripples.

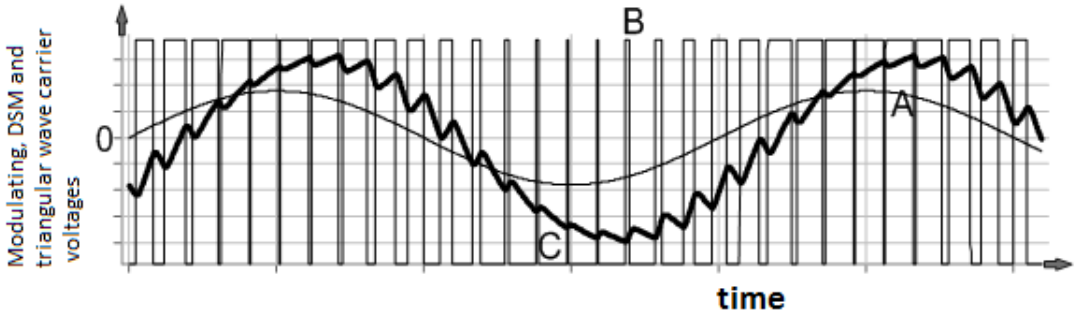

Figure 2.3. Waveforms related to switched-amplifier, A: modulating signal, B: PWM signal, C: after demodulation enabled by low pass filter, amplifier output signal, phase difference between A and C signals arises from filtering process.

Ripple voltage seen in output waveforms of the filter given above is the problem of switched amplifiers which can be regarded as the most important. These waveforms are acquired as a result of simulation and there is the known LC low-pass filter in simulation circuit.

2.2 Pulse Width Modulators

PWM also named as Pulse Width Modulation can be divided into two in terms of creating process. These groups are naturally sampled and uniformly sampled types (Black, 1953).

Naturally sampled modulator is comprised of a simple comparator circuit. Uniformly sampled modulator can be verified by benefiting from a comparator circuit and a sample and hold circuit. Output signals that will emerge when a sinusoidal signal is applied to inputs of both types of modulators are shown in Figure 2.4. The method of Naturally Sampling is benefited to form PWM signal as it's easier to verify in present applications.

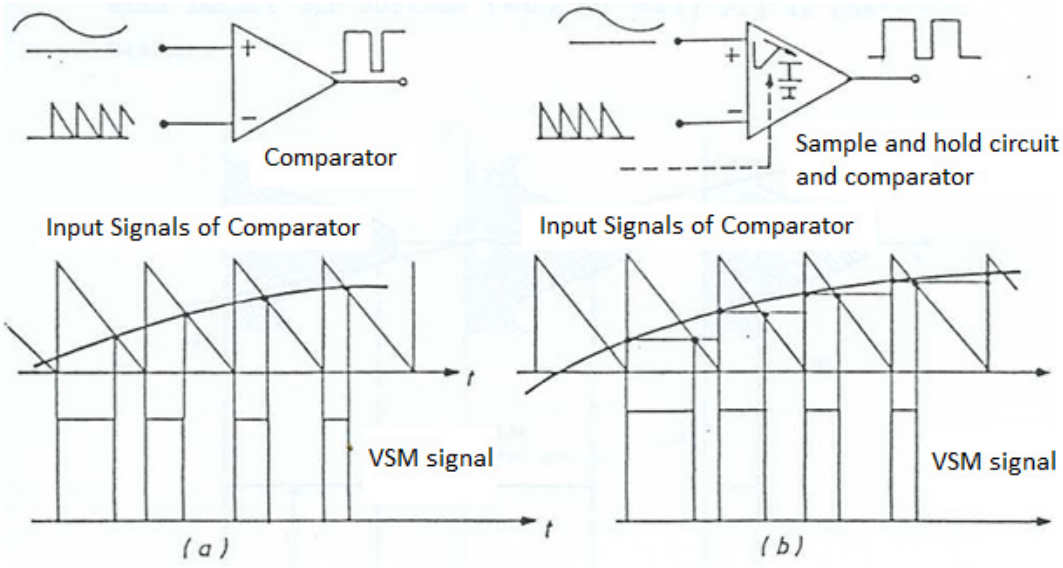

Figure 2.4. Acquisition of PWM signal: Naturally sampling (a) and uniformly sampling (b).

2.3 Spectrum of Naturally Sampled PWM Signal Frequency

The method that will be benefited in frequency analysis is W.R. It's a method that is based on the development of bivariate Fourier series first used by Bennet. This method was published by Black (Black, 1953) .

Let's denote modulating signal $A_c \cos(\omega_c t)$ for the analysis of modulating signal. Let the repetition frequency of pulses be ω_s. Generally, proportion between ω_s and ω_c is not an integer. So PWM signal cannot be periodic. Bennet represented this general PWM signal with three-dimensional structure seen in Figure 2.5.

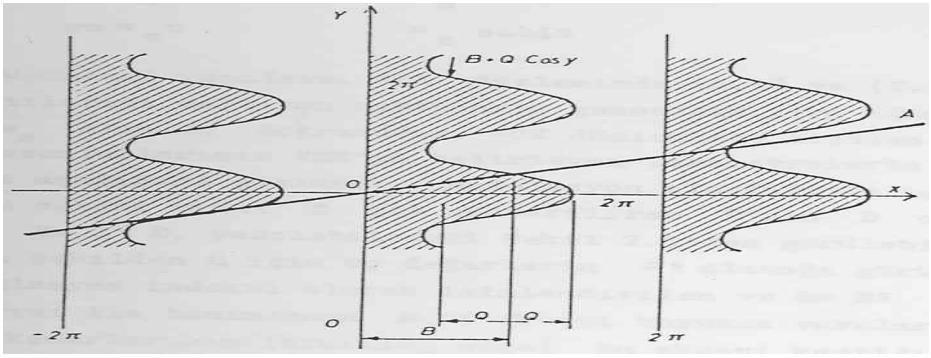

Figure 2.5. Organized structure to analyse PWM.

Let's assume that many walls rise from XOY plane which is at a fixed height and where projections are shown as shaded. It's seen that sides of walls in x=0, x=±2π, x=±4π,… are parallel to Y axis. By taking x' as the distance between two edges, the shape of wall's other sides is defined with $x' = B + Q_{cosy}$. There is a wall at the distance of every 2π along X axis.

The line which will be acquired from intersection of a line passing vertically to XOY plane and from origin with XOY will be showed with OA. The projection to the second plane which is vertical to XOY' including X axis of intersection of the shaded walls with this new plane is shown in Figure 2.6.

If X axis is taken as time in Figure 2.6(a), the structure seen in Figure 2.6(b) becomes PWM signal. In addition, the width of every pulse is determined by the value at the end of pulse of Q_{cosy} term. As a result, PWM signal in Figure 2.6(b) is acquired by naturally sampling.

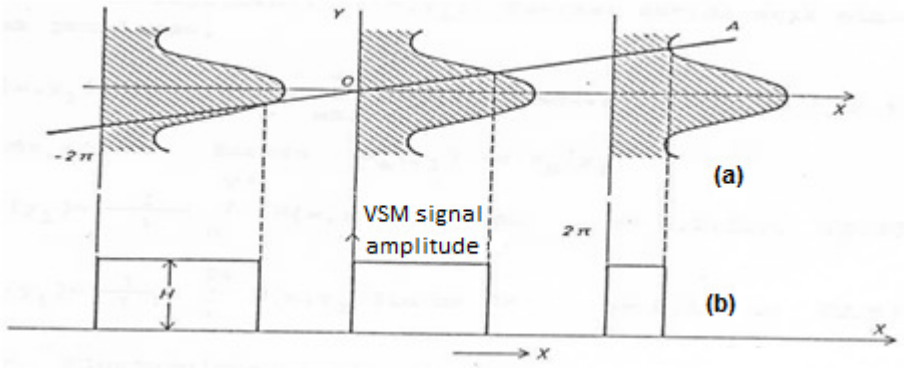

Figure 2.6. Established structure to form naturally sampled PWM signal (a) and PWM signal acquired from this structure (b).

For x and y seen in Figure 2.6 to express PWM signal according to time with a relation,

$x=\omega_s t$ ω_s fixed (2.1)

$y=\omega_c t$ ω_c fixed (2.2)

alternations will be done.

Locus of points providing relations of (2.1) and (2.2) in XOY plane is OA line whose slope is ω_c/ω_s. Relation of B and Q lengths measured in XOY place with parameters determining PWM is as follows: when there is no modulation if pulse width is shown with D, it can be seen from Figure 2.6 that B can be written in terms of D $B=2\pi D$. It's seen from the same figure that extreme values will be $\pm\pi$ for Q.M which is named as Modulation index and defined with the relation of $Q=M\pi$ determines the region in which points that trailing edges of pulses along X axis intersects this axis. If XOY plane edges are divided into squares at the length of 2π the shape of wall projections in every square will be the same.

So H height of a geometric shape formed in an (x,y) point in XOY plane can be defined with dual variable Fourier series whose variables are x and y. If double Fourier series are shown with F(x,y) when $x=\omega_s t$ ve $y=\omega_c t$ are written, height expression is obtained as F(t) along OA line. Intersection of the line including X axis

and vertical to XOY plane with geometric structure creates a series whose pulse widths are equal. When plane is slided provided that it will be parallel to X axis, a new pulse signal whose pulse widths are equal is obtained. Univariate F (x,y_1) Fourier series is enough to show these pulses. In this series y_1 value is the coordinate of the point where plane intersects Y axis.

If univariate F (x,y_1) Fourier series is written precisely,

$$F(x, y_1) = \frac{1}{2} a_o(y_1) + \sum_{m=1}^{\infty} [a_m(y_1) \cos mx + b_m(y_1) \sin mx] \tag{2.3}$$

is obtained. Here $a_m(y_1)$ and $b_m(y_1)$ are;

$$a_m(y_1) = \frac{1}{\pi} \int_0^{2\pi} F(x, y_1) \cos mx \, dx \qquad m = 0,1,2,... \tag{2.4}$$

$$b_m(y_1) = \frac{1}{\pi} \int_0^{2\pi} F(x, y_1) \sin mx \, dx \qquad m = 0,1,2,... \tag{2.5}$$

As all the curves with 2π period along Y axis in the formed structure are periodic, coefficients of $a_o(y_1)$, $a_m(y)$ ve $b_m(y)$ and $b_m(y)$ should be periodic as regards y and so they can be represented with Fourier series as regards y.

From here;

$$a_m(y) = \frac{1}{2} c_{om} + \sum_{n=1}^{\infty} [c_{nm} \cos ny + d_{nm} \sin ny] \tag{2.6}$$

$$c_{nm} = \frac{1}{\pi} \int_0^{2\pi} a_m(y) \cos ny \, dy \tag{2.7}$$

$$d_{nm} = \frac{1}{2} \int_0^{2\pi} a_m(y) \sin ny \, dy \tag{2.8}$$

$$b_m(y) = \frac{1}{\pi} e_{om} + \sum_{n=1}^{\infty} [e_{nm} \cos ny + f_{nm} \sin ny] \tag{2.9}$$

$$e_{nm} = \frac{1}{\pi}\int_0^{2\pi} b_m(y)\cos ny\ dy \tag{2.10}$$

$$f_{nm} = \frac{1}{\pi}\int_0^{2\pi} b_m(y)\sin ny\ dy \tag{2.11}$$

are found. If $a_m(y)$ which will be calculated with (2.4) is written in the relation of (2.7) giving the value of c_{nm},

$$\begin{aligned} c_{nm} &= \frac{1}{\pi}\int_0^{2\pi}\left[\frac{1}{\pi}\int_0^{2\pi} F(x,y)\cos mx\ dx\right]\cos ny\ dy \\ &= \frac{1}{\pi^2}\int_0^{2\pi}\int_0^{2\pi} F(x,y)\cos mx\cos ny\ dx\ dy \\ &= \frac{1}{2\pi^2}\int_0^{2\pi}\int_0^{2\pi} F(x,y)\cos(mx+ny)\ dx\ dy \\ &+ \frac{1}{2\pi^2}\int_0^{2\pi}\int_0^{2\pi} F(x,y)\cos(mx+ny)\ dx\ dy \end{aligned} \tag{2.12}$$

is found. Distinctively for the values of c_{oo} and c_{om};

$$c_{oo} = \frac{1}{\pi^2}\int_0^{2\pi}\int_0^{2\pi} F(x,y)\,dx\,dy \tag{2.13}$$

$$c_{om} = \frac{1}{\pi^2}\int_0^{2\pi}\int_0^{2\pi} F(x,y)\cos mx\,dx\,dy \tag{2.14}$$

is obtained. Similarly;

$$\begin{aligned} d_{nm} &= \frac{1}{2\pi^2}\int_0^{2\pi}\int_0^{2\pi} F(x,y)\sin(mx+ny)\ dx\ dy \\ &+ \frac{1}{2\pi^2}\int_0^{2\pi}\int_0^{2\pi} F(x,y)\sin(ny-mx)\ dx\ dy \end{aligned} \tag{2.15}$$

and from (2.5), (2.10), (2.11);

$$\begin{aligned} e_{nm} &= \frac{1}{\pi}\int_0^{2\pi}\left[\frac{1}{\pi}\int_0^{2\pi} F(x,y)\sin mx\ dx\right]\cos ny\ dy \\ &= \frac{1}{2\pi^2}\int_0^{2\pi}\int_0^{2\pi} F(x,y)\sin(mx+ny)\ dx\ dy \\ &+ \frac{1}{2\pi^2}\int_0^{2\pi}\int_0^{2\pi} F(x,y)\sin(mx-ny)\ dx\ dy \end{aligned} \tag{2.16}$$

is found. If similar operations are also done for f_{nm} ;

$$\begin{aligned} f_{nm} &= \frac{1}{2\pi^2}\int_0^{2\pi}\int_0^{2\pi} F(x,y)\cos(mx-ny)\ dx\ dy \\ &- \frac{1}{2\pi^2}\int_0^{2\pi}\int_0^{2\pi} F(x,y)\cos(mx+ny)\ dx\ dy \end{aligned} \tag{2.17}$$

equation is obtained. If these relations are put into their places in (2.6) and (2.9),

$$\begin{aligned} a_m(y) = \frac{1}{2}c_{om} + \frac{1}{2\pi^2}\sum_{n=1}^{\infty}\Bigg\{ &\int_0^{2\pi}\int_0^{2\pi}[F(x,y)\cos(mx+ny)\ dx\ dy \\ &+ \int_0^{2\pi}\int_0^{2\pi} F(x,y)\cos(mx-ny)\ dx\ dy]\cos ny \\ &+ [\int_0^{2\pi}\int_0^{2\pi} F(x,y)\sin(mx+ny)\ dx\ dy \\ &+ \int_0^{2\pi}\int_0^{2\pi} F(x,y)\sin(ny-mx)\ dx\ dy]\sin y\Bigg\} \qquad m = 0,1,2,... \end{aligned} \tag{2.18}$$

is obtained. Here, it's possible,

$$a_o(y) = \frac{1}{2}c_{oo} + \sum_{n=1}^{\infty}[c_{no}\cos ny + d_{no}\sin ny] \tag{2.19}$$

$$c_{no} = \frac{1}{\pi^2}\int_0^{2\pi}\int_0^{2\pi} F(x,y)\cos ny\ dx\ dy \tag{2.20}$$

$$d_{no} = \frac{1}{\pi^2} \int_0^{2\pi} \int_0^{2\pi} F(x,y) \sin ny \; dx \; dy \tag{2.21}$$

to calculate $a_o(y)$ from this. Eventually,

$$\begin{aligned} a_o(y) = \frac{1}{2\pi^2} \int_0^{2\pi} \int_0^{2\pi} F(x,y) \; dx \; dy + \sum_{n=1}^{\infty} \Bigg\{ \left[\frac{1}{\pi^2} \int_0^{2\pi} \int_0^{2\pi} F(x,y) \cos ny \; dx \; dy \right] \cos ny \\ + \left[\frac{1}{\pi^2} \int_0^{2\pi} \int_0^{2\pi} F(x,y) \sin ny \; dx \; dy \right] \sin y \Bigg\} \end{aligned} \tag{2.22}$$

is obtained. If an expression similar to (2.18) obtained for $a_m(y)$ is formed for $b_m(y)$ and $a_m(y)$, $a_o(y)$ and $b_m(y)$, are put into their places in (2.3), (2.23) is obtained.

$$\begin{aligned} F(x,y) = \frac{1}{2} A_{oo} + \sum_{n=1}^{\infty} [A_{on} \cos ny + B_{on} \sin ny] \\ + \sum_{m=1}^{\infty} [A_{mo} \cos mx + B_{mo} \sin mx] \\ + \sum_{m=1}^{\infty} \sum_{m=\pm 1}^{\pm\infty} [A_{mn} \cos(mx + ny) + B_{mn} \sin(mx + ny)] \end{aligned} \tag{2.23}$$

Here, it is;

$$A_{mn} = \frac{1}{2\pi^2} \int_0^{2\pi} \int_0^{2\pi} F(x,y) \cos(mx + ny) \; dx \; dy \tag{2.24}$$

$$B_{mn} = \frac{1}{2\pi^2} \int_0^{2\pi} \int_0^{2\pi} F(x,y) \sin(mx + ny) \; dx \; dy \tag{2.25}$$

If x and y values given in (2.23) with (2.1) and (2.2) are written to obtain spectrum of PWM signal frequency;

$$F(t)=\frac{1}{2}A_{oo}+\sum_{n=1}^{\infty}[A_{on}\cos(n\omega_c)t+B_{on}\sin(n\omega_c)t]$$
$$+\sum_{m=1}^{\infty}[A_{mo}\cos(m\omega_s)t+B_{mo}\sin(m\omega_s)t] \quad (2.26)$$
$$-\sum_{m=1}^{\infty}\sum_{m=\pm1}^{\pm\infty}[A_{mn}\cos(m\omega_s+n\omega_c)t+B_{mn}\sin(m\omega_s+n\omega_c)t]$$

is obtained.

When components forming frequency spectrum are examined, it's paid attention that first term $A_{oo}/2$ gives DC component of pulses and this term is in fact the area of shaded portion in one of squares whose areas are $4\pi^2$ and formed in XOY plane in Figure 2.6. Second component includes harmonics and modulating signal frequency. Third term is comprised of harmonics and carrier frequency. The last term is the combination of all possible sum and differences of modulating and carrier frequencies.

On XOY plane, they will be defined as A and B which is vertical to this plane and in sequence it will contain OA and OX lines. At the same time, when a specific unit square is taken into consideration with x=[0,2π], y=[0,2π] ,projection of the intersection of A with the wall remaining in this square to B plane represents a period of pulse signal. Rising edge of the pulse is found in x=0. x=[2π,4π] which is another unit square and y′ the point where OA line intersects x=2 π line with y=[0,2π] unit square gives the angle of modulating signal at this time. PWM signal which will be obtained is plotted in Figure 2.7 as F(t).

The phase of modulating signal $\cos\omega_c t$ has been taken as zero in far made analysis. If there is actually a phase angle like θ, $y=\omega_c t+\theta$ should be written. In the new situation, modulation is determined by an OA line whose slope is ω_c/ω_s just the same and as far as from origin to Y axis. But it's only meaningful in the event that proportion of phase difference ω_s/ω_c is whole number or more clearly periodic to PWM signal (Black, 1953).

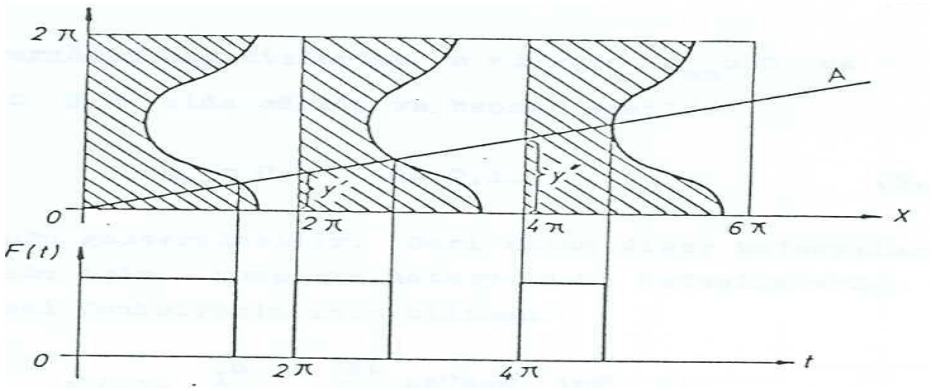

Figure 2.7. Acquiring PWM from the geometric structure suggested by Bennet.

2.4 Calculation of PWM Signal's Harmonic Components from the Parameters of Magnitude

By transmitting to complex notation, calculation of coefficients of A_{mn} and B_{mn} given with (2.24) and (2.25) can be shortened.

$$A_{mn} + iB_{mn} = \frac{1}{2\pi^2} \int_0^{2\pi} \int_0^{2\pi} F(x, y) e^{i(mx+ny)} \, dx \, dy \tag{2.27}$$

From Figure 2.5, F(x,y)=H (height of wall) is written for [0, $B+Q_{cosy}$] values of x and F(x,y)=0 is written for values within the range of [$B+Q_{cosy}$, 2π].

If these found values are put into their places given with (2.26) to calculate complex number,

$$A_{mn} + iB_{mn} = \frac{iH}{2\pi^2 m} \int_0^{2\pi} [e^{i(mB+mQ\cos y+ny)} - e^{iny}] \, dy \tag{2.28}$$

is obtained.

In the last relation, e^{iny} term doesn't bring a component to definite integral for n values which are different from n=0. In addition, as m is seen at denominator, extra calculation is necessary for m=0. For H which represents height of walls, it can be

H=1 and this means that pulse amplitude is 1. From coefficients, A_{oo} and A_{on} (n=1,2,…) can be calculated as follows.

$$A_{oo} = \frac{1}{2\pi^2}\int_0^{2\pi}(B+Q\cos y)\,dy = \frac{B}{\pi} = 2D \tag{2.29}$$

$$A_{on} = \frac{1}{2\pi^2}\int_0^{2\pi}[B\cos ny + \frac{Q}{2}(\cos(n+1)y + \cos(n-1)y)]\,dy \tag{2.30}$$

From the relations above, A_{on}=0 and A_{o1}=M/2 are obtained for n>1and similarly it can be shown as,

B_{on}=0 n=0,1,2,… (2.31)

For the calculation of rest of the coefficients, if you benefit from identities in complex notation and the known definition of Bessel function,

$$J_n(z) = \frac{i^n}{2\pi}\int_0^{2\pi} e^{iz\cos\phi}e^{in\phi}\,d\phi \tag{2.32}$$

ordered expressions whose values are comparatively short can be obtained . When all the coefficients which will be calculated are written in the series into their places,

$$\begin{aligned} F(t) = {} & D + \frac{M}{2}\cos\omega_c t + \sum_{m=1}^{\infty}\frac{\sin m\omega_s t}{m\pi} \\ & - \sum_{m=1}^{\infty}\frac{J_o(m\pi M)}{m\pi}\sin(m\omega_s t - 2\pi mD) \\ & - \sum_{m=1}^{\infty}\sum_{n=\pm 1}^{\infty}\frac{J_n(m\pi M)}{m\pi}\sin\left(m\omega_s t + n\omega_c t - 2\pi mD - \frac{n\pi}{2}\right) \end{aligned} \tag{2.33}$$

is obtained.

Calculated spectrum is for a rectangular wave which is changing between 0 and 1 and its average duty-cycle value is D. In addition, it’s clear that this spectrum in Figure 2.7 is for single-edge modulation PWM.

2.5 Multiplier Phase Detectors

Analog Multipliers are one of two different phase detector groups which are mostly benefited in the application. Ex- Or type gates which works with digital signals are also included in this group. Multiplier Phase detectors don't have memory feature. In other words, any output is certain with current inputs. Mentioned memory feature is found in Charge-Pump type Phase detectors but as aforesaid memory feature may cause continuously to malfunction in some control circuits (Karaca, 2001). In literature, it's often mentioned that Multiplier Phase detectors are more immune against noise. It has been reported that Charge-Pump type Phase detectors are indeed very sensitive against noise (Baker, 1989). This condition can create a serious problem especially in frequency control circuits which are using charge-pump type detectors (Karaca, 2005a).

In Phase Locked Loop(PLL) circuit which will be mentioned later in the thesis and creates square wave of f_o frequency, there won't be this malfunction possibility (Karaca, 2001). It's benefited from a charge-pump type phase detector for the purpose mentioned in the thesis work. A multiplier type phase detector appears in the part that malfunction condition of frequency control circuit designed in the thesis can occur. In this part of the circuit, it's benefited from AD633 and MLT04 analog multiplier integrated circuits of Analog Devices Inc. Company. It's understood from the literature entering index that it's benefited mostly from these integrated circuits in other analog multiplier applications, as well.

2.6 Analysis of Multiplier Type Phase Detectors for Two Sinusoidal Inputs Application

Let $v_1 = A_1 . Sin(\omega_1 t)$ and $v_2 = A_2 . Sin(\omega_2 t + \phi)$ signals be applied to an analog multiplier input. In this condition that input sinusoidal signal frequencies are different, the output is in this form;

$$v_o = Kp . A_1 . A_2 Sin(\omega_1 t) . Sin(\omega_2 t + \phi) \quad (2.34)$$

Here, the one coming from Kp analog multiplier circuit is fixed and for AD633, it's given as (1/10) in its catalog (http://www.analog.com/UploadedFiles/Data_Sheets/AD633.pdf).

By using from trigonometric identities and using the abbreviation of $K=Kp. A_1 A_2$;

$$v_o = (1/2) . K. \{Cos[(\omega_1 - \omega_2) t - \phi] - Cos[(\omega_1 + \omega_2) t + \phi]\} \quad (2.35)$$

can be written. In the last expression, it's seen that average value of v_o output will be zero. In other words, if output of multiplier circuit is applied to a low pass filter, filter output will be zero. It's understood that time constant should be chosen according to a component of lower frequency for $\mathbf{v_o}$ starting out from the expression written above for choosing time constant of filter which takes an average value in the application. In other words, time constant $(\omega_1 - \omega_2)$ frequency should be chosen at a value enough to weaken. If the proportion between ω_1 and ω_2 is for example 100, filter can be chosen in such a way that it can filter even the smaller one of time constant from ω_1 and ω_2 .

If one of the mentioned frequencies is switching frequency and the one that has a smaller value is modulating signal frequency, time constant of filter for taking average value can be chosen at a value that will weaken switching frequency enough.

The graphic in Figure 2.8, frequencies are chosen as 1 kHz and 100 kHz and simulation outputs of a RC low filter chosen to weaken 100 kHz with multiplier circuit output has been shown.

Although filter at 1 kHz frequency doesn't provide weakening, if ripples on the filter output signal are ignored from the output signal shown in the figure as dark, it's seen that output will be zero. From here, it is seen with simulation that there isn't 1 kHz component in multiplier signal. It's understood from the trigonometric relations above that there are components of 99 kHz and 101 kHz in multiplier signal. In the thesis, in the design of frequency track circuit, while designing cutoff frequency of filter after the process of multiplier circuit, this feature of multiplier will be taken into account.

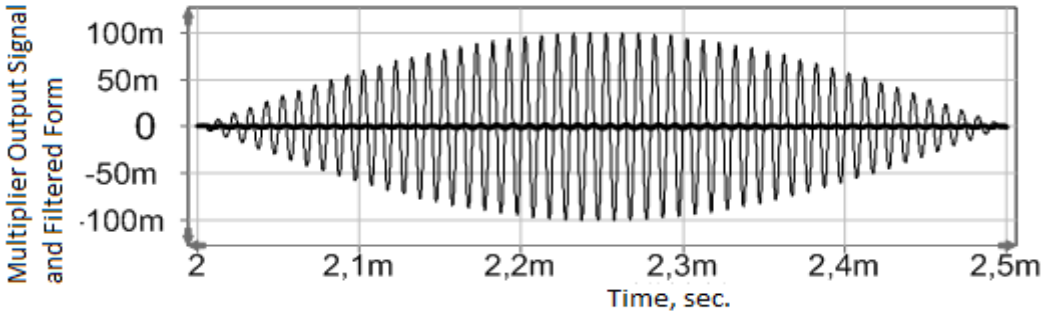

Figure 2.8. Output of a multiplication circuit whose inputs are 1kHz and sinusoidal signals 100 kHz (slim-line waveform) and form of corner frequency of this output after the process of low pass filtering which is 20 kHz (bold-line waveform).

On the other hand, in the special case of $\omega_1 = \omega_2$, multiplier output is;

$$v_o = (1/2) \,.\, K.\, \{ Cos\,(-\phi) - Cos\,[\,(2.\,\omega_1)\,t + \phi\,]\,\} \qquad (2.36)$$

and in this condition, average value of output is

$$v_o = (1/2) \,.\, K.\; Cos\;(\; -\phi\,) \qquad (2.37)$$

According to the last acquired result, if there is phase difference of $\phi = 90^{o}$ between sinusoidal and equal frequency inputs, it's seen that output average will again be zero in this special case. It is benefited from this feature of multiplication of sinusoidal signals in the design of Frequency Control Circuit(FCC) in the thesis.

Simulations are done with MLT04 integrated circuit for the purpose of evaluating also visually the results acquired above. This simulation circuit is seen in Figure 2.9.

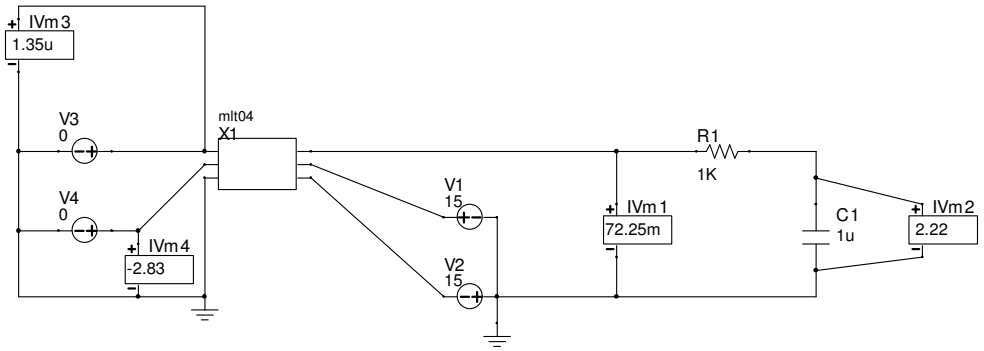

Figure 2.9. Simulation circuit to see the signal emerging after low pass filtering being multiplied with sinusoidal signals.

In this circuit, I_{Vm3} and I_{Vm4} oscilloscopes show input signals, I_{Vm1} shows multiplier output and I_{Vm2} shows output of low pass filter circuit put in order to see the average of multiplier output. Acquired simulation results are seen in Figure 2.10 and Figure 2.11.

This result can be deduced from the information analyzed above related to multiplier circuits: let's apply sinusoidal signal of f_1 frequency to one of the multiplier circuit inputs and a signal that contains many sinusoidal components to the other input. When the output of multiplier circuit is filtered with a low pass filter, only one correct voltage will emerge at the filter output. Amplitude of this correct voltage will contain the information related to phase difference between sinusoidal component of f_1 frequency from the components existing in sinusoidal signal and the other signal. It has been benefited from this feature of multiplication operation in the design of frequency control circuit of thesis work.

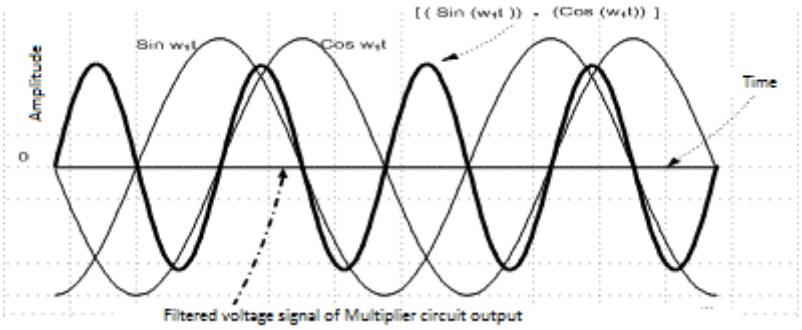

(a)

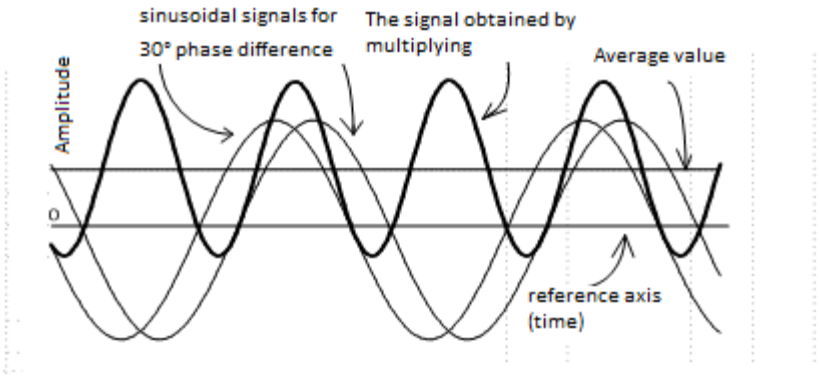

(b)

Figure 2.10. Emerging signal with filtering of multiplying two sinusoidal signals with a phase difference is 90° (a), filter output for 30° phase difference and their frequencies are the same.

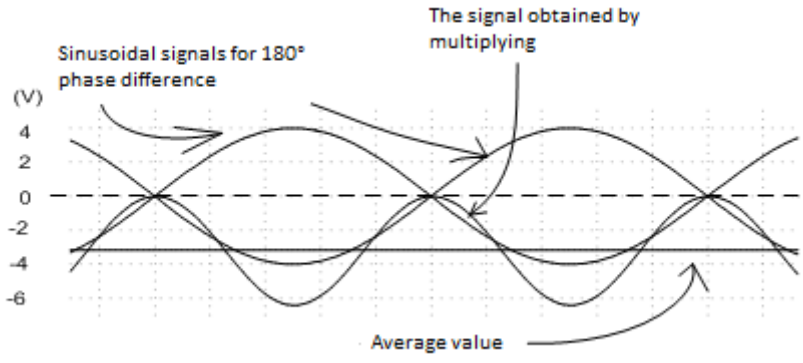

Figure 2.11. Averaged value signal of filter output for 180° phase difference between multiplication signs.

CHAPTER THREE
EVALUATION OF THE PROPOSED NOTCH FILTER CIRCUIT EFFECTIVENESS IN CLASS-D AMPLIFIERS

3.1 Analysis and Evaluation of LC-Filter for Switched Amplifiers

Verification of filter consisting of L, C and load resistance for switched amplifiers with element values seen in Figure 3.1 for the purpose of comparison takes place in experiment studies.

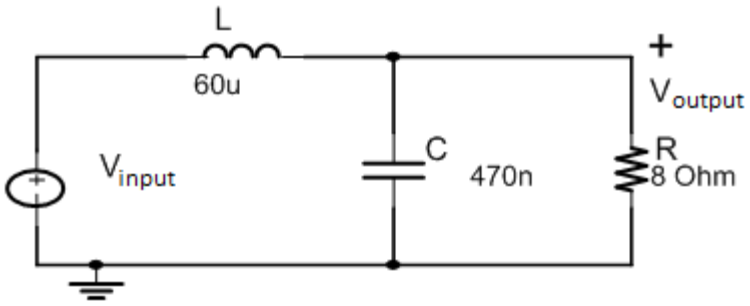

Figure 3.1. Low pass filter circuit the known LC- for switched amplifiers, this drawing is constructed with seen elements values and notch filter suggested in different places of this thesis.

If it's required to calculate Q quality factor and Transfer function of a filter circuit, relations given below are obtained.

$$T(s) = \frac{\frac{1}{LC}}{s^2 + s\frac{1}{RC} + \frac{1}{LC}} \tag{3.1}$$

$$Q = R\sqrt{\frac{C}{L}} \tag{3.2}$$

If the terminals of a filter's transfer function are conjugate, duplicate or reel, it provides filter characteristics to take the forms seen in Figure 3.2. If it's assumed that load resistance in filter is fixed, calculation according to which one of the

characteristics seen in the Figure 3.2 is wanted, selection of L and C values become a design problem.

It's understood that as frequency increases, filter gain will decrease with the proportion of 40 dB/decades over corner frequencies from the graphic and function of transfer. LC filter with this aspect is superior to notch filter that will be suggested in the thesis. But it's clear that it'll provide the least weakening for basic component which has the highest amplitude but the lowest frequency in PWM.

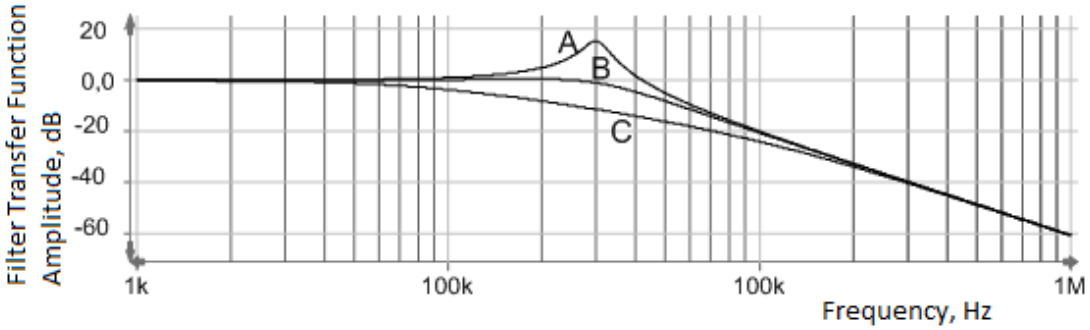

Figure 3.2. Transfer function plotted for different conditions of known LC- filter's transfer function terminals, A: conjugate roots, B: duplicate roots, C: real roots.

The spectrum of filter output and a PWM signal spectrum with double-edged modulation are seen in the Figure 3.3.

The component which has the least frequency among spectrums is the modulating signal. It's seen that filter input and output of amplitude remain the same. It's seen that it's component of just 100 kHz and sidebands are much weakened in the filter output. As amplitude axis hasn't been chosen as dB, much weakened components aren't seen on the simulation graphic. But the spectrum of filter output with this form reveals the aim of thesis and working principle of switched amplifiers. While the known filter filters well its high frequency harmonic components, the component of f_o frequency and sidebands are seen on the spectrum. In case that amplitude of modulating f_c = 1 kHz signal is less, as is understood from spectrum, high frequency harmonic components on the filter output will reveal the distortion effect which is seen more easily.

It's met with publications in which ripple components are proposed to be extracted from the voltage on output load mostly with an analog active circuit to be able to obtain a pure output signal by decreasing repeated ripple components at f_o frequency in switched power amplifiers. Publications in which this method is suggested has taken place in literature for a long time (Karaca, 1987), (Van Der Zee, 1999), (Walker, 2003). When this schema is thought as a whole, linear active circuit which tries to destroy ripple voltage at the output with this method and adds ripple component onto output load as negative in these methods will cause the efficiency of the amplifier which will be obtained to be less.

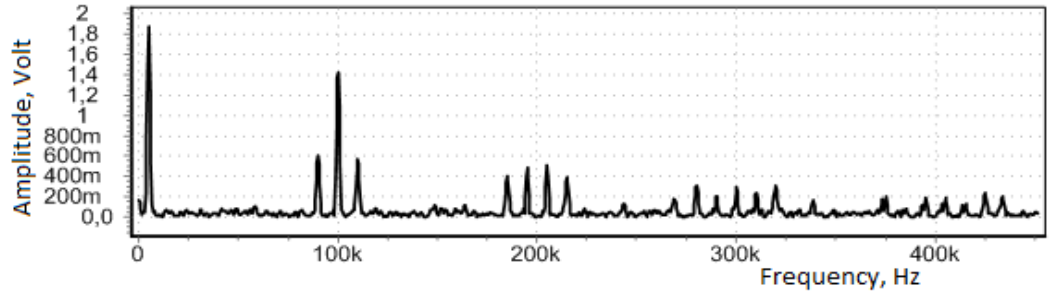

(a)

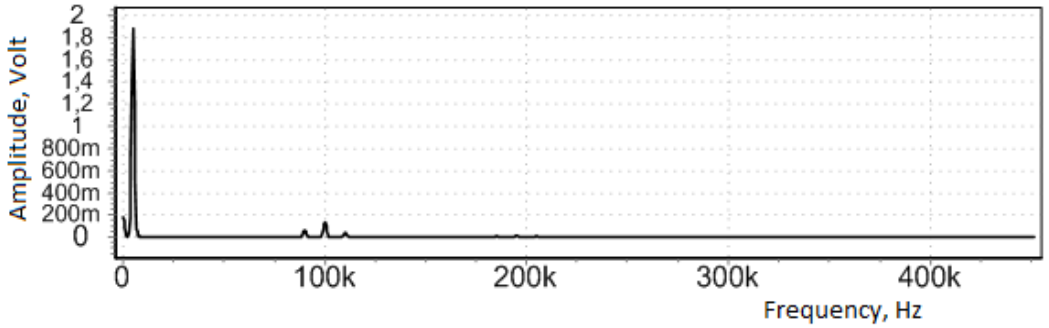

(b)

Figure 3.3. Frequency spectrum of PWM signal applied to LC- filter input (a), filter output spectrum.

For this reason, a new concept is tried to be developed in the thesis. In this concept, a filter topology is searched to acquire a pure output signal as much as possible for the thesis amplifiers by examining PWM frequency components.

3.2 Evaluation of PWM Spectrum for an Active Filter Design

A PWM signal whose amplitude is between -1 and 1 and average values is 0 will be output of a switched amplifier before filter. If this signal is called as $F_1(t)$, $F_1(t)$ spectrum can be written from the relation of (2.33) in General Information. As to be remembered, this relation has been found for a pulse signal which changes between 0 and 1. The spectrum of given amplifier output, for one-sided PWM modulation by writing $F_1(t) = 2(F(t) - 1/2), \quad D = 0.5$ in the relation of (2.33),

$$F_1(t) = M\cos(\omega_c t) + 2\sum_{m=1}^{\infty}\frac{\sin(m\omega_s t)}{m\pi} - 2\sum_{m=1}^{\infty}\frac{J_0(m\pi M)}{m\pi}\sin(m\omega_s t - \pi m) - 2\sum_{m=1}^{\infty}\sum_{n=\pm 1}\frac{J_0(m\pi M)}{m\pi}\sin(m\omega_s t + n\omega_c t - \pi m - \pi n/2) \tag{3.3}$$

is written. Double-edged PWM (whose carrier is triangular wave) spectrum can be created easily from this spectrum (Tan, 2003) and the spectrum below is found.

$$F_2(t) = M\cos(\omega_c t) + 4\sum_{m=1}^{\infty}\frac{J_0(m\pi\frac{M}{2})}{m\pi}\cdot\cos(m\omega_s t)\sin(m\pi k) + 4\sum_{m=1}^{\infty}\sum_{n=\pm 1}^{\pm\infty}\frac{J_n(m\pi\frac{M}{2})}{m\pi}\cdot\cos(m\omega_s t + n\omega_c t)\sin(m\pi k + n\pi/2) \tag{3.4}$$

Coefficients of switching frequency and frequency components of its harmonics in the spectrum can be calculated from the relation above for both types of PWM. For this purpose, the MATLAB code has been prepared that in Appendix A. Graphics produced by the MATLAB code are given in Figure 3.4 (a) and Figure 3.4 (b).

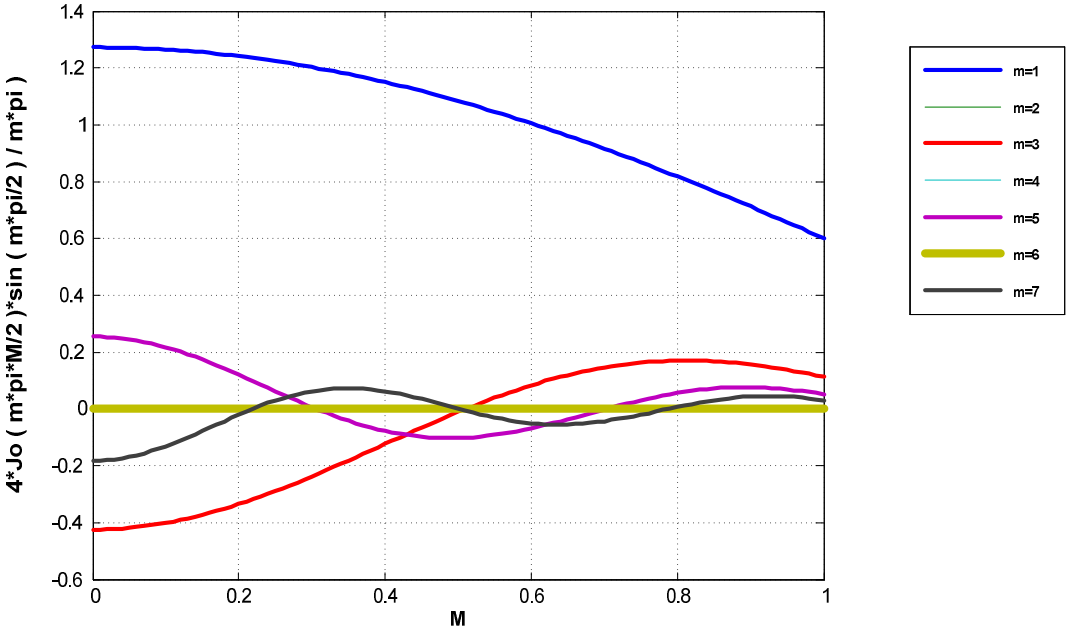

(a)

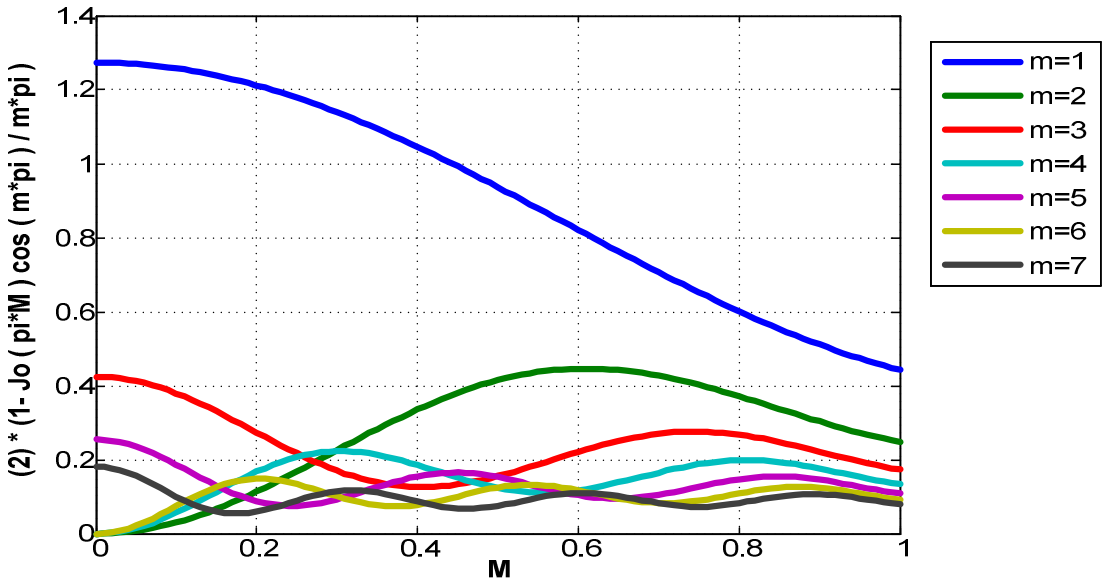

(b)

Figure 3.4. Coefficients of f_s, 2 f_s, 3 f_s, 4 f_s, 5f_s, 6f_s, 7f_s frequency components in PWM spectrum with double-edged modulation (a), coefficients of f_s, 2 f_s, 3 f_s, 4 f_s, 5f_s, 6f_s, 7f_s frequency components in PWM spectrum with single-edged modulation (sawtooth) (b), it's note to worth that double carrier harmonics don't occur when PWM is acquired by sawtooth carrier.

Let it be wanted to do an investigation for amplitudes of harmonics according to each other for M values which are different modulation indexes by benefiting from this relation. The reason of this is to aim to weaken well components in switching frequency of filter topology PWM which will be suggested in the thesis with notch characteristic. Let it be chosen the value of M=0 as starting. In this condition, a square wave changing between +1 and -1 will be obtained. For different M, n, m values, another MATLAB code calculating $J_n(m\pi M)/m\pi$ is written and the results are given in Table 3.1(Appendix B).

It can be shown from the definition of Bessel functions that third term in $F_1(t)$ given in (40) for square wave will be zero. Apart from this, in Table 3.1 for M=0, $J_{-1}(0)$, $J_1(0)$, $J_2(0) = 0$ are read.

As a result, for M = 0, the spectrum of PWM signal transformed into square wave can be written in the form of;

$$F_{1k}(t) = 2\sum_{m=1}^{\infty}\frac{sin(m\omega_s t)}{m\pi} - 2\sum_{m=1}^{\infty}\frac{J_0(0)}{m\pi}sin(m\omega_s t - \pi m) \tag{3.5}$$

If m=1 is written for basic component, the known amplitude value below is calculated.

$$A_1 = \frac{2}{\pi}sin(\omega_s t) - 2(0,318)sin(\omega_s t - \pi) = 1.273\,sin(\omega_s t) = \frac{4}{\pi}sin(\omega_s t) \tag{3.6}$$

When m = 2 is written for the second harmonic calculation, it can be shown that the term in (3.5) abbreviates each other and as a result, zero is obtained. In a similar way, it seen that it will be $A_3=(1/3)A_1$ ...$A_m=(1/m).A_m$ ... and the spectrum of the known square wave can be acquired.

At peak condition in which modulation depth is M=1, if component amplitudes at the frequency of 1, 2, 3 multiples of switching frequency are calculated from the relation of (3.3);

$\frac{2}{\pi}\sin(\omega_s t) - 2(0{,}0968)\sin(\omega_s t - \pi) = 0.443\sin(\omega_s t)$ and from here A_1=0.443 is found. Again, from (3.3) for $2\omega_s$ angular frequency component;

$$\frac{1}{\pi}\sin(2\omega_s t) - 2(0{,}0351)\sin(2\omega_s t - 2\pi) = 0.248\sin(2\omega_s t) \tag{3.7}$$

for $3\omega_s$ angular frequency component ;

$$\frac{2}{3\pi}\sin(3\omega_s t) - 2(-0{,}0192)\sin(3\omega_s t - 3\pi) = 0.250\sin(3\omega_s t) \tag{3.8}$$

is found. From here, A_2=0.248 and A_3=0.174 is calculated. It can be seen from the relation of (3.3) that amplitudes of all components under and over switching frequency will be symmetrical. Amplitudes are calculated as like that; for the first sideband as (n=1, n= -1) 0.181, for the second as 0.3; for component amplitudes (M=1, m=2, n=1, 2) around two times more components of switching frequency respectively as 0.067 and 0.09.

When amplitudes of components in PWM are compared for different M values, for M=0 namely for the state of square wave ω_s frequency component has the amplitude of three times more than the component of the highest amplitude coming after itself. Although M increases, this proportion decreases, even in the case of M=1, amplitude in its frequency is twice more than the amplitude of component which has the closest amplitude.

From here, it's clear that characteristic will affect performance of attenuation value of ω_s in PWM signal filtering. Instead of a filter whose frequency with characteristic changes as much as 20dB/decades or 40dB/decades, filters which has a notch-shaped attenuation at exactly ω_s can provide a better performance.

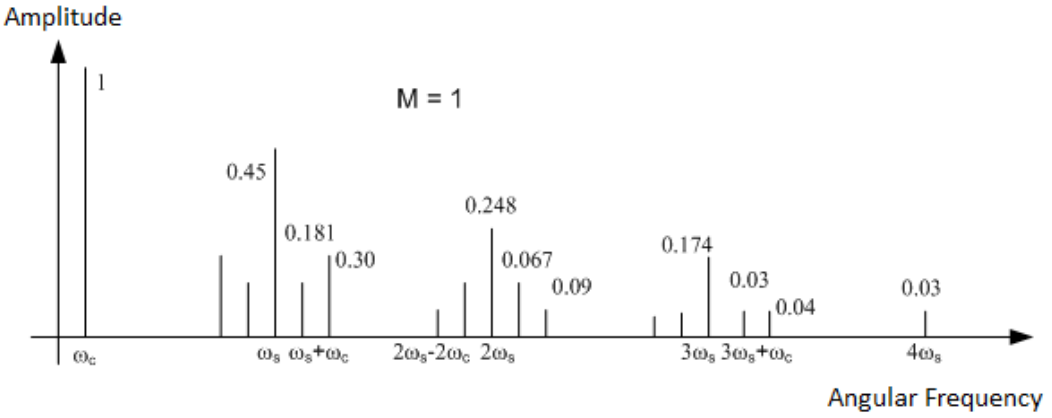

(a)

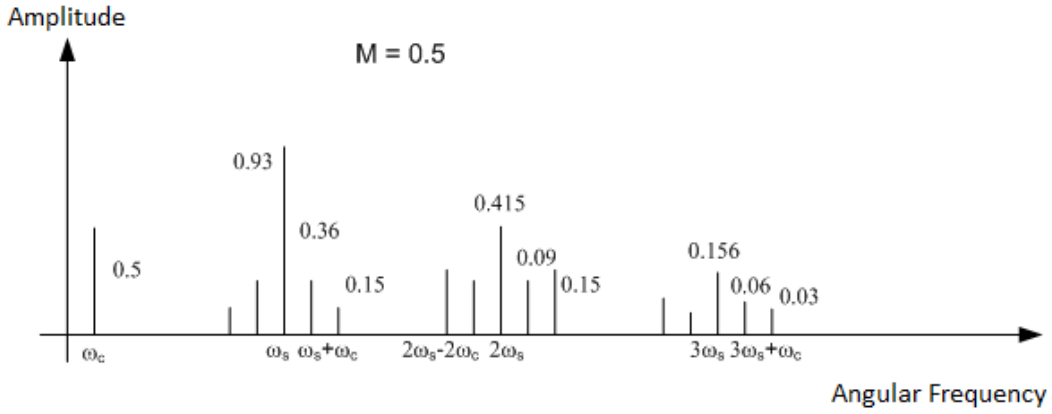

(b)

Figure 3.5. Calculated component amplitudes of PWM signal's frequency spectrum given in the correlation for M = 1 (a), for M = 0.5 component amplitudes (b).

3.3 Selecting Topology of Class-D Amplifier Filter

As known, transmission line filters has an important place in Microwave applications. Recently, publications in which integrated structure resembling to transmission line filter also in power electronics applications has often taken place in literature (Sheen, 2000), (Yin, 2007). To be remembered in the thesis proposal, this trend was predicted to be researched of the application in switched amplifiers. Nowadays, studies on verified power electronics filters with multi-resonance mass elements as well as transmission line filters have been (Phinney, 2005).

As the result of simulation studies, when its characteristic is thought as output filter of switched amplifiers, a very striking filter topology is acquired. In this filter circuit given in Figure 3.6 (a), R2 represents output load resistance and R1 represents an open circuit connected to avoid the failure of simulation programme. In the (b) section of the same figure, Bode amplitude characteristic simulation of the filter is seen.

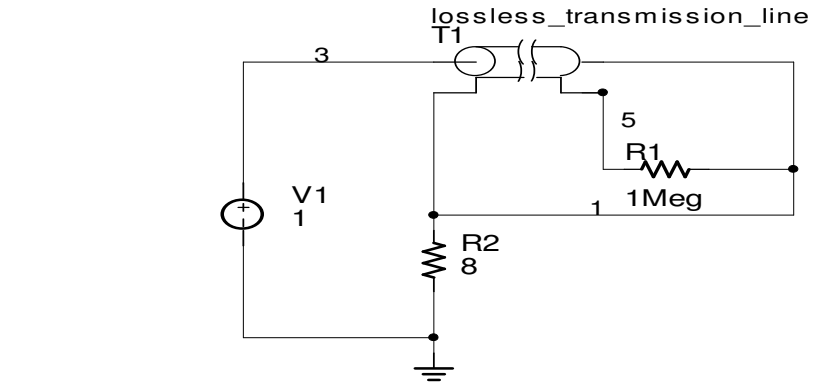

(a)

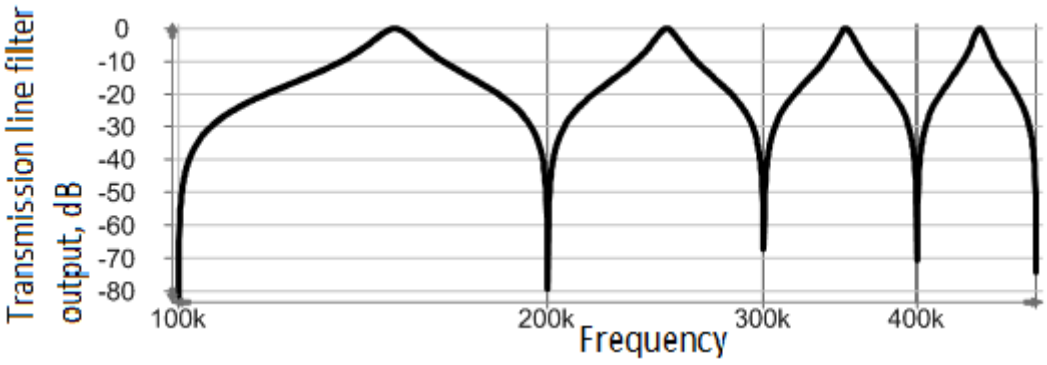

(b)

Figure 3.6. A transmission line filter designed for switched amplifiers in simulation environment (a), output signal in case of input signal is a sweeped sinusoidal signal (b). As 1 Volt is selected for V1 source amplitude, output filter taken upon 8Ω will have transfer characteristic.

When PWM frequency spectrum is remembered, it's seen that this filter can provide a very good ripple rejection in an amplifier whose switching frequency is 100 kHz. If f_s, $2f_s$ $2f_s$ $3f_s$ ... frequency and components which will emerge around

them are small enough nearby f_c, f_s seen in equation (3.3), it will be attenuated in the form of f_s=100 kHz as can be seen from the figure.

In condition that transmission line in filter is with losses (when lost values which can be met in the application are accepted), it takes the attenuation values up to -80 dB, -60 dB. It's seen that cable length giving the result of this simulation (Figure 3.6(b)) is over 1000 m. Studies are made on discrete filter structures of similar results which are more suitable for verification and take less place.

There are solenoid coils each of which is wounded one after the other with 200 winding numbers on aluminium rod at the length of about half meter in Figure 3.7. In this photograph, only the coil above is seen. This experimental element is wounded on aluminium rod to make it more successful with this form in the application (the information provided by simulation results) and being less of this experimental element characteristic impedance which has been created by inspiring from a similar transmission line in implementing literature.

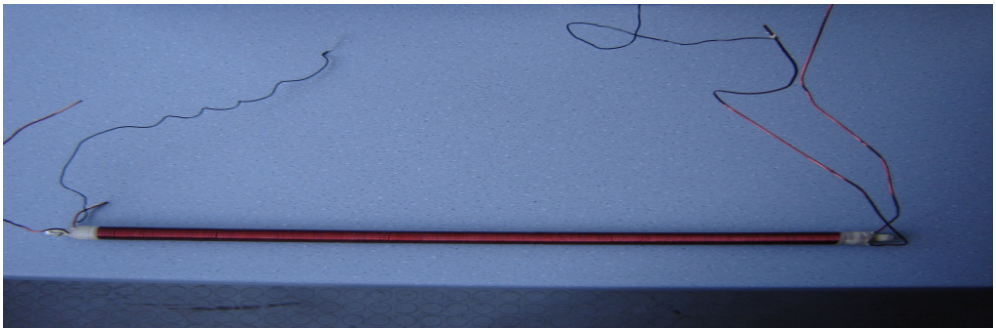

Figure 3.7. Transmission line filter comprised of over and over wounded Solenoid coil.

It's benefited from this prototype transmission line in verification of filter circuit given in the figure. Prototype filter is connected to 4395A Network Analyzer device over measurement amplifier whose output resistance is so low and verified input resistance is 50 Ohms for experiments. Oscillator output of the device is connected to input of measurement amplifier and amplifier output is connected to transmission line. To be driven with a small impedance source of the Filter is provided with this measurement amplifier. With this method, instead of Bode diagram which will be

obtained by being driven with a 50 Ohms resistance of source (the technique used in high frequencies), here, conventional transfer function is experimentally obtained as in Figure 3.8 by driving with a small internal resistance of source.

As can be seen from the obtained experimental diagram, as well as that prototype of verified transmission line isn't suitable for the use of consumer electronics in consideration of its physical sizes, its notch frequency is 2.86 MHz even with this size. In other words, it can provide success for switched amplifiers whose switching frequency is chose as 2.86 MHz. In addition, as transmission line characteristic is tried to be created with solenoid coils (for the purpose of being able to decrease transmission line physical size), attenuation values which appear at 100 kHz and its multiplies seen in simulations emerge as attenuation values which differs gradually at 2.86MHz and its multiplies in experiments.

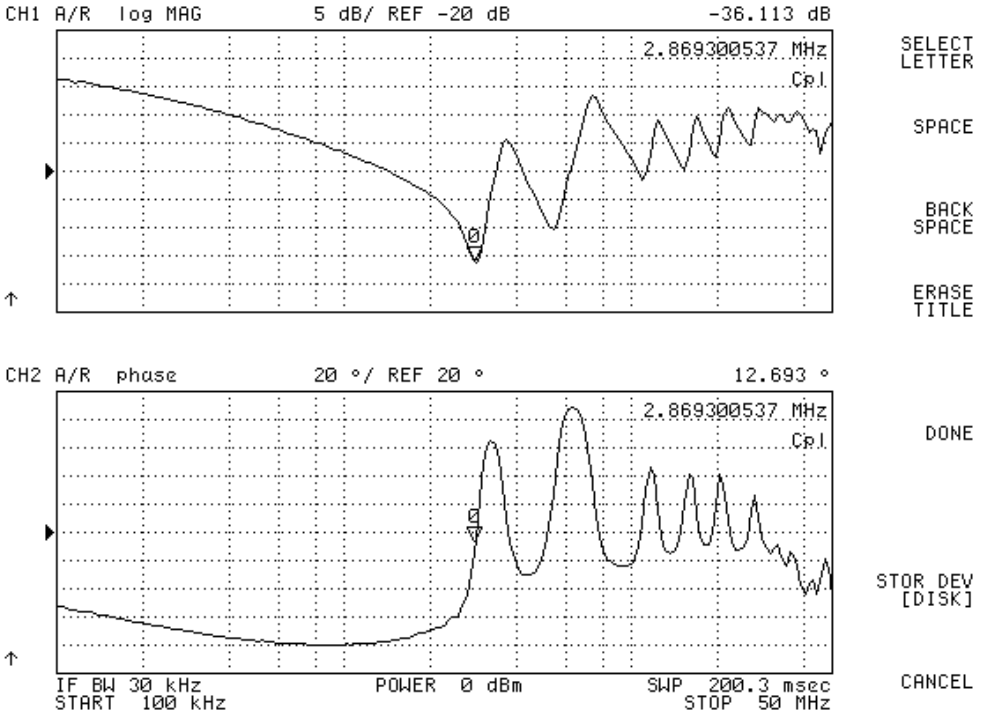

Figure 3.8. Amplitude (above) and Phase (below) characteristics of experimental transmission filter.

3.4 Transfer Function of the Notch Filter

From the simulation studies of verified filter with lumped elements, it has been seen that the filter seen in Figure 3.9 and classified as notch filter because of its characteristic gives good results for PWM signal and it's mostly worked with this filter in the experiment. When notch filter is chosen instead of LC- type filter in switched amplifiers, Transfer Function should be first calculated to be able to evaluate performance in terms of ripple voltage.

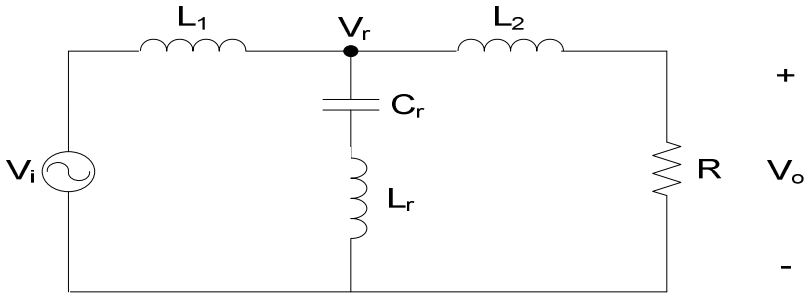

Figure 3.9. Notch filter designed with ideal elements.

Let the element values of this notch filter be chosen as below:

$L_1 = L_2 = 30\ \mu H$, $Lr = 5\ \mu H$,$Cr = 470$ nF, $R = 8$ Ohms .

When filter elements are accepted as ideal, V_0/V_i Transfer Function of the composed circuit in Figure 3.9 can be calculated as below.

$$\frac{V_O(s)}{V_i(s)} = \frac{R(L_r C_r s^2 + 1)}{C_r[L_2 L_r + L_1(L_2 + L_r)]s^3 + RC_r(L_1 + L_r)s^2 + (L_1 + L_2)s + R} \quad (3.9)$$

Zeros of found transfer function corresponds $\omega_o = 1/(\sqrt{LrCr})$ which is notch frequency of filter (Koroglu, 2001). Although there is resistance (R) in filter circuit, as seen, quality factor Q of zeros is not finite.

V_0/V_i Transfer Function can be written as simplified as below in a frequency as far as ($\Delta\omega$) from notch frequency. In this relation, the second and higher degree of terms of ($\Delta\omega$) are ignored.

$$\frac{V_O}{V_i} = -\frac{2R\left(\frac{\Delta\omega}{\omega_0}\right)}{R[1-C_r(L_1+L_r)\omega_0(\omega_0+2\Delta\omega)]+j\{(L_1+L_2)(\omega_0+\Delta\omega)-[L_2+L_1(1+L_2/L_r)](\omega_0+3\Delta\omega)\}} \qquad (3.10)$$

In this relation, it's paid attention that frequency terms are in the form of $\omega_o+(\Delta\omega)$, $\omega_o+2(\Delta\omega)$, $\omega_o+3(\Delta\omega)$ and it's seen that its amplitude and angle, denominator won't change much around notch frequency for element values of $L_1 = L_2 = 30$ µH, $L_r = 5$ µH , $C_r = 470$nF chosen in prototype filter. Numerator is ($\Delta\omega$)= 0 namely zero in notch frequency. It's understood from here that amplitude of Transfer function will also be zero. In addition, as the sign of numerator will change when input frequency of filter goes over ω_o from a little bit under of ω_o, there will occur Phase change of 180º.

Transfer function which is measured by connecting to filter output of A channel and input of B channel of measurement device is given in Figure 3.9. It's understood from this gotten measurement result that it's at the value of f_o = 107.5 MHz. Theoretically, it's calculated that the values given above and the value which f_o should take are about 104 kHz. The difference between them may result from value tolerances and parasitic components of filter element.

MATLAB Bode diagrams which are formed by being written at the transfer function of element values given in the beginning.

As seen in the last composed relations, it's expected that V_o voltage in the frequency of ω_o ($\omega_o = 1/(\sqrt{L_r C_r})$ zero or it's very small in real conditions. For this reason, it's benefited from V_r voltage instead of V_o in the design of frequency control circuit.

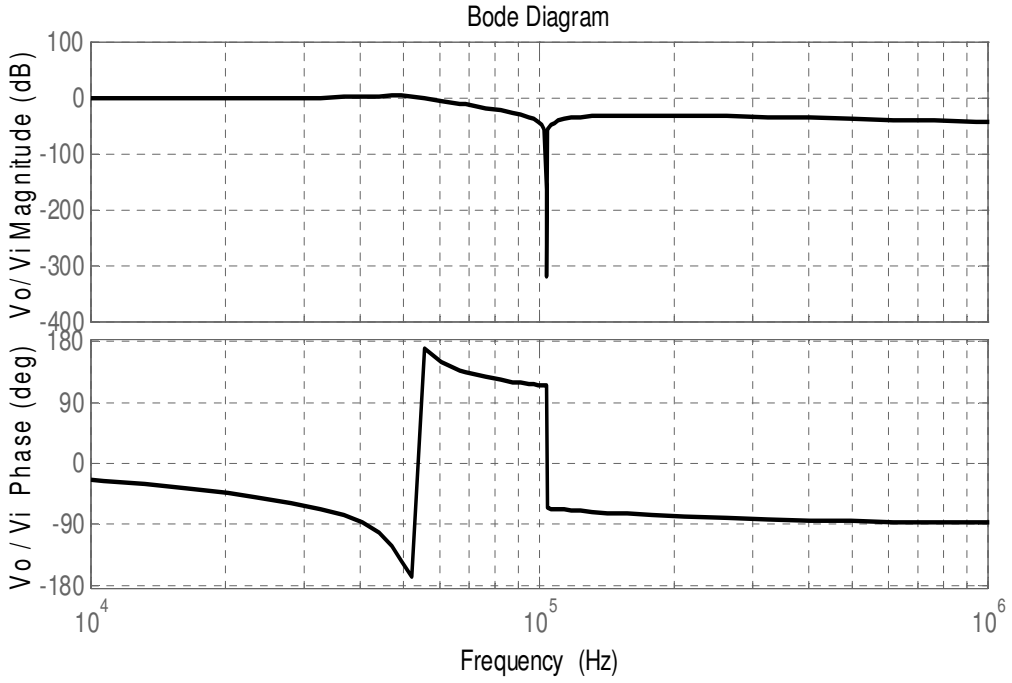

Figure 3.10. V_o Amplitude and Phase characteristics are plotted with (3.9)

In addition, there won't be any need for 90° phase shift circuit with this choice in the design of frequency control circuit. If similar relations are searched for V_r :

$$\frac{V_r}{V_i} = \frac{(R + L_2 s)(L_r C_r s^2 + 1)}{C_r[L_2 L_r + L_1(L_2 + L_r)]s^3 + RC_r(L_1 + L_r)s^2 + (L_1 + L_2)s + R} \tag{3.11}$$

$$\frac{V_r}{V_i} = -\frac{2\ [R + jL_2(\omega_0 + \Delta\omega)]\dfrac{\Delta\omega}{\omega_0}}{R[1 - C_r(L_1 + L_r)\omega_0(\omega_0 + 2\Delta\omega)] + j\{(L_1 + L_2)(\omega_0 + \Delta\omega) - [L_2 + L_1(1 + L_2/L_r)](\omega_0 + 3\Delta\omega)\}} \tag{3.12}$$

are obtained.

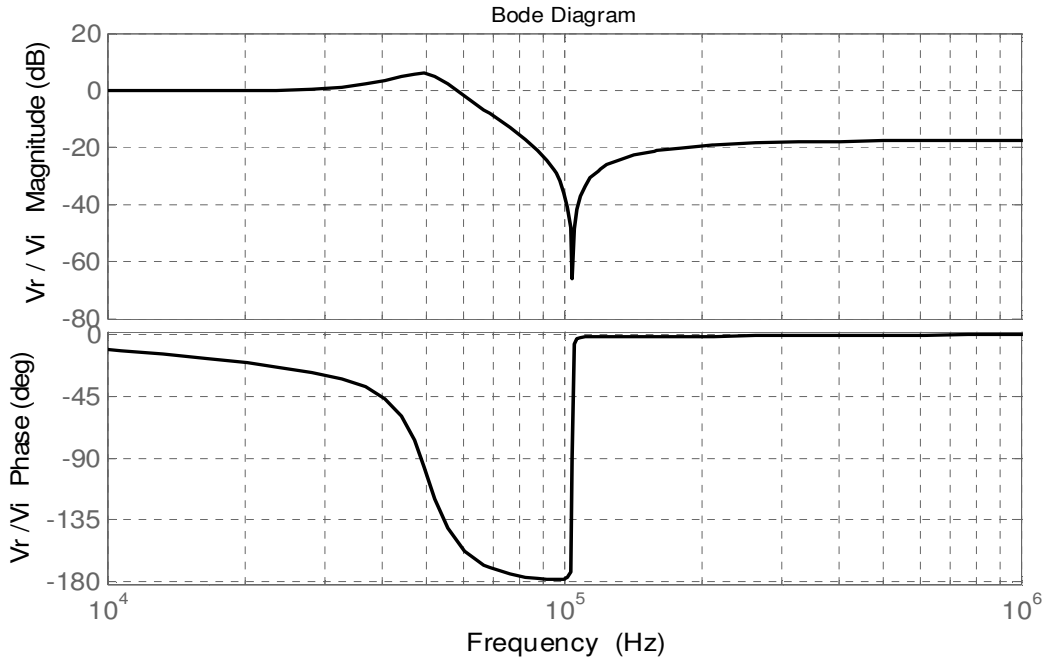

Figure 3.11. V_r Amplitude and Phase characteristics are plotted with (3.11) MATLAB calculated from transfer function.

In laboratory, characteristic of a verification done with given element values is found as below.

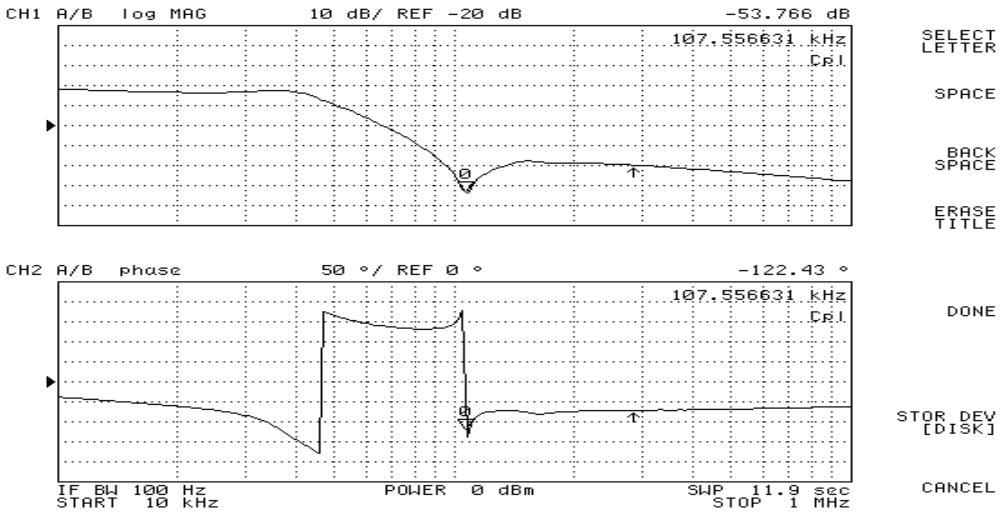

Figure 3.12. Measurement results of experimental notch filter Amplitude and Phase characteristics.

From the characteristic of experimental measurement given above, attenuation in ω_o is theoretically under the found (Figure 3.10) in real conditions. It's understood from the relations above that load resistance R of filter isn't effective on notch attenuation. r resistance which represents losses of L_r and C_r is added to the filter to be able to approach real conditions. As r resistance seen in the circuit in Figure 3.13 below doesn't represent a resistance which is connected to verified filter and inductances of L_1 , L_2 are chosen equally, these are shown with L.

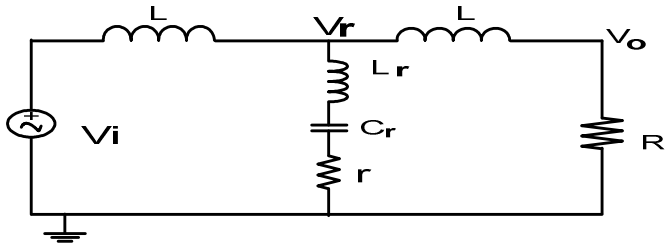

Figure 3.13. As filter circuit is chosen at the same value in two inductances experiments in the circuit when losses determining notch attenuation are represented with r, these are shown with L in the diagram above.

In the new condition, transfer function can be composed as below.

$$\frac{V_o}{V_i}=\frac{R(L_rC_r\,s^2+srC_r+1)}{C_r[(2L_rL+L^2)]\,s^3+(LRC_r+2rC_rL+L_rRC_r)\,s^2+(2L+rRC_r)\,s+R} \tag{3.13}$$

$$\frac{V_r}{V_i}=\frac{(R+sL)(L_rC_r\,s^2+srC_r+1)}{C_r[(2L_rL+L^2)]\,s^3+(LRC_r+2rC_rL+L_rRC_r)\,s^2+(2L+rRC_r)\,s+R} \tag{3.14}$$

If it's wanted to calculate V_o voltage for $(\Delta\omega)$ change around ω_o in lossy case again, the transfer function below can be written.

$$\frac{V_o}{V_i}=\frac{-2R\sqrt{L_rC_r}\,(\Delta\omega)+jrR\sqrt{\frac{C_r}{L_r}}+jrRC_r(\Delta\omega)}{-R-2r-4\sqrt{L_rC_r}\,(R+r)(\Delta\omega)+j(rRC_r+2L)\left[\frac{1}{\sqrt{L_rC_r}}+(\Delta\omega)\right]-j\frac{L(2L_r+RL)}{L_r}\left[\frac{1}{\sqrt{L_rC_r}}+3(\Delta\omega)\right]} \tag{3.15}$$

When (Δω)=0 is written from this last relation, it's understood that attenuation in notch frequency is finite and depends on r resistance value. If Q quality factor of attenuation in notch frequency is looked for;

$$Q = \frac{1}{r}\sqrt{\frac{L_r}{C_r}} \tag{3.16}$$

can be calculated. L_r can be chosen as big and C_r can be chosen as small as well as choosing elements whose losses of L_r and C_r are low to verify quality factor Q as high. But if the limit is exceeded in this choice, filter attenuation decreases quite in the frequencies just on ω_o of filter. For this reason, it's clear that selection of the values of L_r and C_r elements will be a design problem which requires measurements, also takes into consideration losses of available L_r , C_r elements and design conditions.

By applying square wave to the input of experimental filter (Prototype switched amplifier input is provided by making short circuit), image of oscilloscope screen given in Figure 3.14 (a) has been taken with V_o and V_r voltages of the filter.

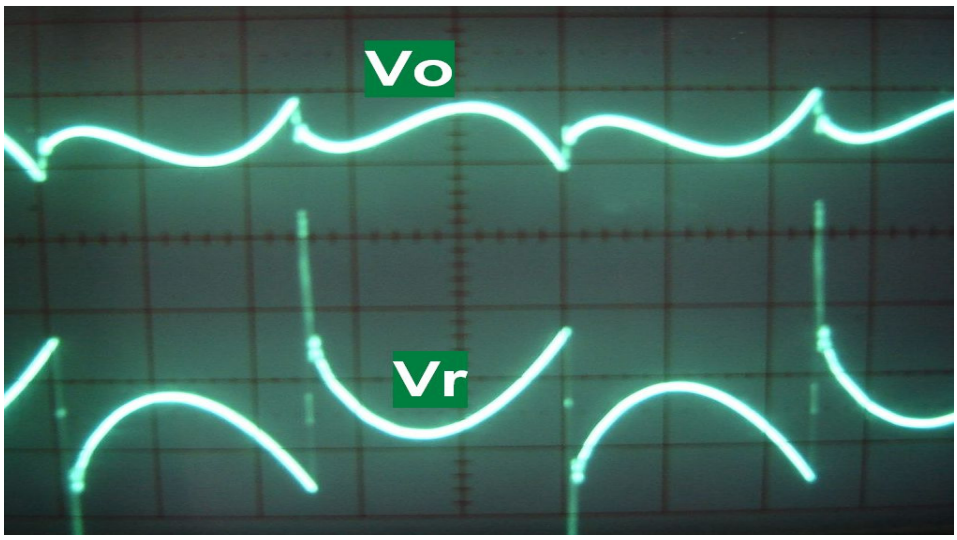

V_0: 0.25 V/DIV **V_r:** 1.5 V/DIV **Time/DIV:** 2µs / DIV

(a)

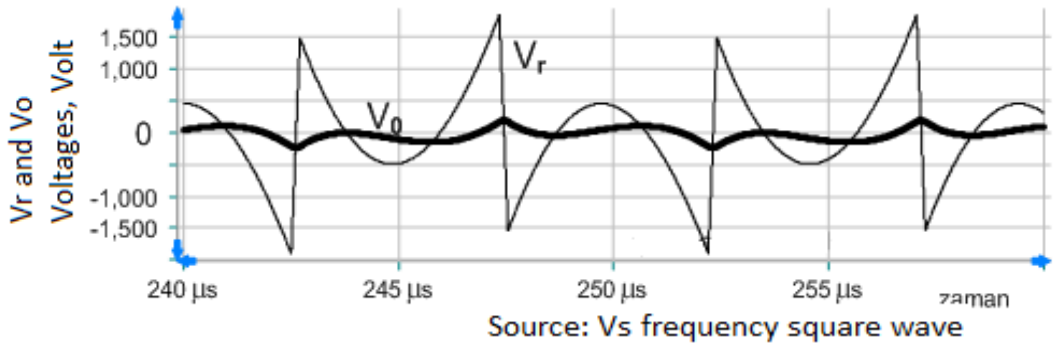

(b)

Figure 3.14. Experimental figures taken when filter input amplitude is applied to a square wave changing between +15 V and -15 V and angular frequency ωo (Δω= 0) (a), simulation results of the same conditions (b). If you pay attention, you'll see that there are very short-term spike-shaped pulses occurring at the moment of switching in V_r. These pulses are due to capacity of parallel value a few pF and leakage of L_1 inductance.

Simulation results of the same voltages are given in Figure 3.14 (b). It can be observed that signal format created by taking out the basic component in a square wave is close to V_r voltage seen in experimental result. From here, function of notch filter is understood in a better way.

3.5 Evaluation of Ripple Current Passing Through L_r - C_r Handle of Notch Filter Comparing with Ripple Current Passing Through Load Resistance

The principle of success in switched amplifiers of notch filter is based on almost all of current component of f_o frequency passing through L_r - C_r handle of the filter, not passing through load resistance. It can be expected that this current will take the highest value in condition of $f_s = f_o$ and it will be close to a sinusoidal current format of f_s frequency. But it's understood from experimental and simulation results below that the second part of this prediction is not correct.

It has been seen that this current whose duty-cycle is 50% (square wave) for a filter input voltage is very close to triangular wave. This condition can only be explained by thinking that L_r - C_r handle will pretend to be consisting of only L_r for upper harmonic components of f_s. In this condition, resistance of components (L_1+

L_r) passing through this handle for harmonics will be as if harmonics of a square wave connected between its ends. This simplified result has been created by ignoring harmonic currents which will pass through L_2 inductance. Indeed, as all prototypes are chosen as L_2 = 30 µH and L_r = 5 µH, this acceptance can be done by ignoring a certain error.

Zero voltage has been applied to the prototype input which has been verified with TDA7490 where experimental waveform below is taken and in the condition, filter input is in the form of square wave. In addition, the condition of $f_s = f_o$ = 104 kHz has also been created. Square wave voltage is +15, - 15 Volts and R load resistance has been chosen as 6 Ohms. As the signal which will be amplified isn't connected to amplifier prototype input, currents of filter elements will be only ripple current in this condition. Resistance (R) and L_r currents have been recorded as seen in Figure 3.15.

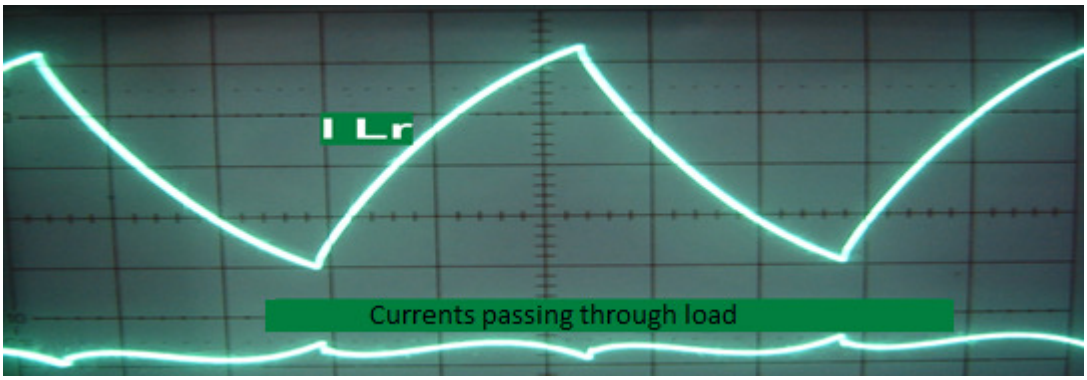

Figure 3.15. $f_s \approx f_o$ (f_o= 104 kHz) and currents passing through load, $\mathbf{i}_{Lr}$: 0.5 A/DIV, $\mathbf{i}_R$: 0.1 A /DIV, time: 2 µs/DIV when compared in terms of peak-to-peak values is about 50 times bigger than load ripple current.

It has been understood that experimental form of $\mathbf{i}_{Lr}$ current arises from the losses of magnetic core with copper resistance of L_1 inductance. In other words, in condition that L_1 is without loss, simulation results exactly conforms to the laboratory results when a resistance of 1 Ohm which represents high frequency losses is connected to L_r - C_r current L_1 resistance which is read as triangular wave.

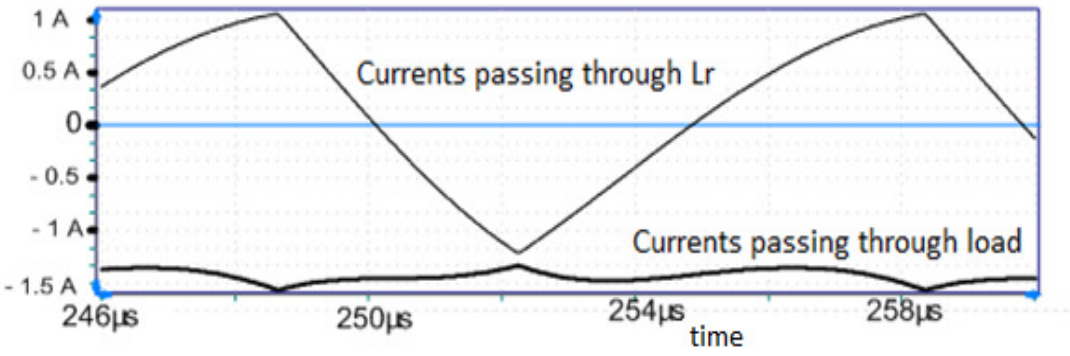

Figure 3.16. $\mathbf{i}_{Lr}$ under the condition of $f_s \approx f_o$ and simulation results of currents passing through load, amplitude of load resistance current format has been multiplied 3 times while drawing to be able to read it from graphic explicitly.

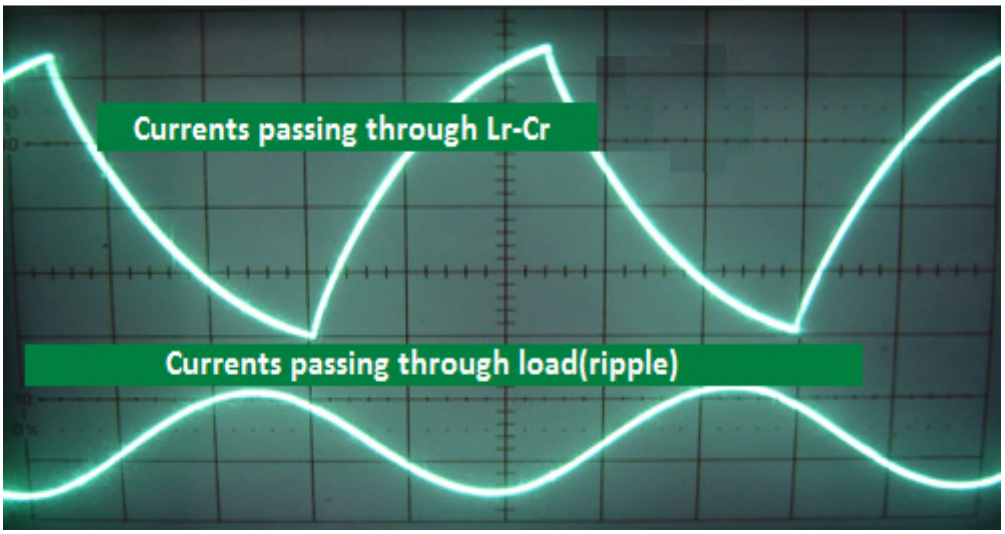

Figure 3.17. In case of that f_s, f_o is under 15 kHz, $\mathbf{i}_{Lr}$ and currents passing through load, $\mathbf{i}_{Lr}$: 0.5 A/DIV, $\mathbf{i}_R$:0.2 A/DIV, time:2 µs/DIV, when compared in terms of peak-to-peak values $\mathbf{i}_{Lr}$ current is about 7 times bigger than load ripple current.

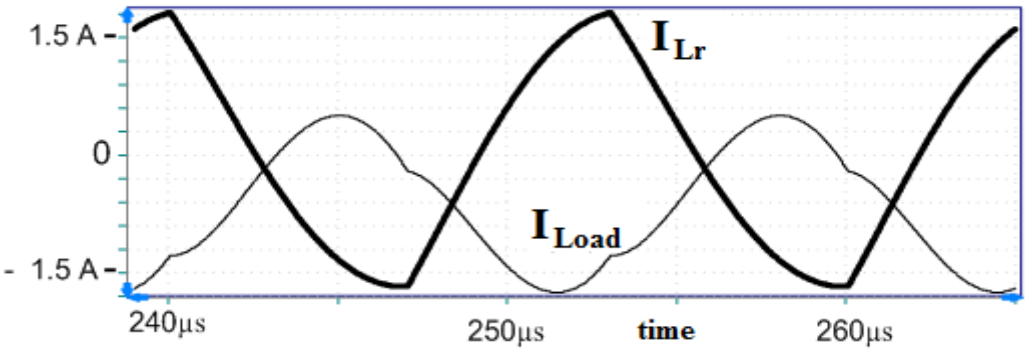

Figure 3.18. $\mathbf{i}_{Lr}$ in case of that f_s , f_o is under 15 kHz and simulation results of currents passing through load , amplitude of load resistance current format has been multiplied 3 times while drawing to be able to read it from graphic explicitly.

The current (ripple current) which passes through L_r - C_r handle of the filter doesn't increase in condition that $f_s = f_o$ condition is provided. This current increases when it takes even lower values than f_s notch filter. It's seen that the current increases as the factor which determines the current is the value of L_1 impedance and as frequency decreases, impedance will decrease, as well. Let it be accepted that the current passing through L_r - C_r handle during small change around f_o of this current f_s with the aim of simplification. But ripple voltage, which is created between ends of L_r - C_r handle of this current whose amplitude is accepted as fixed, changes with frequency and this amplitude takes the lowest value under the condition of $f_s = f_o$. In other words, L_r - C_r handle creates a current path with a very small (zero in ideal condition) impedance.

So serially connected L_2 – R handle can be modelled in the form in which it's driven from a source of small amplitude and small impedance from the aspect of ripple voltage under the condition of $f_s = f_o$. As a result, the current passing through R (load) resistance is about 1/50 of the current passing through L_r - C_r handle from the aspect of amplitude in notch filter. In condition that load ripple current f_s is under f_o about 15 kHz, this proportion increases up to 1/10. An interesting result seen from again simulation and experimental results is that the current passing through load increases although the current passing through L_r - C_r handle increases when it starts to take values which are over $f_s = f_o$ = 104 kHz. This observation can be explained with working principle of simplified filter above.

3.6 Comparison of Switched Amplifier Suggested Filter in the Thesis Work with LC Filter

The simulation circuit seen in Figure 3.19 has been designed in order to compare the filter suggested in the thesis work with the known LC filter of switched amplifiers from the aspect of performance of ripple attenuation. In these circuits, it has been chosen as f_s = 100 kHz. It has been based on the choice of this value so that the numbers in the graphics can be compared more easily.

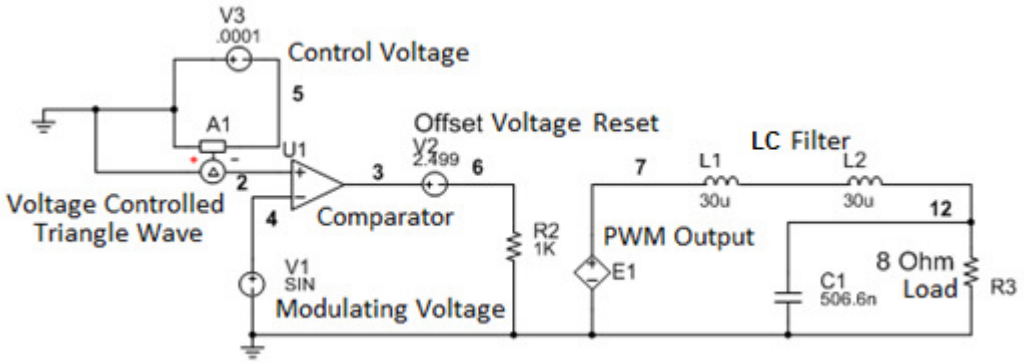

(a)

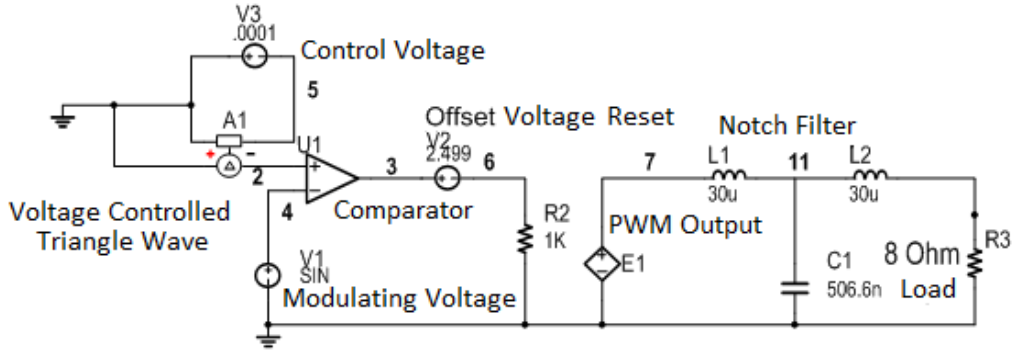

(b)

Figure 3.19. Simulation circuits to compare filter performances, Switched amplifier with LC filter (a), simulation circuit of switched amplifier with notch filter (b).

C1 capacitor in Figure 3.19 (a) is calculated to make notch frequency of the suggested notch filter at exactly this value ($f_s = f_o$) and it has been found C1= 506.6 nF (in application circuits, it's at the standard value of C1 = 470 nF. When L3

resonance inductance of filter in this circuit is taken out of the circuit and C1 capacitor is connected to the ends of R3 load resistance, the known LC-filter in Figure 3.19 (b) will be obtained.

For this filter circuit, being exactly at 100 kHz of PWM switching frequency isn't so important for its performance but switching frequency and notch frequency should be equal to be able to benefit from the characteristic of notch filter. As known, there will be only one L element instead of L1 and L2 inductances in the classic filter, but here only one inductance isn't connected to be able to compare more easily from the aspect of view of filters by taking equivalents.

In all the simulations at this chapter, PWM amplitude is at the value of 1 Volt and is taken from the ends of E1 dependent source.

Let modulation depth be wanted to compare ripple signals of both filters for small PWM signals. For this aim, modulation depth is chosen as zero, namely a square wave instead of PWM. E1 is provided to be square wave by assigning the value of V1=0 (Figure 3.19) in simulation circuits. Voltages occurring on output load (resistance of 8 Ohms) are comprised of only ripple component and it's seen in Figure 3.19.

When the amplitudes of this two different ripple voltage waveforms are compared, activity of notch filter suggested in the thesis is clearly seen. But increasing of modulation depth in the evaluation done in this report before causes to decrease the amplitude of basic component of 100 kHz in PWM. In turn, it causes to increase the amplitudes of 200 kHz and other double and single harmonics. PWM signals with high modulation depth can provide a better performance to make better the performance of classic filter at high frequencies. Modulation depth is provided to be very close to 1 value by making V1 resistance seen in Figure 3.19 as V1=0.99 Volt to be able to make comparison. It hasn't been chosen as exactly M = 1 not to have lost PWM pulses.

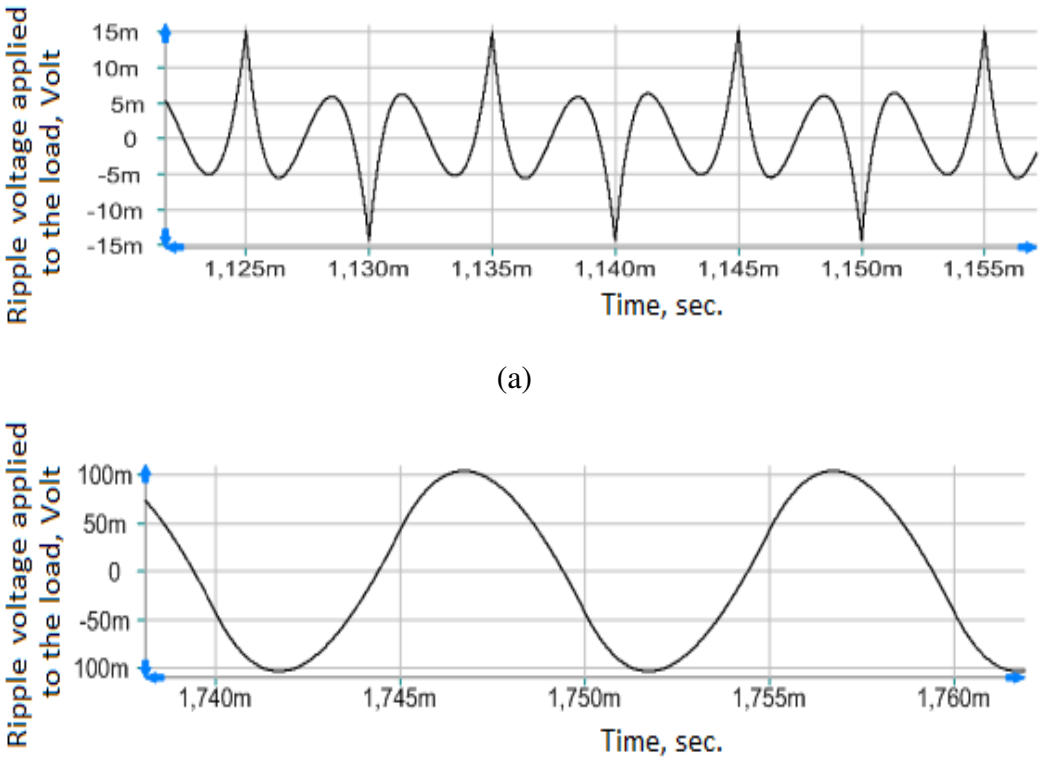

Figure 3.20. Thesis work filter ripple voltage (a), classical filter ripple voltage (b) , if you pay attention, in the second type of voltage, weight of 100 kHz frequency is very much and ripple signal is comprised of almost an 100 kHz frequency sinusoidal signal.

Output waveform of classic filter (a) and frequency spectrum obtained with FFT (b) are seen in Figure 3.20 below.

From the evaluation of (a) part of this figure, it's realized that ripple voltage has increased around zero crossings of the signal. In addition, it's understood from the evaluation of the figure that although modulation depth is at the highest value that it can take, the amplitude of 100 kHz amplitude component is over other harmonics and also this condition can be observed from the plotted waveform according to time.

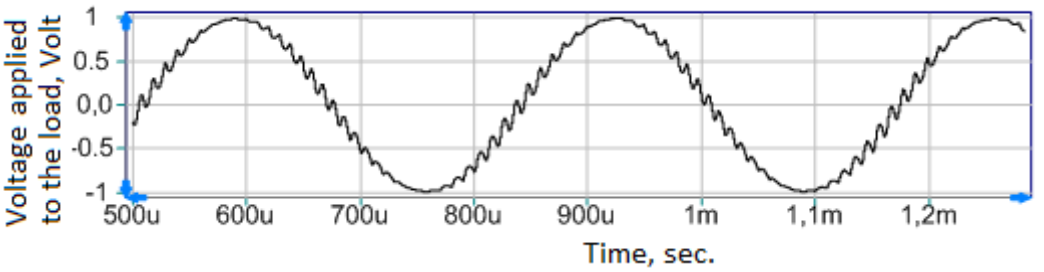

(a)

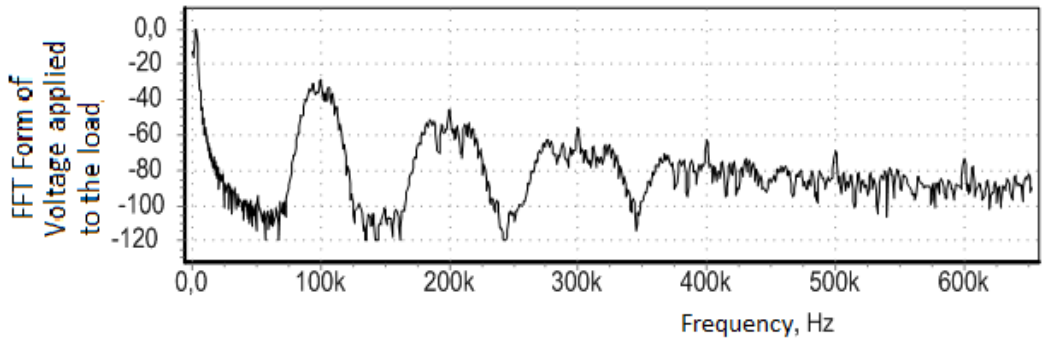

(b)

Figure 3.21. PWM signal (M=0.99 and f_c= 3 kHz) output obtained in result of demodulation with classical LC- filter (a),frequency spectrum of output signal (b).

Simulation results of the circuit in which only notch filter (instead of classic filter) takes place and under the same conditions are given in Figure 3.22. It's clearly seen that output signal contains less ripple component. The attenuation that occurs at the value of -100 dB at the frequency of 100 kHz basic component which stays as the component which has the highest amplitude even for this modulation depth is striking although it seems to be superior to suggested classic filter at harmonic frequencies (200 kHz, 300 kHz,...).

It's seen from Figure 3.22 (b) that f_s component weakens greatly and side bands just around f_s are under the amplitude of the same side band given in Figure 3.21. As well as observing that there is a better attenuation in the third and upper harmonics of the classic filter whose output spectrum is given in Figure 3.21 (b), it's seen that amplitudes at these frequencies are small for both of the compared filters. This

condition without doubt results from amplitudes of these components' being relatively small in PWM input spectrum.

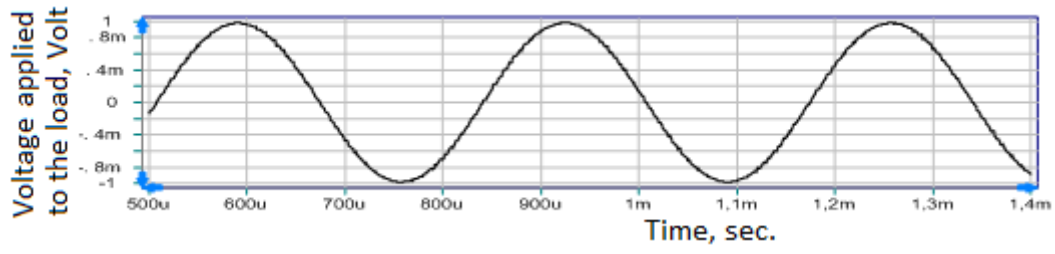

(a)

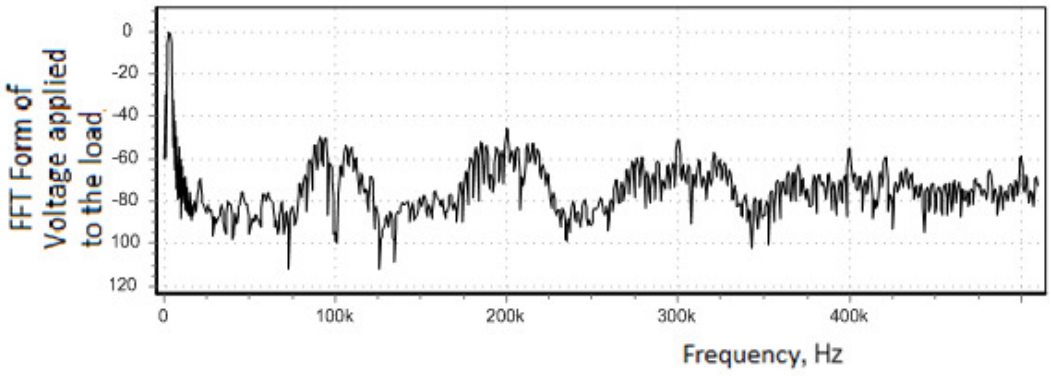

(b)

Figure 3.22. PWM signal (M=0.99 and f_c=3 kHz) output obtained in result of demodulation with notch filter (a), frequency spectrum of output signal (b), simulation result has been taken under the condition of f_s= f_o=100 kHz, it's striking in spectrum that amplitude occurring exactly at f_s= f_o=100 kHz is very low.

3.7 Selection of Filter Magnetic Core

After determining Filter Topology, verification of it has been made with different ferrite core types. At first, experimental results didn't result as expected. An important distortion, which may be related by core characteristics has been seen. To change core air gap could be a solution to this problem but as worked with cores in toroid geometry (with the notion of Electromagnetic compatibility), there isn't a possibility of such a solution.

Many experiments have been made with different turn numbers and many magnetic core types for the solution of these problems. Eventually, a test which has been made with toroid-shaped magnetic cores taken from a broken Desktop power supply has given the expected output waveform. It has been seen that these magnetics whose one side is white and the other are yellow exist in power supply of every brand of computers. It's reported that this type of cores aren't ferrite but iron powder type. It has been seen that transformators from ferrite material in computer power supplies and filters are verified with correct voltage with this type of cores whose performance is reported to be good in the frequency band of 1 MHz (PE – COILS) with correct voltage.

Mentioned core type is used for L_1 and L_2 inductances of thesis filter. Cores, whose losses are reported to be less (Amidoncorp) for Lr inductance in filter, again in the type of iron powder coded with red colour are used. As Lr cross-section carries only high frequency ripple currents, it can be chosen as small according to L_1 or L_2 cross-section. But as can be seen in the proceeding parts of the report Lr current amplitude is around the value of 1 Ampere for symmetrical supplied prototypes of 12-15 volts. These values are measured for L_1 and L_2 inductances verified with Impedance Analyzer feature of 4395A Device taken in the scope;

L= 30.3 μH, leakage parallel capacity is measured as Cp= 7.7 pF and leakage parallel resistance as Rp = 1.5 kOhms. The change of angle or impedance module of L_1 or L_2 according to frequency is seen in Figure 3.23.

Here, it's reported that Change graphic with the frequency of angle is not sharp but relatively slow and losses of the core or inductance are too much (Agilent 2006). Indeed, it has been observed that this type of cores become warmer than ferrites during experiments. It's understood that this warm stems from high frequency losses, this type of cores are optimized for power filters which conducts direct current or low frequency with Electromagnetic Interference Filters. When it's started to the experiments with this type of cores, as also mentioned above, distortions named as

spike which are extremely short-term in filter output. It's clear that except distortions created by mentioned spike pulses.

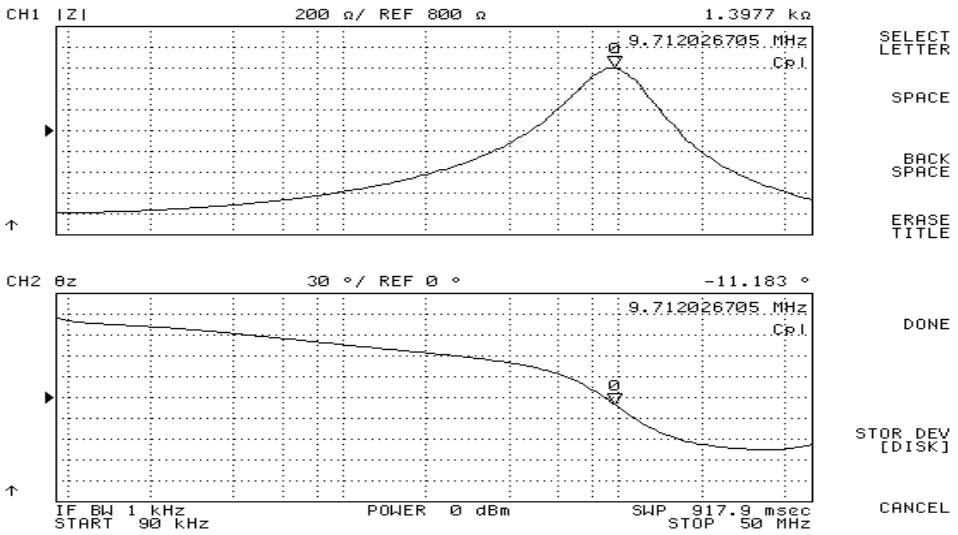

Figure 3.23. Changing of impedance modules of L_1 and L_2 inductances taking place in notch filter with frequency. As seen, parallel resonance emerges due to parallel coil leakage capacity of 9.7 MHz frequency.

It can also cause distortions on electronic elements in some topologies and cause Electromagnetic interference problems. It's observed that resistance value representing losses after 20 MHz in taken measurements with the measurement device mentioned above again decreases rapidly. It's understood from Rp-frequency seen in Figure 3.24.

Mentioned Rp resistance is a parameter which represents losses of inductance with parallel resistance. It was plotted to understand that rapidly decreasing of Rp after 20 MHz frequency by plotting again impedance amplitude in addition to this result taken from the device of Impedance Analyzer has nothing to do with parallel resonance. The feature of inductance losses increasing at high frequencies provides to weaken well as a result of spike-shaped switching although it's through power loss path.

One of the features of iron powder based cores is that its linearity is very good as small distances between iron particles in extender creates an effect of scattered air gap. Cross-section of the core chosen in the thesis is about 1 cm^2 and toroid inner diameter is 1.6 cm, outside diameter is about 2.1 cm. In prototypes, wound numbers of L_1 and L_2 are 23 rounds and these round numbers provide inductance of 30 µH value. Relative permeability of construction material which is mentioned as mix26 in information notes is known as 75 in the information notes (PE-MAGNETICS) of producing company. It has been seen in the measurements that the value of relative permeability is about 70.

It has been observed from experimental observations that density value of saturation magnetic flux of the mentioned magnetic cores is so high that it can't be compared with Ferrites and it has been seen that this feature, relatively small core cross-section and consequently core volumes (when compared with ferrites) will be enough in the application.

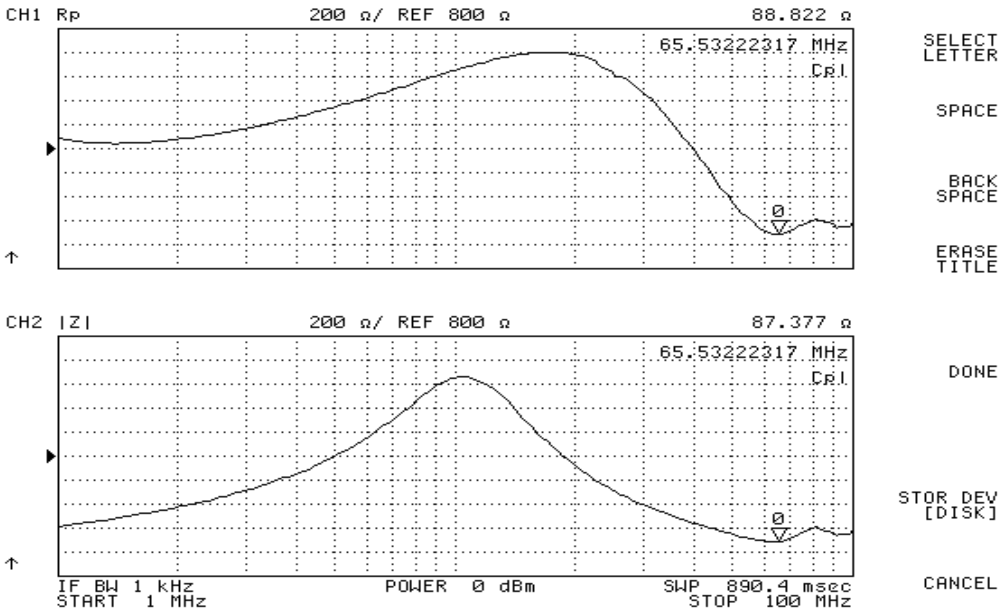

Figure 3.24. Changing of parallel resistance parameter of L_1 and L_2 inductances and impedance amplitude with frequency.

3.8 Comparison of Proposed Notch Filter and Classical LC-Filter in Terms of Economic and Volume Aspects

In this chapter, there will be the economic (from the aspect of element sizes, element costs) comparison of the classic LC filter with notch filter. As seen in Figure 3.25(b), notch filter contains a L3 inductance which doesn't exist in classic filter. But only ripple currents pass through the handle where L3 exists. The reason for this is that C1 capacitor stops the current component of f_c frequency. In whole of the thesis work, it will accepted that PWM modulating signal of f_c frequency is a sinus (the assumption made while PWM frequency spectrum is obtained). It will be seen in the proceeding parts of the report that ripple current form of mentioned L3 (Figure 3.25 (b)) is akin to triangular wave.

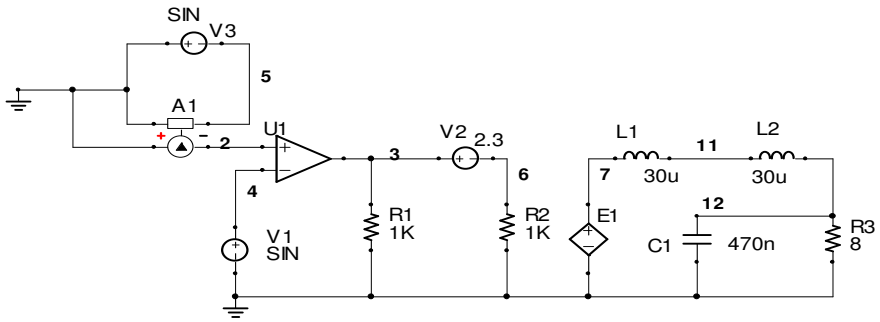

(a)

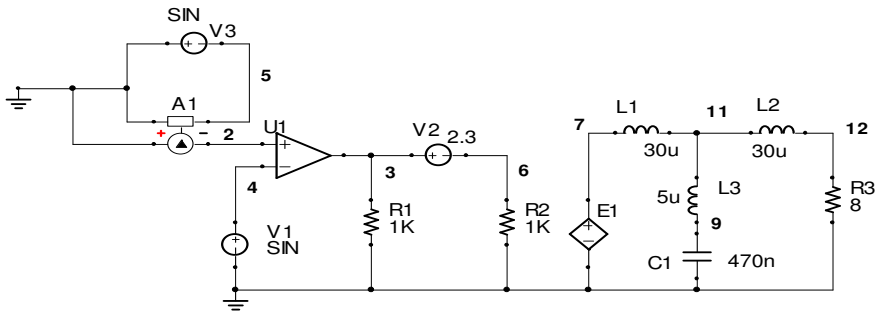

(b)

Figure 3.25. Switched amplifier circuit with classic LC- filter (a), amplifier circuit with notch filter (b).

On the other hand, peak value passing through L1 and L2 in the same prototype cab reach the value of 1.5A (for the values of modulation depth which is close to 1). Therefore, L1 and L2 core cross-sections should be chosen higher than the cross-section necessary for L3. Another reason of this is that L1and L2 values are higher than L3.

Let notch filter L1 and L2 core cross-actions be S_1 and winding numbers be (equal) N_1. Let L inductance core cross-section which comes instead of these in classic filter be S and winding numbers be N. Cores are chosen in the structure of toroid for both filters in the thesis so that voltage inductance of the emission which is transmitted as Electromagnetic by output stage of switched amplifier.

On condition that magnetic core material characteristic will be the same, size evaluation can be done as below for L with L1 and L2. Mentioned inductances will be the same in both filter types. Let the peak value of this current be I. To prevent cores from entering saturation, by thinking that p is a parameter determined by core material, the conditions of $p \langle N_1 \mathbf{I} / S_1$ and $p \langle N \mathbf{I} / S$ should be provided. Here $N_1 \mathbf{I}$ or $N \mathbf{I}$ is in the size of ampere. Let it be thought that it's worked in the saturation limit of the core for both filters. From here "$N_1 \mathbf{I} / S_1 = N \mathbf{I} / S$" can be written. This relation becomes simple in the form of "$N_1 / S_1 = N / S$". When L1 inductance existing in classic filter circuit is thought as being twice more than L1 inductance in notch filter for the purpose of comparison, L = 2 L1 is written and after that, if it's remembered that inductances are directly proportional to squares of winding numbers and cross-section, L = 2 L1 relation can be expressed in the form of "$N^2 S = 2. N_1^2 S_1$" . By combining this last relation with the relation found before above $N_1 / S_1 = N / S$, as a result "$S = (2)^{(1/3)} S_1$" or "$S \cong 1.25 S_1$" is obtained. Let it be accepted that inner and outer radius of toroid cores in classic and notch filters are equal and only their heights are different to be able to make a simple evaluation. In this condition, that can be said for core volume or weights. Instead of a core of 1.25 unit volume in classic filter, two magnetic cores each of which is 1 unit volume are needed. In addition this, switching amplifier circuit should contain a frequency tracking circuit to enable PWM switching frequency to be at full filter

notch frequency. The cost of parts of frequency control circuit suggested in the thesis is under 6 – 7 TL and when this circuit is added to amplifier plaque which should be, it's understood that the space that it will cover be less when passive elements and surface mounted (SMD) integrated circuit are used. It's understood from the simulations above that ripple performance which will be obtained will be very striking as well as cost increase which will be brought by the concept suggested in the project especially in magnetic monitoring applications where it's so important for ripple voltage to be low and in high-powered switched amplifiers.

3.8.1 Comparison of Proposed Notch and Classical LC-Filter in Terms of Ripple Reduction Effectiveness

Classical LC-Filter circuit performance in switching amplifiers may be sufficient but proposed Notch Filter gave much desirable results in our experimental work. However when the Figure 3.2 and Figure 3.10 are compared it is understood that classical filter give much more attenuation at very high frequencies.

When overall performance is considered however notch filter give less ripple distortion since it provides very much attenuation at switching frequency at which ripple voltage frequency has much more amplitude.

3.9 Evaluating Suggested Filter Performance Experimentally

A correct voltage which has been obtained by being divided with a potentiometer from a DC. Supply source has been applied to the input of the circuit which controls f_s frequency by breaking off frequency control loop of switched amplifier which is verified in laboratory. Ripple amplitudes are compared by choosing switching frequency f_s, f_o frequency of filter over and under about 10 kHz. PWM modulating signal has been chosen as a sinus wave of 1.5 kHz frequency taken from a signal producer. It has been found that f_o frequency of filter is at the value of about 104 kHz with good approximation with measurements.

In addition, L_r inductance by making it external to the circuit and C_r element by connecting parallel between 8 Ohms load ends chosen from a non-inductive resistance have been resorted to the condition of the known LC- low-pass filter. Recorded waveforms are as below:

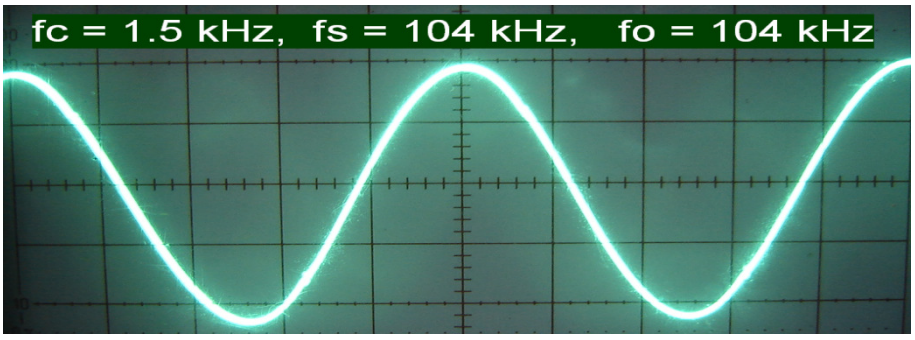

(a)

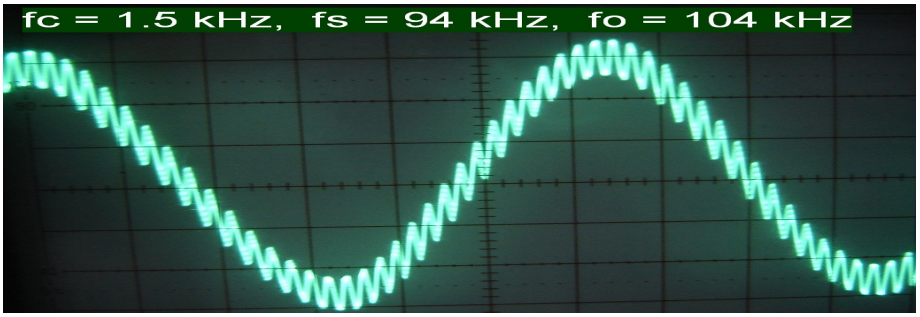

(b)

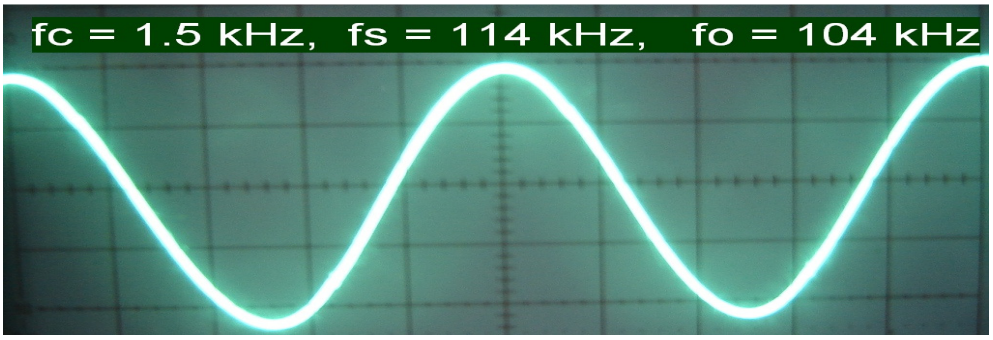

(c)

Figure 3.26. Waveform of load voltage, switching frequency equal to notch filter frequency $f_s = f_o$ (a), f_s, f_o below 10 kHz(b), f_s, f_o above 10 kHz (c).

It seen that notch filter from waveforms provides the condition of the highest performance as expected under the condition of $f_s = f_o$. Ripple voltage is higher in the condition of $f_s \ll f_o$.

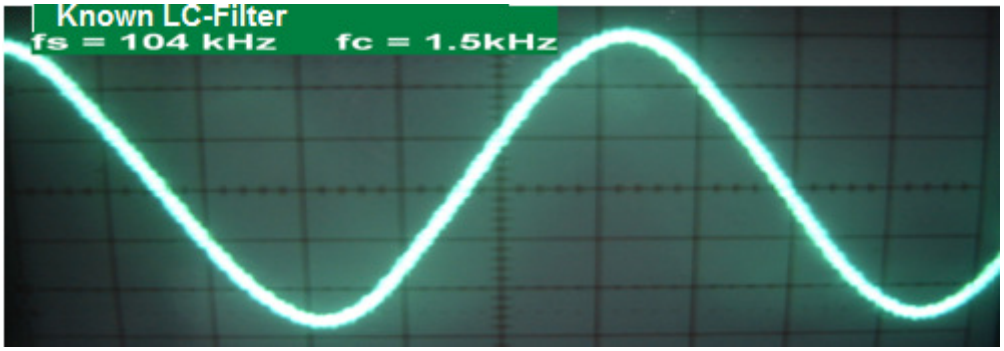

Figure 3.27. Output waveform when notch filter is replaced by the known LC- filter topology with the same elements.

It's understood from the Figure 3.27 that performance of LC- filter chosen in the applications almost as standard for switched amplifiers is quite under the condition in which $f_s = f_o$ is provided and with notch filter.

3.10 Ripple and Phase Correlation Methods

These methods are examined below by thinking that Ripple and Phase Correlation methods will be a good choice in the application of f_s tracking f_o with an analog control circuit.

3.10.1 System Control with Ripple Correlation Method

An application suggested for frequency control of an parallel type inverter having the purpose of induction heating (Karaca, 1991), has been summarized. As known, if switching frequency of parallel inverter f_s is equal to load resonance frequency (f_r), load current amplitude takes the lowest value and a study in which desired zero voltage switching is fullfilled. In Figure 3.28 below, main lines of the change of this type of load current amplitude of an inverter with f_s has been given.

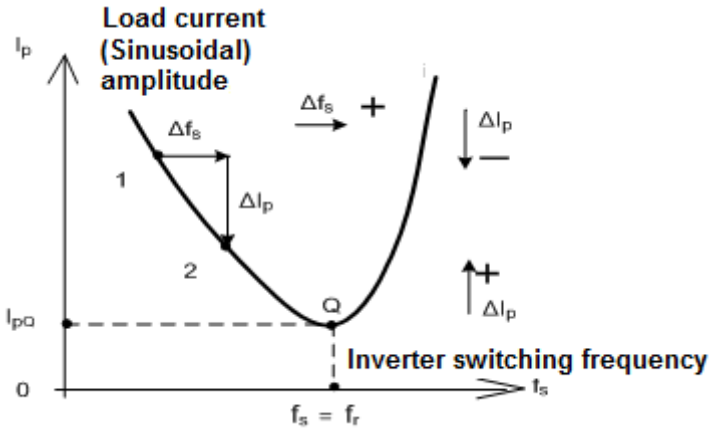

Figure 3.28. f_r Resonance frequency is the change of load comprised of a parallel resonance circuit with f_s driving frequency.

f_s is controlled by being watched with a digital circuit in the suggested application (Karaca, 1991). If when f_s is increased as much as Δf_s, the read I_p current is lower than its previous value, namely if ΔI_p current change is negative, f_s is increased once more (as much as Δf_s) and this condition continues until it's observed that ΔI_p starts to increase when f_s is increased. Working point of zero voltage switching is obtained in this way. But after reaching Q working point in Figure 3.28, the change of I_p is examined by changing continuously f_s a step further. Eventually, even if Q point seen in Figure 3.28 shifts (f_r is changing) because of various factors (for example, change in temperature of heated workpiece), this digital control system enables f_s to track f_r.

Although this basic approach is a technique which is known all along, it has started to get attention in power electronics circuits in recent years (Lymar, 2006),(Esram, 2006).

The method can be applied to a J(x) function or in other words, J(x) seen in Figure 3.29 can be applied between ranges of x_1 and x_2 in which it provides this condition.

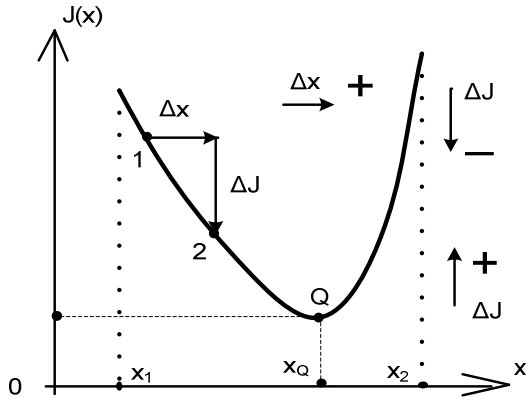

Figure 3.29. General form which J(x) system function ought to be in controllable range (x_1 – x_2) to be able to apply for the purpose of keeping J(x) function at minimum.

In the application given as an example in the beginning, it's seen that $I_p(f_s)$ corresponds to J(x) and x to f_s. It can be benefited from u(t) signal ,which is given below and obtained from the relation known as correlation control rule, as a control input which enables J(x) function to stay at the minimum value (Balog, 2002).

$$u(t) = -k\int_0^t \frac{dJ(x(\tau))}{d\tau}\frac{dx}{d\tau}d\tau \qquad (3.17)$$

It can be said that as ripple word which passing in the name of this method known as ripple correlation control bears the same name with the known switching ripple voltage or current, at first it makes difficult to understand the method. Working principle of the method for continuous systems which doesn't include switching can be understood from Figure 3.29 and the relation of (3.17). But in an application found in literature (Esram, 2006), it's seen that ripple signals which are input for the application of the method are provided by choosing ripple voltages emerging as a result of switching with high-pass filters. In other words, in some applications, it can be benefited from the ripple voltage which occurs as a result of switching that is also the target of this thesis to apply the method of Ripple Correlation Control.

The method can be applied by choosing peak value or average value of amplitudes in J(x) circuit in Figure 3.29 in switched power conversion systems. In the application example, induction heating given above is applied in the form of conversions at small intervals in switching frequency from outside for the aim of ripple control. There may not be any relation between ripple current or voltages which are existing in switched system and ripple amplitudes created for the purpose of control. This condition depends on implementation form of the method.

An interesting application of control method with ripple correlation has already been suggested in reference of (Lymar, 2006). Here, J(x) function seen in Figure 3.29 has been chosen the average of effective value of ripple voltage emerged as a result of switching. In this paper, the value of one of output filter elements of a switched power source is controlled in a way that output ripple noise will be the least.

This application which also includes an integrated circuit designed for the measurement of analog effective value chooses x amplitude, which is mentioned in the method, as switching frequency. Ripple amplitude of the method is chosen as a signal of much lower (500 Hz) frequency than switching frequency.

This ripple voltage which is created by an integrated circuit (a different signal from ripple voltage which will be as a result of switching) modulates switching frequency. In other words, ripple which is necessary for the method is formed outside and the value of f_s frequency is modulated by this sinus voltage. $u(t)$ control voltage seen in the relation of (3.17) presented in this application changes the value of a filter inductance over orthogonal control winding. So, by taking effective value average of ripple voltage composed -as a result of switching as J(x), the value of a filter element is controlled in a way that it will be at the least value. This application seems to be similar with thesis work studies and its aim. It's tried to decrease much switching ripple voltage by keeping notch filter attenuation, which is chosen as switching frequency in the thesis, at a point that will be the highest.

3.10.2 System Control with Phase Correlation Method

It was later realized that the method above (Lymar, 2006) suggested for switched power sources is not suitable for the thesis work. Ripple signal frequency applied to the system from outside for the purpose of control in the literature above has been chosen around 500 Hz (f_s is modulating the value with a sinusoidal signal at this frequency). Component filter at this frequency which can exist in the signal that will be amplified will change the spectrum of PWM signal and this may cause control circuit to produce a frequency with more or less mistake. Experiments show that this prediction is correct.

For this reason, Phase Correlation method (Balog, 2002) has been adopted to control f_s frequency in the form that will be $f_s = f_o$.

Vo/V_i amplitude characteristic of notch filter and phase characteristic of filter center node voltage (V_r) are seen in the simulation result given in Figure 3.30. Sharply changing of (V_r) phase at 180º in notch filter can make phase correlation method successful.

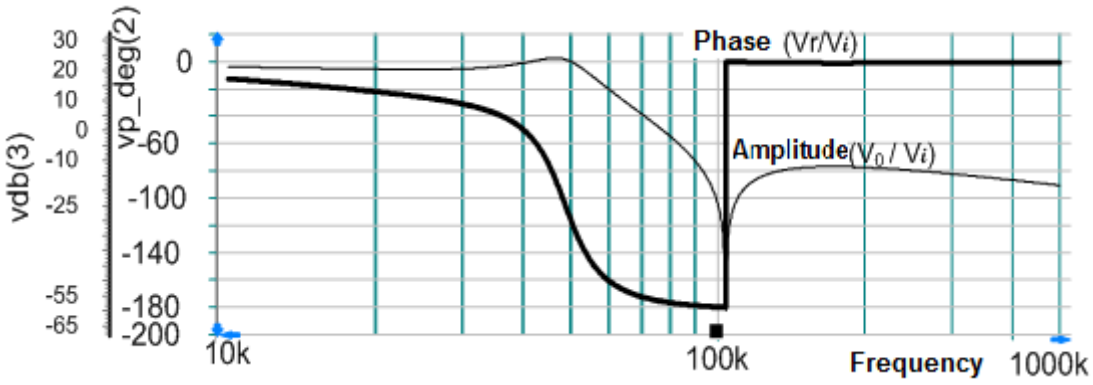

Figure 3.30. Notch filter I (V_o/ V_i) I and {Phase (V_r / V_i)} frequency characteristics, it's the simulation result of values of selected elements in prototypes.

In addition, the value of {Phase (V_r / V_i)} being at -90° in f_o notch frequency can abbreviate frequency control circuit to a certain extent. For example, if phase

difference at this frequency was 0°, -90° phase shifter of a circuit would be needed to add to the control circuit.

{Phase (V_r / V_i)} value which is necessary for phase correlation method is obtained by multiplication and subsequent filtering. But V_r and V_i aren't sinusoidal signals. In addition, there are many components at the same frequency in them. To be able to apply phase correlation method in this type of applications, it's suggested to benefit from a sinusoidal oscillator (at f_s frequency) in the related publication (Balog, 2002). In the thesis prototypes, this sinusoidal signal is comprised of V_i which is PWM signal with FCC technique.

Block diagram given in Figure 3.31 shows the adaptation of phase correlation method in the thesis.

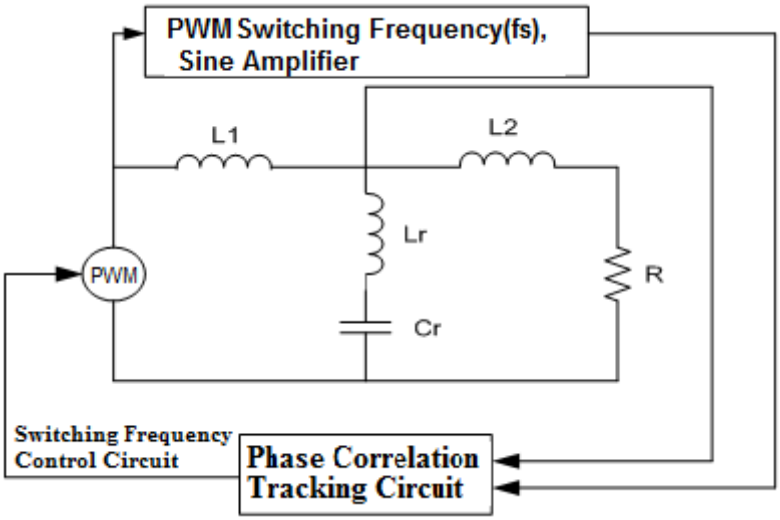

Figure 3.31. Block diagram of phase correlation monitoring circuit and PWM switching frequency simplified to control.

Phase correlation tracking circuit is based on this result which is realized with multiplication circuits in the experimental work. Let a sinusoidal signal of f_s frequency be applied to one of a multiplier circuit inputs and a signal in which contains many sinusoidal components to the second input. When the output of multiplier circuit is filtered with a low pass filter, only the correct voltage will

emerge at the filter output. Amplitude of this correct voltage will contain the information related to phase difference between sinusoidal component of f_s frequency from the components existing and the other sinusoidal signal. If the mentioned phase difference is -90˚ and this is the case under the condition of $f_s = f_o$, average value of the output of multiplier circuit will be zero. This is the output point of adapting to thesis prototypes of phase correlation method. This averaging process is provided with an integrator circuit and either f_s is changed or f_o can be changed for the condition of $f_s = f_o$ with an integrator output.

3.11 Shifting Filter Frequency Characteristic with Controlled Inductance

To change the value of an inductance which is wounded on magnetic core by benefiting from nonlinear characteristic of the core is a technique that is known for a long time. Recently, it's seen that this technique is benefited in power electronics applications (Lymar, 2006), (Brandt, 1994). Inductance verification whose value can be changed electrically is based on stimulation of one of orthogonal windings wounded on the same core with the correct voltage (Polivka, 1983).

Pot-core type core structure which is seen in Figure 3.32 is quite suitable for verification of orthogonal windings. In this type of cores, a cylindrical cavity is left just from the centre as also seen from the figure and the coupling coefficient K between coils coiled in ferrite core with up-and-down movement of a cylindrical screw, which is made up of again ferrites and can be put here, can be changed.

An orthogonal coil can be wounded to the invisible coil in ferrite as seen in the figure instead of ferrite adjusting rod to this cavity. Two different inductances, which use only one core with these two coils but have no coupling among them electrically, can be verified (Polivka, 1983). But when the current passing through one of the coils magnetizes the core until it reaches the saturation limit, the other coil is affected and its inductance decreases. The current controlling inductance value is usually applied to the coil named as orthogonal coil seen in the figure. Mentioned correct current can be determined by a control circuit and is applied with a current source of

operational amplifier (Lymar, 2006). In this type of application schemes, a circuit with verified operational amplifier drives the orthogonal coil over a discrete transistor and there is relatively a power loss on this transistor. In addition, an important distortion may be said as it's worked in the region of core which cannot be accepted as linear because of characteristic of the method. So, it's resorted to control carrier frequency of PWM signal applied to the filter in the place which will slide the characteristic of filter's frequency by controlling one of them from filter inductance values in the thesis work.

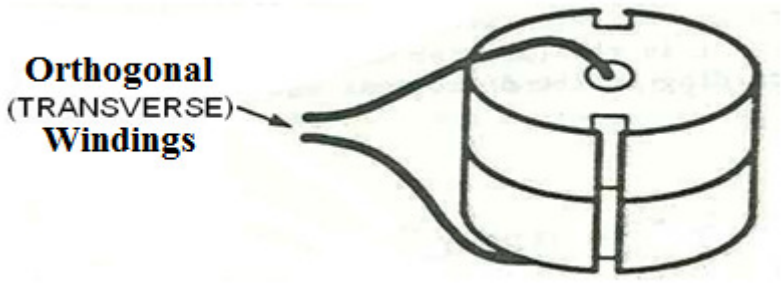

Figure 3.32. Magnetic core (pot-core type) and one of orthogonal windings, the other winding is not seen as it stayed inside of two-piece core.

This control has been made by transmitting a correct current to resistance element existing between reference and frequency control foot of integrated circuit from the output of control circuit in TDA7482, TDA7490 and the other similar integrated circuits which exists commercially. Mentioned resistance element determines the current of a current source in the integrated circuit. This current source fills a capacity element which is again connected to integrated circuit from outside and f_s frequency sawtooth voltage emerges by being discharged at once with a transistor in integrated circuit when ramp-shaped voltage comes to a certain level. The method shown in Figure 3.33 is thought and experimented for verified thesis prototypes and TDA7482 and TDA7490 integrated circuits. When it's seen that the result is successful, it has been applied to all integrated circuits and all the verified prototypes. As known in literature, frequency control isn't mentioned with this

method. It's resorted to slide frequency of filter characteristic with orthogonal coil which has been examined in the applications seen in literature, mostly in this report (Lymar, 2006), (Balog, 2002).

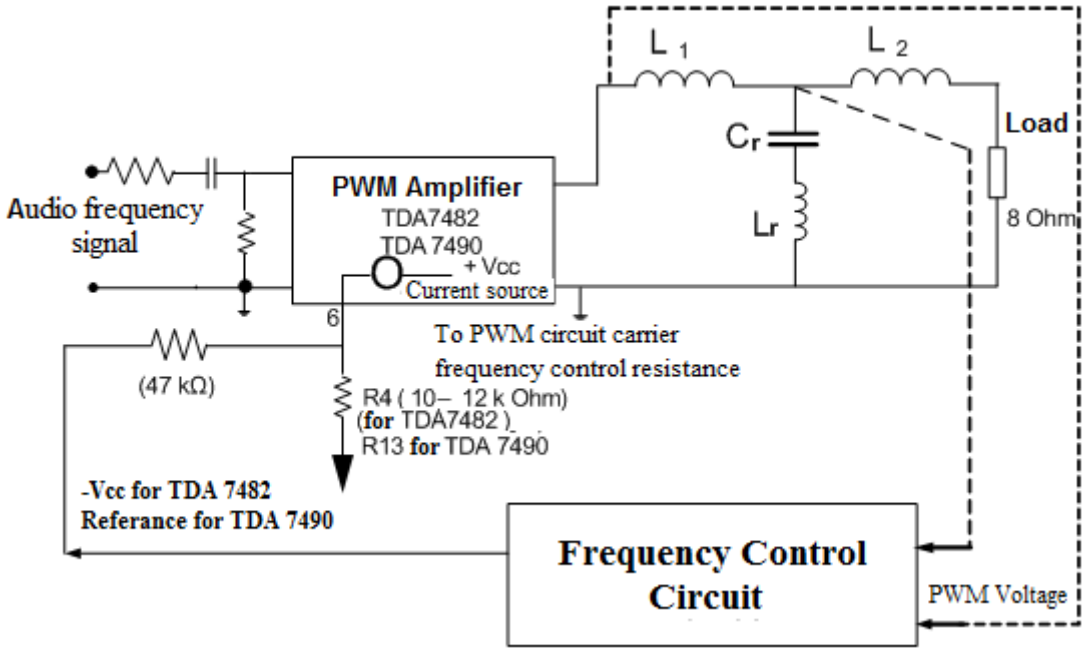

Figure 3.33. Tracked path in thesis prototypes to equate ω_s frequency of PWM with ω_o notch frequency of filter.

3.12 Necessity of Frequency Control Circuit

Frequency control circuit enables to equate f_s frequency of triangular or sawtooth wave to be equal to f_o frequency of notch filter. Change of working conditions especially temperature, change of parameters with time circuit elements, change in supply voltage of the circuit makes frequency control circuit indispensible. When switched amplifier with notch filter was first started to work, even if $f_s = f_o$ is obtained with tuned elements, this equality may not be maintained with the factors mentioned above. On the other hand, in condition that this equality isn't obtained from Figure 3.30, it's understood that even LC filter performance can't be attained from the characteristic of notch filter.

For this reason, by producing a control voltage with frequency control circuit, either Lr inductance value in the filter is controlled by an orthogonal coil or f_s frequency $f_s = f_o$ condition can be obtained by injecting a small correct voltage to the node which determines frequency of integrated circuit producing PWM with this control voltage. The second method is preferred as it's easier to apply in the thesis work. Control circuit(Figure 3.34) is designed in such a way that it will rely on Phase correlation method which has been studied in this report.

One of circuit inputs is PWM signal in the filter input. This signal is converted to a square wave of f_s frequency with the help of a FCC circuit. Then this square wave is brought closer to f_s frequency sinus and an analog circuit which is verified with operational amplifier. It has been seen that sinus signal generated from experimental observations is quite pure. The reason not to try to obtain sinus signal of f_s frequency directly from PWM signal is that amplitude of the basic component in square wave is bigger and fixed. FCC circuit which is verified for this purpose contains CD4046 integrated circuit and LM311 integrated circuit. This circuit provides possibility of a phase shift which can also be adjustable with potentiometer. It has been understood that phase shift feature (Karaca, 1996) is necessary to be able to meet effects which can arise from finite bandwidths and delay of elements in the circuit although it's at a small extent.

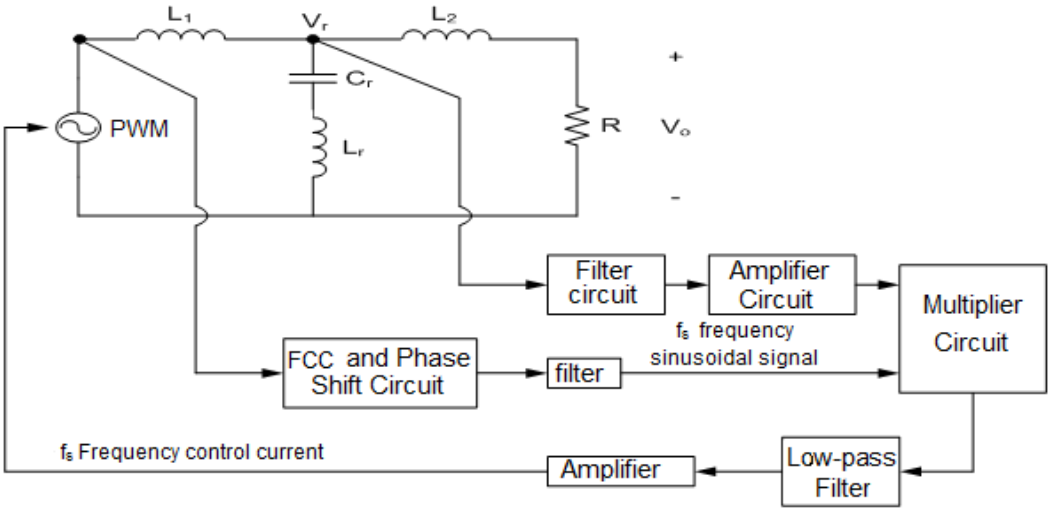

Figure 3.34. Block Diagram of designed frequency control circuit. The whole circuit can be interpreted as a Multiplier type PLL circuit.

There is the component of f_s frequency which is attenuated by notch characteristic as well as component of many frequencies in V_r which is the other input of frequency control circuit. As control circuit will benefit from phase of this component, sinusoidal signal of f_s frequency in it will be provided to be amplified by amplifying and making V_r pass through passive band-pass (50 kHz – 150 kHz) filters. This obtained signal and sinusoidal signal of f_s frequency is multiplied by benefiting from AD633 integrated circuit. Multiplication sign is filtered with low-pass filter and amplified. Instead of benefiting from an analog integral receiver circuit, this method has been followed. The reason of it is that because of finite bandwidth of amplifiers which is included by integral receiver circuits in fact for the signals which change very slowly, it will show the behaviour of an active low-pass filter (Karaca, 1999).

3.13 Control Circuit of PWM Signal Frequency

Sinus generator circuit with designed PWM switching frequency is seen in Figure 3.35 (a). Input of the circuit is PWM signal and this signal is applied to a FCC circuit. This circuit (FCC) is also a circuit of digital signal phase shift and this is suggested in literature (Karaca, 1996). In FCC phase shift circuits which is mentioned frequently in literature, phase shift is provided by adding a DC signal (with operational amplifier circuits) to the control signal in FCC. PLL circuit which is created by integrated circuits produces square wave in switching frequency. Stages (filter and amplifier stages) comprising of operational amplifiers (LM318) and passive elements following this (RC) make square wave signal approach to sinus signal at the same frequency quite well. A signal of the same frequency resembling to sinus can be formed from PWM signal without initial PLL circuit. But as amplitude of basic component in square wave is higher, this method has been followed in the thesis for a signal which resembles to sinus more.

A verification of ripple correlation monitoring circuit is given in Figure 3.35. Voltage (V_r voltage) taken from the middle node of notch filter passes through amplifier circuit and RC filters designed with values which will pass frequencies around 100 kHz.

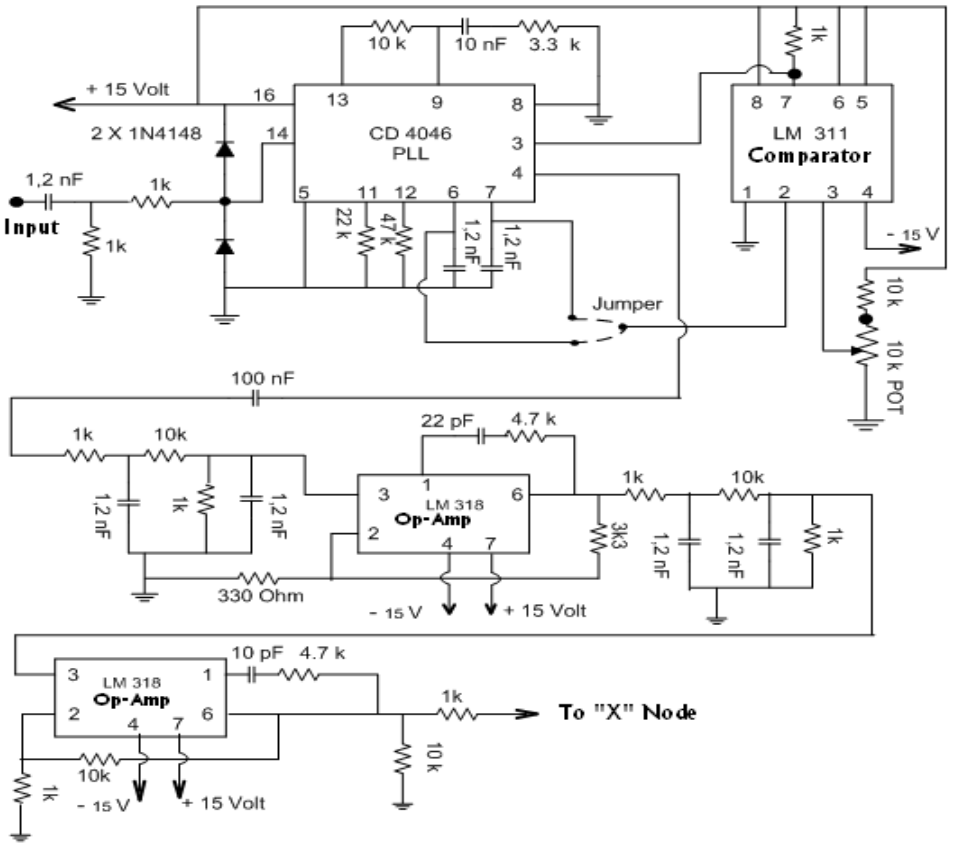

(a)

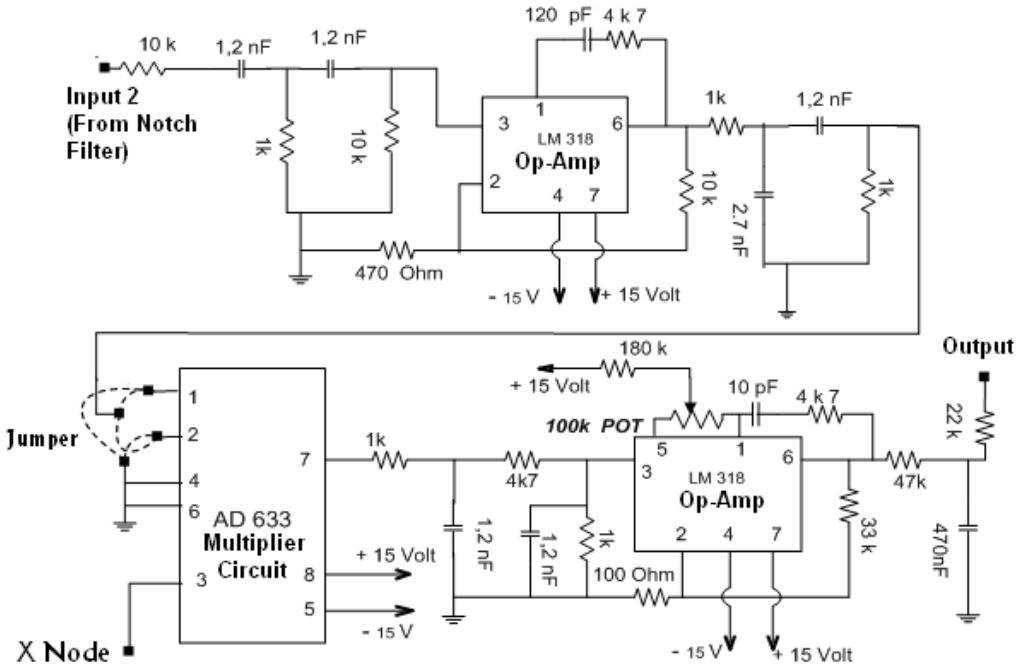

(b)

Figure 3.35. The first page of frequency control circuit diagram realized and tested (a), second page of it (b).

Output of this circuit which can be thought as a narrow band amplifier and LM381 verified is applied to input of AD633 multiplier circuit. The produced f_o sinus signal is connected to the other input of multiplier circuit. Output of multiplier circuit is applied to low pass filter circuit.

V1 source in the circuit seen in Figure 3.36 below models switched amplifier output antecedent to filter in the physical circuit. In other words, it's a PWM signal. It's not possible that phase correlation control method can produce correct control voltage with application of V1 source to control circuit in this application. The reason of it is that PWM forms again components at many frequencies in number 2 node which can be said to be midpoint of filter of component of many different frequencies in PWM. If number 2 and 4 nodes of circuit in the figure are applied to the input of a control circuit filter by multiplying voltages, the output of filter is created in the form of average total of many multiplying components. Another factor which makes the method more impossible to apply is that the amplitude which emerges by multiplying f_s frequency voltages from mentioned multiplication components is normally much lower than the amplitude of other components. After applying a sinusoidal signal whose frequency changes to notch filter circuit (Figure 3.36, V1 input) and filtering the output which wiil emerge bu multiplying it with the voltage at no. 2 node of filter seen in the same figure, K will be fixed K. It's seen from number (37) relation that it will appear in the form of $Cos\ (-\phi)$. Here, ϕ 2 and Number 4 node voltages are phase difference.

As well as benefiting from sinusoidal signal of f_s frequency formed with filtering and FCC technique from PWM signal in the thesis control circuit (Johns. D), it's applied as a sinusoidal source which produces V1 pure signal in the results and simulation circuit in Figure 3.36 (a). Frequency of this signal is changed between 10 kHz and 500kHz and it's composed with the expression of cos [- Ph(V2*V4)] which is written in simulation programme of output graph.

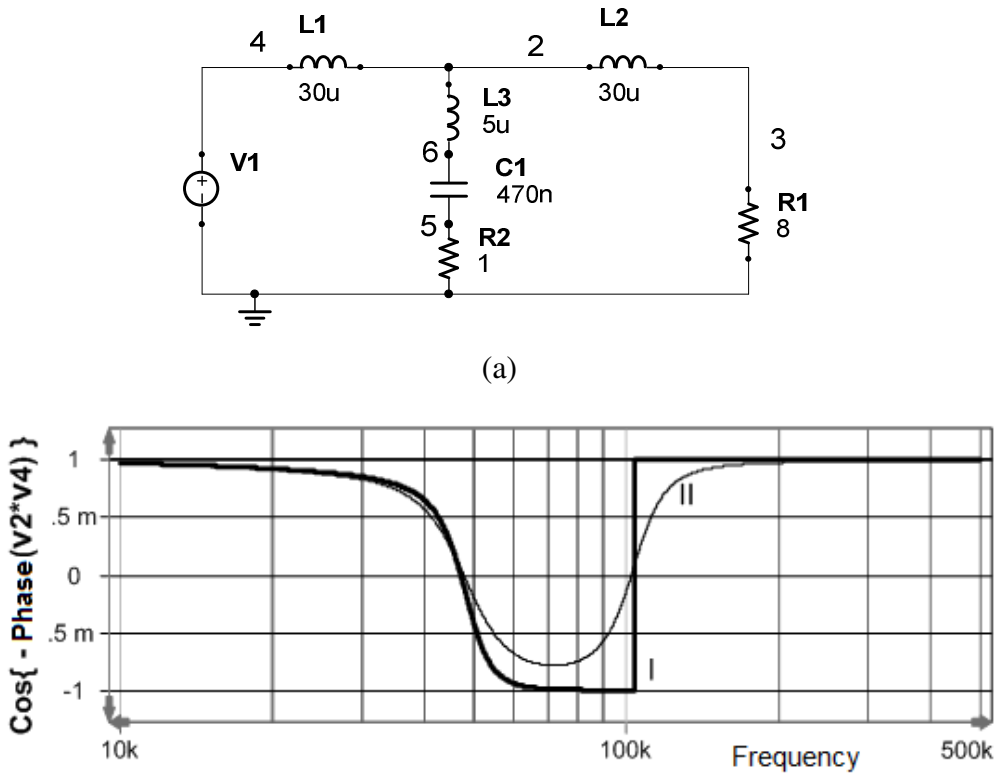

Figure 3.36. Simulation circuit for filter phase correlation (a), changing of output calculated by the correlation of cos [- Ph(V2*V4)] with frequency, condition of I : R2 = 0 and II: R2 =1. R2 resistance seen in simulation circuit falls against the r resistance passing in transfer functions.

As remembered, this expression has been obtained by writing 1 for the purpose of simplification instead of (1/2) K term in the relation of (2.37) mentioned before. R2 resistance seen in simulation circuit is connected to investigate the effect of parallel arm losses which is in the middle of filter that creates notch characteristic of FCC method performance benefited for frequency control.

Obtained simulation result is seen in the Figure 3.36. It shows that the method will work even for the condition of R2=1 Ohm which seems quite pessimistic for prototype circuits of R2 resistance which represents the losses of L_r and C_r carrier frequency of PWM signal can be controlled with a loop benefiting from the characteristic seen in Figure 3.36(b). The loop can be applied to PWM integrated circuit in a way that the frequency which cuts 0 axis Figure 3.36(b) will be switching frequency of the signal. Since there are two points (approximately 37 kHz and 103

kHz) that provides this condition as will be seen from the figure, 103 kHz in which filter notch attenuation characteristic occurs should be selected as operating point. FCC circuit which produces sinusoidal signal at f_s frequency from PWM signal gives out at least 60 kHz frequency output. So, control cycle is enabled to carry operating point of prototype to the point of 103 kHz frequency. The average of multiplication process is zero at this frequency as seen from Figure 3.36 and the signals of outputs at both sides are different. Control loop can be completed by connecting over a big resistance in a way that integrator output will inject current to the frequency control resistance (integrated circuit is connected from outside) of integrated circuit that produces PWM by applying multiplication process to an integrator circuit input instead of a low pass filter.

Because of finite open loop gain of operational amplifiers, it can be shown that operational amplifiers verified with an integrator circuit can be modeled in fact by cascade connection of low-pass filter and amplifier circuit.

CHAPTER FOUR
SIMULATION WORK

4.1 Comparison of Notch Filter with LC Filter in a Simulated Environment with Element Values in Prototypes

Transient simulation results of circuits seen in Figure 4.1 below done with B2 Spice have been obtained for the purpose of being able to evaluate efficiency of Notch Filter suggested in the thesis with simulation. Classic Switched Amplifier seen in Figure 4.1(a) contains LC filter circuit. When L1 and L2 inductances are thought as one inductance whose value is 60 μH in this circuit, C1=470 nF and R3=8 Ohms creates the known LC filter.

Although filter input signal, PWM parameters and signal levels are all chosen as the same in the circuit of the same figure (b), only the topology of output filter is changed. Equivalent L inductance whose value is 60 μH is changed as seen in Figure 4.1(b) with two inductances whose values are the same (30 μH) and there is no magnetic coupling between them. Suggested notch filter is created by connecting parent node of filter capacitor to the node where L1 and L2 inductances are connected to each other.

PWM carrier frequency in all the simulation circuits here is taken as 103.6 kHz which is notch frequency of the suggested notch frequency. In addition, modulation depth is chosen as M = 0.8 and peak value of PWM signal is taken as 12 V. Modulating signal frequency is chosen as f_c=1 kHz.

Voltage in the ends of load resistance seen as R3 in simulation circuits is given in Figure 4.2 for both of the circuits. Time intervals in which simulation is made are chosen the same and simulations are shown from 500 μs so that the first transient waves which will appear when the circuit is first run (also present in the application) won't make the comparison difficult. As can immediately be seen from the

comparison of Figure 4.2(a) and Figure 4.2(b), notch filter provides a better ripple attenuation.

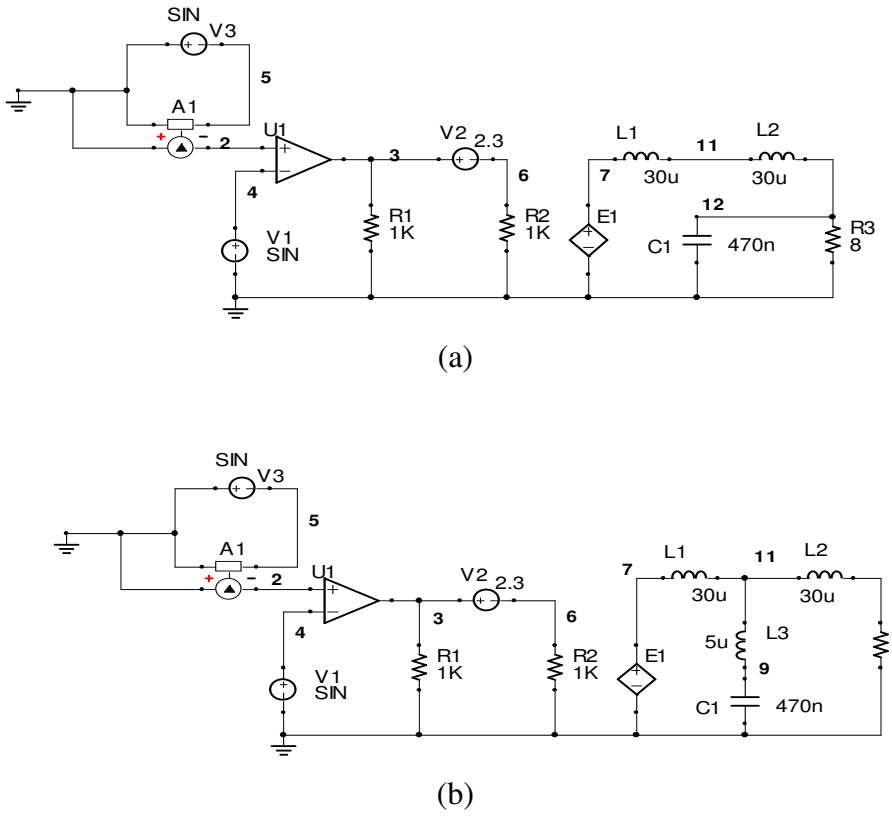

Figure 4.1. Switched amplifier circuit with classic LC- filter (a), amplifier circuit with notch filter (b).

Another point that takes attention is that activity of voltage of output waveform of notch filter increases more around zero crossing. Classic filter becomes more active in regions close to peak values of output signal than relatively zero crossing region of its own signal. The cause of this view can be explained from PWM spectrum. Amplitude of f_s frequency component is high in PWM spectrum at low voltage levels of modulating signal while other upper frequency amplitudes are relatively low. When modulating signal amplitude or modulation depth is increased, carrier frequency component in PWM spectrum isn't anymore as high as it was when compared with the other upper carrier harmonic frequency components. Notch filter provides its highest attenuation in notch frequency (PWM carrier frequency has been chose in these simulations, $f_o = f_s$). There will be a limit in which attenuation of

classic filter will be better at upper frequencies of the carrier than notch filter. The reason of it is that notch filter attenuation slope is increases with frequency 20dB/decades (because of L2 and R3 resistance) and this slope in classic LC filter is L (L = L1 + L2) and 40 dB/decades because of C1 capacitor .

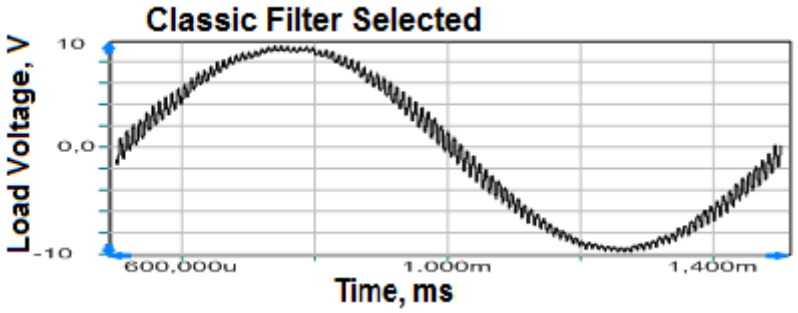

(a)

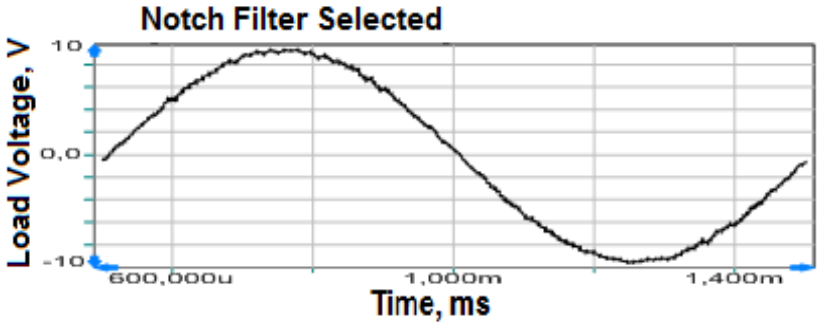

(b)

Figure 4.2. Simulation result of output voltage of classical filter (a), simulation result of output voltage of notch filter (b), simulation time period is chosen as 0.5 ms and 1.5 ms.

The result given below in Figure 4.3 are taken by admitting chosen time intervals given in Figure 4.2 above between 0.98 ms and 1.02 ms. These figures give information about the comparison of ripple amplitudes around zero crossing of output signal with ripple waveforms which both filter topologies give. In these figures, it should be taken into account that scaling of vertical axis is different for both conditions.

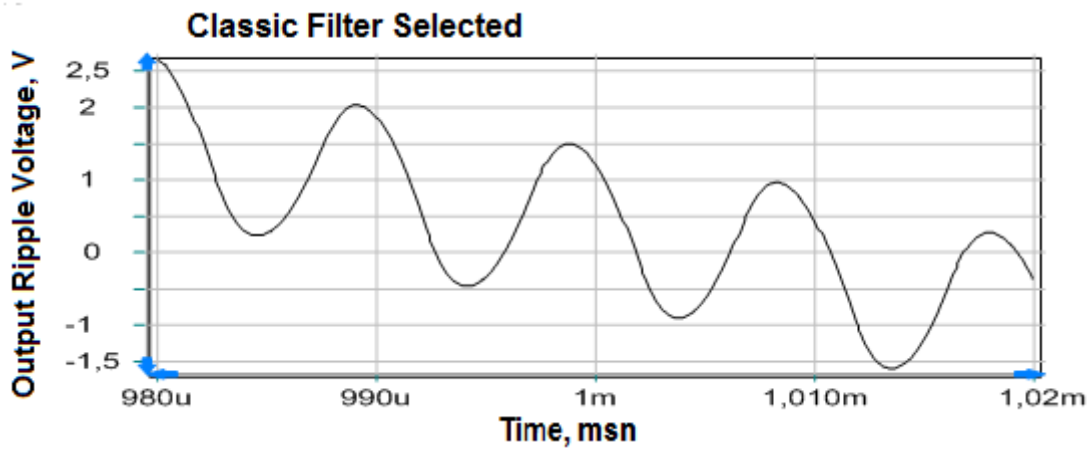

(a)

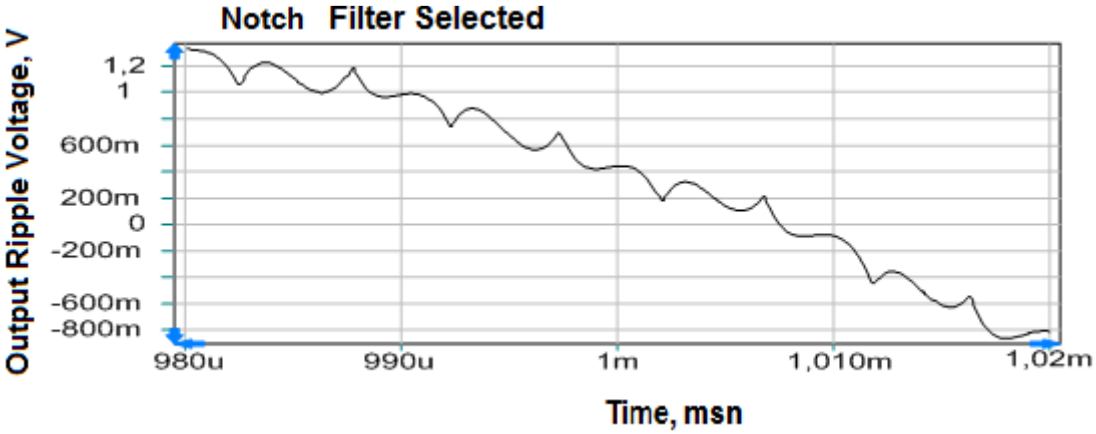

(b)

Figure 4.3. Simulation waveforms whose level of output signal is taken around zero, for classical filter (a), for notch filter (b).

4.2 Simulation Circuit of Verified Frequency Control Circuit

As a new filter circuit has been suggested by leaving the filter on which worked in previous periods of the work, frequency control circuit should also be changed. For this reason, simulation circuit has been changed. The new simulation circuit has been designed also in B2 Spice simulation programme which has been used. Obtained PWM signal is then applied to the filter input.

There aren't models of CD4046 PLL integrated circuit although there is an integrated circuit which is quite mature and well known. For this reason, square wave signal whose Duty – Cycle values is 50% and it has switching frequency is provided with the additional circuit which has U2 comparator in it. It can't be reached to triangular wave which is benefited for PWM from the outside of integrated circuit in switched amplifier integrated circuits of today. For this reason, it's benefited from an additional FCC circuit in verified prototypes. But as both it's not possible to reach aforesaid triangular wave signal in simulation circuit and there is no modelling, output signal in Figure 4.4 of FCC integrated circuit has been created at the ends of E2 controlled voltage source in simulation circuit. This square wave signal is converted into a pure sinusoidal signal of f_s frequency between the ends of R17 resistance by amplifying and filtering with successive layers.

This sinusoidal signal has been applied to the input of an analog multiplier circuit. The signal taken from the middle node (Figure 4.4, number 8 node) of switched amplifier output filter suggested in the study is applied to the other input of multiplier circuit again by amplifying and passing it through analog signal processing filter. A high-pass filtering is also needed as PWM has its modulating signal which is wanted to be taken (only this signal is wanted to be in the ideal condition) from switched amplifier output and there is much more bigger amplitude that other components on the mentioned middle node. C6, C7 which exist in the circuit and resistances connected to these provide aforesaid high-pass function. Mentioned High-pass filter function isn't necessary theoretically. The reason of it is that a sinusoidal is applied to the other input of multiplier circuit. This low frequency component which exists only in one of the inputs won't affect in the voltage which occurs when multiplier circuit output is filtered. But this modulating signal component with mentioned relatively big amplitude trails X3 operational amplifier seen in the Figure 4.4 to saturation. For this reason, high-pass filtering circuit is needed for the purpose of processing the mentioned signal. Cutoff frequency of this filtering has been chosen approximately 20 kHz by assuming that upper frequency limit of the modulating signal will be around 20 kHz. As output filter which is suggested in the thesis and comprised of L1, L2, L3, C1 and load attenuates ripple

amplitudes well and ripple component amplitude of f_s frequency, which is wanted to be applied alone to the input of multiplier circuit in the ideal condition, is quite small. For this reason, block gain which contains verified X3 with LM318 integrated circuit has been kept as high. Multiplier circuit output has been applied to A1 oscillator control input with E5 controlled voltage source path after a low-pass filtering circuit.

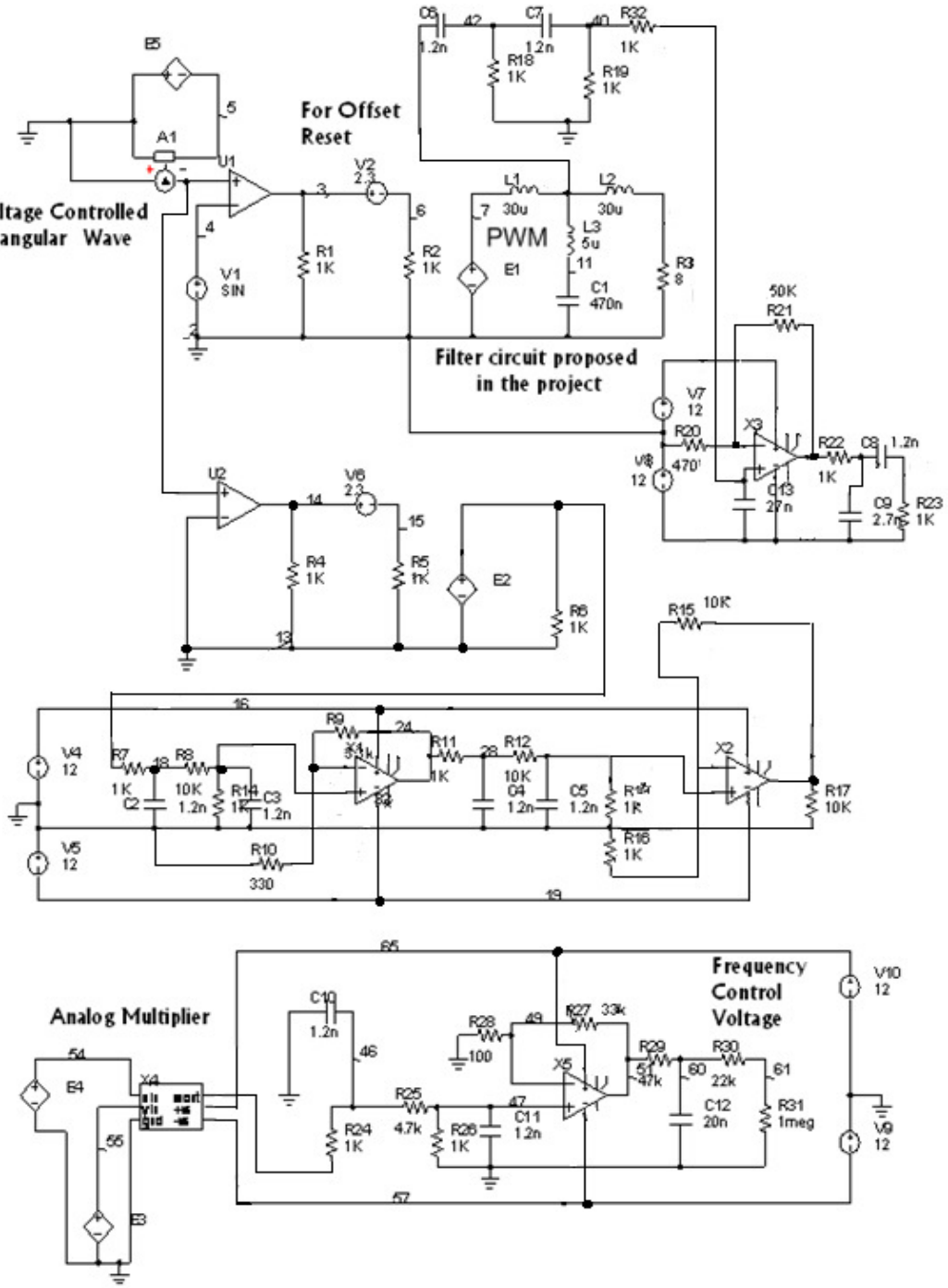

Figure 4.4. Simulation circuit of verified frequency control circuit.

All the operational amplifiers are in the type of LM318 in prototypes and simulation circuit (amplifiers named as X by the Programme). Multiplication circuit output has been amplified with X5 after being filtered again in a way that low frequencies will pass. A problem met in prototypes is that there can be an offset voltage of X5 integrated circuit in simulation circuit in real application. This causes f_s value of switched amplifier to be produced not exactly at notch frequency of output filter but a little bit above or below of it which contains an adjusted resistance has been connected to offset adjusting feet of X5 integrated circuit for the solution of this problem in prototypes. Once this resistance is set with the help of oscilloscope, there is no need to change it again. As offsets can be chosen as zero in the programme in simulation circuits, mentioned adjustment circuit hasn't been verified in simulation.

4.3 Simulation Results of Prototype Amplifier

Evaluation of prototype amplifier and especially filter ripple performance has been made with established simulation circuit. Starting switching frequency from the wished value has been enabled in simulations by assigning different values to C12 capacitor initial voltage in the section which produces frequency control voltage in simulation circuit.

Simulation results have been given in Figure 4.5 and the voltage on output load has been demonstrated with frequency control voltage in these results. When control voltage reaches the value of zero in the simulation circuit, $f_s = f_o$ equality is reached. In the first of simulation results, starting voltage of V= +10 Volt has been assigned to C12 capacitor as initial condition. f_o parameter of filter is at the value of about 103.6 kHz. f_s with initial voltage which has been given starts from the value of 60 kHz. Obtained simulation graphic is seen in Figure 4.5(a). At first, ripple distortion in amplified signal at the output is very high and after about 1 ms, ripple component decreases quite with approaching of f_s to f_0 value. But only this part of the figure won't be enough to prove the performance of suggested filter. The reason of it is that as f_s increases, frequency of components in ripple increases in this condition and

eventually attenuation of filter increases, as well. In other words, as time goes on in Figure 4.5(a), decrease of ripple distortion is provided by both factors.

For this reason, a second simulation graphic has been formed in Figure 4.5(b). This graphic has been obtained by choosing C12 capacitor voltage starting condition as - 10 Volts. f_s starts from the value of 200 kHz with the starting condition given to the circuit. As can be seen from this graphic, as time control voltage approaches towards zero and this shows f_s approaches to the value of f_o = 103 kHz, ripple distortion is a little bit improved. But this is an important result and f_s value, ripple distortion which will occur in chosen condition of 200 kHz is provided when it also takes the value of f_s, 103.6 kHz.

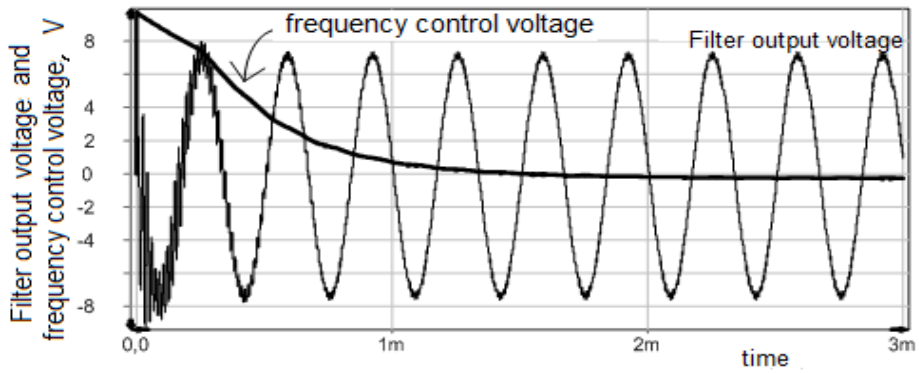

(a)

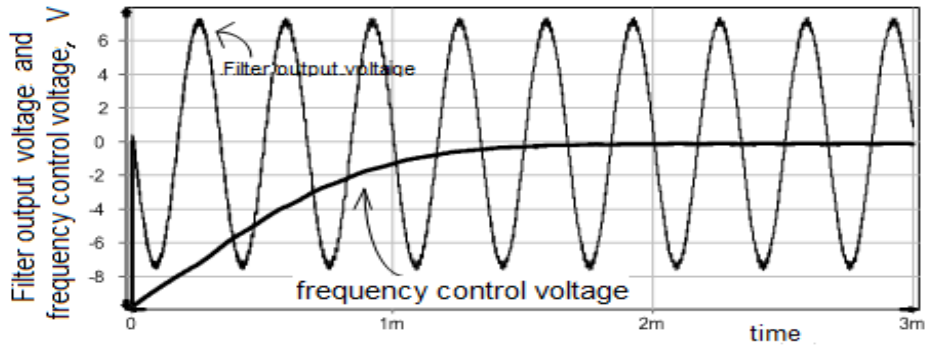

(b)

Figure 4.5. During the reach of PWM's f_s frequency from 60 kHz to $f_o \approx 104$ kHz value, simulation of amplifier load voltage (filter output voltage) (a), during the reach of f_s 's value from 200 kHz to $f_o \approx 104$kHz, simulation of amplifier load voltage (filter output voltage) (b).

As a result of simulation, ripple performance of f_s value which will be obtained is provided in the condition that f_s is twice more with suggested notch filter which becomes equal or very close to f_o frequency. So f_s value doesn't need to be high from the aspect of ripple performance. As known, choosing f_s as low decreases the average value of switching losses. This will increase the efficiency of amplifier and eventually performance of amplifier and notch filter will have been increased.

CHAPTER FIVE
MEASUREMENT AMPLIFIER

5.1 Measurement Amplifier Design for Experimental Work

Input resistance of input terminals (R/A/B) of 4395A Spectrum/Circuit/Impedance analyser device is 50 Ohms. It's understood that output resistance of sweep oscillator of the device is fixed as 50 Ohms according to high frequency techniques. The circuit is directly driven from sweep oscillators and reading is done from R/A/B inputs in the practice of measurement of characteristics of two-port networks in device's application notes. 4395A that can be considered to have low-frequency (upper frequency limit is 500 MHz) in its class is designed according to the technique above which is used in high frequency measurements. In other words, two-port networks that will be tested is driven by a source of 50 Ohms output resistance and the signal taken from output port is applied to one of the input terminals (R/A/B) of 50 Ohms input resistance. It's understood that Bode characteristics are measured in this condition at high frequency measurements. When upper limit of frequency for measurements is seen enough up to 10th harmonic of PWM switching frequency, it can be said that remaining under 2 MHz will be suitable. It has been thought that protrusion of Bode diagram in the conventional sense can be done by making reading with a measurement channel whose input resistance is very big and by driving impedance with a very small source for this upper frequency limit. Internal resistance of the device which will be tested is provided through the help of measurement amplifier which is planned to be driven with a small source. In reading process related to the device which will be tested, it's benefited from 418000A active probes which is suitable for this device and also a product of the same manufacturer (Agilent). These probes charge about 100 kOhms the loop to which it's connected but terminal resistance of probe which is connected to 4395A device (Figure 5.1) is 50 Ohms output resistance. A measurement amplifier is necessary to acquire Bode diagrams of thesis work filters in accordance with driving with known low impedance and reading technique with high impedance input filter. In a survey, it's seen that there is no commercially available amplifier which is suitable for this

purpose. In addition, it's seen that prices of the ones that will be made suitable for the purpose with a wideband transformator start from a few thousands USD. For this reason, measurement amplifiers with different earnings are verified benefiting from AD815 integrated circuit of Analog Devices Company. These verified amplifiers take place in measurement setup seen in the Figure 5.1.

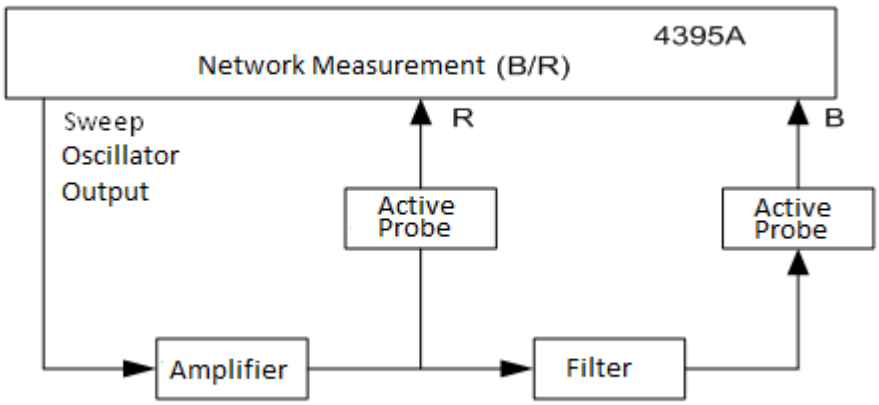

Figure 5.1 .Measurement setup of filter Bode diagram, (input impedance of active probes is 100 kOhms, output impedance is 50 Ohms).

Input resistance of prototype measurement amplifiers is 50 Ohms, output resistance is designed under one Ohm value. An important advantage of measurement with amplifiers is that it provides to make measurements with amplitudes of about 10 Volts instead of signal amplitudes which sweep oscillator is at most 1 Volt. With this approach, it will be provided that nonlinear characteristics of filter magnetic elements (which will appear in real applications) will rebound to measurement results. Another reason which makes important doing filter measurements as buffered with amplifier as seen in Figure 5.1 is impedances of filter input and output whose inductive value is high. In case that filter is directly connected to measurement device, it's thought that there is a possibility that inductive currents destroy input of measuring channels with output of sweep oscillator of 4395A Network device. For the same reason again, freewheeling diodes are connected between (+) and (-) feedings and output loop of verified measurement amplifier. So, filter input which is highly inductive is avoided to make output transistors of amplifier break down. Circuit drawing of measurement amplifier has

been shown in Figure 5.2 and D1, D2, D3, D4 diodes seen in this drawing are chosen in the type of 1N4148 and they are mentioned freewheeling diodes.

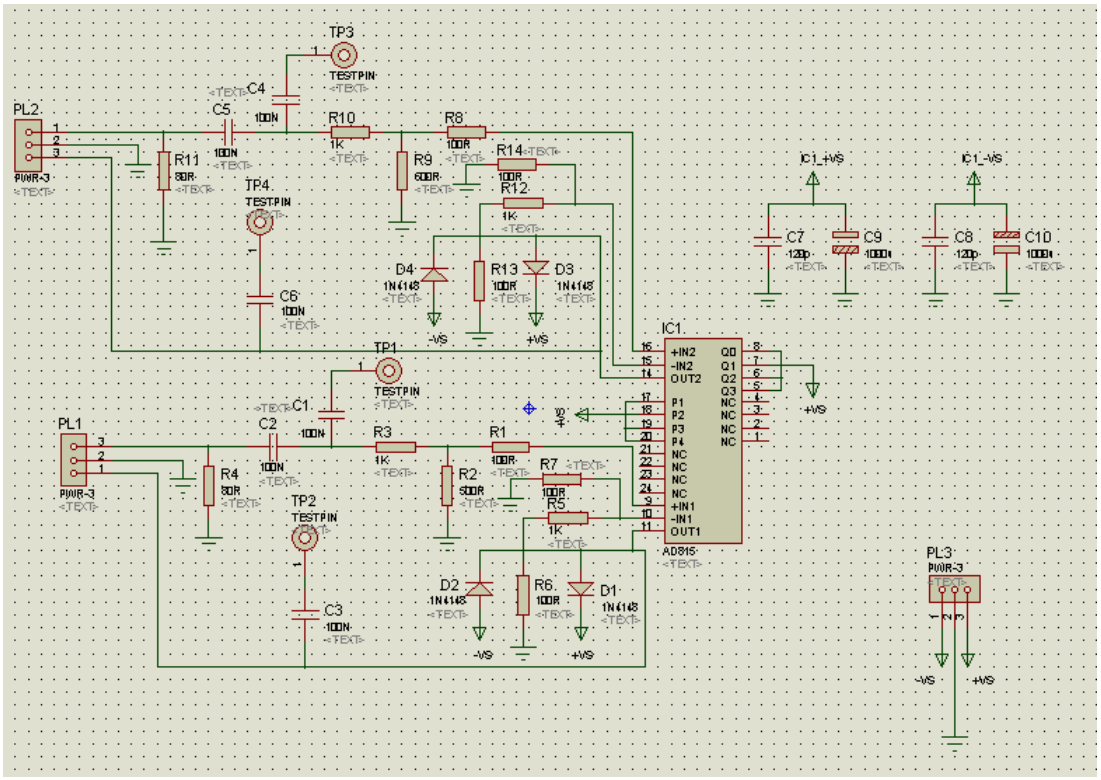

Figure 5.2. Drawing of verified measurement amplifier.

Picture of realized amplifier has been given in Figure 5.3.

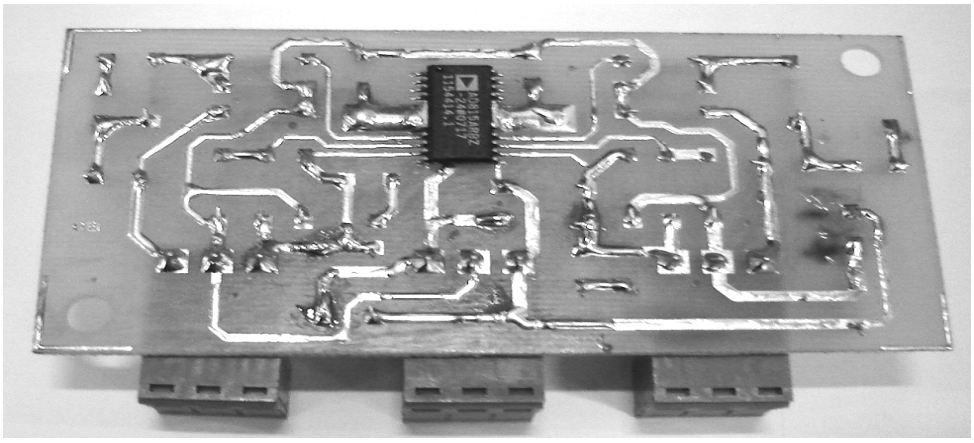

Figure 5.3. View of measurement amplifier.

Bode amplitude and phase diagram obtained with the help of Network analyzer of verified measurement amplifier are given in Figure 5.4.

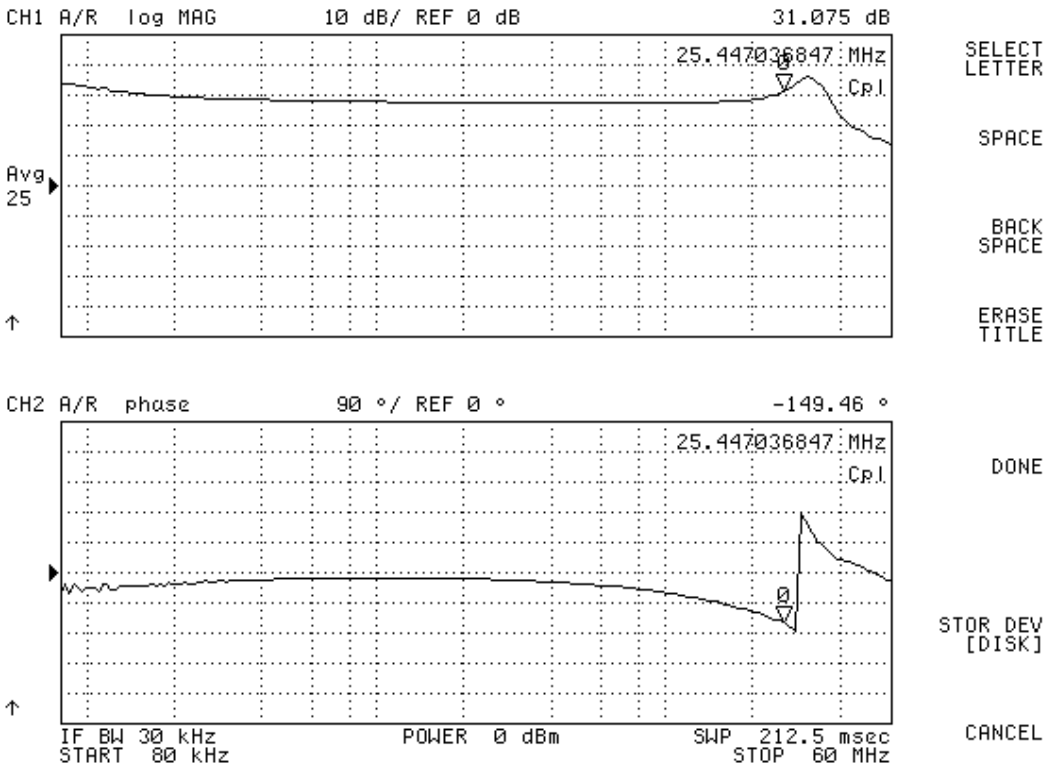

Figure 5.4. Gain amplitude of measurement amplifier – characteristic of frequency (above), characteristic of gain phase – frequency (below).

As maximum output current of AD815 integrated circuit within verified amplifiers is 400mA, it has been enough in measurements, but it's understood that while working, it's necessary to cool integrated circuit with a small fan to cool it enough.

CHAPTER SIX
DISCUSSION ON EXPERIMENTAL RESULTS

6.1 Filter Performance Evaluation Taking into Account Filter Element Parasitic

It has been observed experimentally that performance of notch filter which is worked with shows an important change with parasitic component of L_r and C_r elements and it has been also confirmed with simulations. The most effective parasitic value is the losses of L_r and C_r elements or r resistance which represents these losses in Figure 3.17. It has been observed with the experiments that complying with design conditions presented as suggestion to be able to decrease the value of this equivalent circuit element (r) as possible gives effective results.

a) Magnetic core size of L_r inductance can be chosen much smaller than core sizes of L_1 and L_2 inductances which are at the same circuit. The reason is that the current of low frequency doesn't pass through L_r inductance contrary to L_1 and L_2.

It can be accepted as its reason that C_r capacitor doesn't conduct mentioned PWM signal component.

But the most important difference between L_r with L_1 and L_2 cores should be core material. It has been seen in prototype tests that L_1 and L_2 inductance cores (made up of Mix 26, yellow – white coloured) get hot (PE – COILS). This heating is less in other types of cores with the same copper wire winding. Core has been connected to Q (Quality) factor's being given as middle in the information notes of this mentioned material. But it has been seen that this mixture enables to verify inductances which can carry big current with a small cross-section as linearity of cores made from the material given as 26 is quite good and saturation values are high. It's seen that there are at least two cores of this type in power sources of all desktop computers. It has been seen that losses of this type of cores occur at high frequencies, for example; it has been seen that losses are less for a few kHz in the measurements made with Impedance Analyzer. It has been realized that losses which increases rapidly over a

few hundred kHz are useful in the thesis application and short-term spike shaped distortions which occur during switching weaken in an effective way by creating snubber effect. One the reasons which makes it an indispensable material in mentioned computer power supplies is that it is thought to be protecting semiconductor switches with mentioned snubber effect.

b) The core of filter L_r inductance has been indicated with red colour code in subsequent tests and it has been changed with cores with high Q value and it has been seen that filter performance gets better. As a result, it's understood that the core of L_r inductance should be made up of a material with high Q value.

c) Enameled copper wire has been used for L_1 and L_2 in prototypes. Then it has been seen that using Litz wire for L_1 and L_2 doesn't affect the performance at an appreciable degree. Contrary to this situation, choosing Litz wire for windings of L_r inductance evidently has increased the performance of weakening ripple voltage of thesis filter.

d) It was explained above with its reason that cross-section of L_r inductance core can be chosen smaller than core cross-sections of L_1 and L_2 . But decreasing winding number to reach the same inductance value and choosing core cross-section relatively high instead of verifying L_r with high winding number and a core with small cross-section can be useful for increasing filter performance. The reason of this is that it's possible to decrease losses at a certain degree by decreasing winding number.

6.2 Notch Filter Inductor Core Type(Material) Selection

It has been observed in the experiments that the distortion which will be created by non-linearity of magnetic core characteristic is much more in the condition that magnetic core has one inductance element than the condition that the same core is a part of transformator. This condition has been investigated below without theoretically making a comprehensive analysis.

Let an operational amplifier whose gain is quite high but nonlinear and a feedback amplifier circuit be designed. Input signal amplitude - gain characteristic of the amplifier which will be obtained may be improved enough to be accepted as linear (because of feedback). Transformator can be thought as a feedback magnetic circuit. It's seen that such an effect appears in transformator applications. It seems to be possible to reach a similar result over the circuit in Figure 6.1 in which there is a simplified equivalent circuit of the transformator.

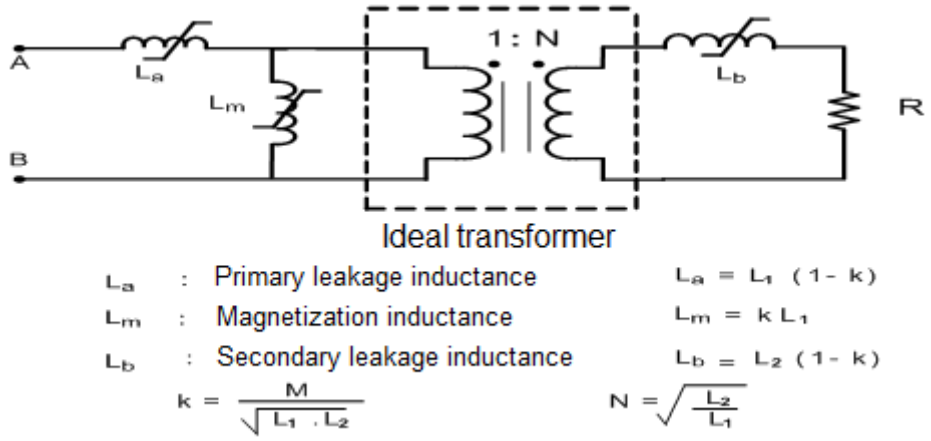

Figure 6.1. Simplified equivalent circuit of the transformator

In this equivalent circuit, L_1 and L_2 respectively show primary and secondary self inductances and represent coupling coefficient with k. Nonlinear characteristic of L_m magnetization inductance in the transformator equivalent circuit which uses one core will create a little distortion in the current of R resistance in equivalent circuit in nonlinear characteristic and the characteristic of magnetic materials is actually always like that. The reason of it is that L_m in transformators is designed in a form that it will take the value as highest as possible. In this condition, the distortion which will arise from core characteristic at output will arise from leakage inductance of L_a and L_b in the condition that output impedance of voltage source applied between A-B is different from zero and it's actually like that. If coupling coefficient is designed close to the value of 1, it's understood from the relations given in the Figure that the value of these inductances will be small.

The circuit at the right side of ideal transformator of the same Figure 6.1 can be thought as single in inductance condition. In this condition, L_b is at the value of L_2 anymore. Because of nonlinear characteristic of core, if a current of high frequency and smaller amplitude with a correct current which changes slowly goes through this inductance, inductance value may be changing at an extent that should be paid attention with correct current which passes through it. For this reason, it's benefited from cores of iron powder type which contains scattered air gaps instead of ferrite cores with high permeability ferrite cores in the thesis filter. Scattered air gaps enables to improve linearity. The worth of this approach is to verify cores whose linearity is good with more winding numbers and inductances which can be verified with less winding numbers with cores of high μ_r (its linearity isn't good). It's known that the mentioned problem of nonlinearity is met in audio amplifiers which uses switched amplifier of an establishment that works in the field of television design and production. Both experimental studies and this type of information in switched amplifier show that linearity of filter inductances is very important whichever filter topology has been chosen.

6.3 Evaluation of Power Electronic Switch Types for the Class-D Amplifier Circuit

One of the most important mistakes that can be done in design of switched amplifier stage verified with discrete elements is that benefiting from reverse connected diodes in MOSFET switches in the connection of Half-Bridge or Full-Bridge. Reverse recovery current of mentioned diode elements are quite high and this current passes also through another MOSFET during switching. Short-term over current which repeats at the moment of every switching is a short-term short-circuit current at the same time. This current decreases the efficiency but except this effect, it can cause to distort MOSFETs at its output stage which is more important.

Because of the mentioned reasons, it's benefited from HiperMOSFET elements in prototypes which have been verified with discrete elements. Reverse diodes which exist in HiperMOSFET that has started to be produced recently are diodes which is

fast and whose recovery currents are less. Two schottky diodes are connected around each of MOSFETs in another prototype. One of these is connected to MOSFET serially in such a way that MOSFET won't ever enable the diode in itself to conduct current and the other one is connected to the source (reference) from input node of inductance for inductive current of inductance which is just at the input of it.

It has been seen that using this known techniques is very important. It's understood that solutions resembling to this problem in switched amplifier integrated circuits (like TDA7482 and TDA 7490) which also includes output stage are applied in integrated circuit. From this aspect, a problem isn't encountered in prototypes operating with aforesaid integrated circuits. Supply current spikes which seems to be possible in measurement of supply source currents with a wideband current probe haven't been seen in circuits verified with TDA7482 or TDA7490.

Notch filter suggested in the thesis provides more success than it has provided in amplifiers on which is worked in switched amplifier power sources. If switched source is designed in a way that it will work around wave-space proportion of 50% (by providing necessary conversion ratio in this way by choosing transformator topologies),the amplitude of the second harmonics can be assured to be very low. In this condition, the basic component which takes the highest value as will be seen in Figure can be weakened with notch characteristic.

CHAPTER SEVEN
CONCLUSIONS

Application of switched amplifiers to volume up goes up to thirty years before and widespread usage of it has been seen recently. Almost most of semiconductor firms have a product which resembles to TDA7482 which has been used in this thesis. The reason of this proliferation is thought to be arising from developing new semiconductor technologies which are more suitable to verify this type of amplifiers as well as that electronic devices which has also audio feature are sold more.

It's thought that technologies, which produce relatively more resistant MOSFET when compared with the old ones, and a design, which will decrease this problem in TDA7482 and TDA7490 whose output MOSFETs are again in integrated circuit, take place. It has been observed in the experiments made that TDA7490 integrated circuit is quite successful. Cross-over distortion is a matter just as it is in Class-B amplifiers in switched amplifiers. While being worked with small output voltages in thesis experimental studies made with TDA7482 and TDA7490, the effect of cross-over distortion which is apparent hasn't been met. Cross-over distortion occurs with a very different mechanism from Class-B amplifiers in switched amplifiers. In transmission case, voltage drops which will occur on diodes (semiconductor switches) and MOSFETs causes this problem. It has been seen that this problem has been reduced to a degree that can't be noticed in TDA7482 and TDA7490 which Bipolar, CMOS and DMOS semiconductor production technologies are used in their production.

On the other hand, it has been seen that ripple noise (repeated in switching frequency) at output signal is excessive in experimental studies made with filter element values and in filter topology whose own datasheet is given. That explanation has been made for this condition. TDA7482 class integrated circuits, which are produced for devices which have greater power than handheld one especially for TV and home cinema systems, find application usually as switched audio amplifier. Ripple distortion which is clearly seen in oscilloscope screen, when this signal is

converted into audio after being applied to a speaker, obtained voice quality will be affected a little from ripple noise on (output voltage). The reason of it is that it has been connected to the mechanisms reported below.

1- It can be said that ripple noise which is clearly observed on oscilloscope screen and exists on speaker voltage won't appear as sound ripple noise again at its own frequency. But vibration of cardboard sheet (cone) which produces phonogram in speaker is determined with speaker current. Both the reality that ripple noise on this current will be little (high frequency components on the voltage applied and a speaker inductive load is carried on current by being much weakened) and not responding of cone again to high frequency current components because of its mechanical inertia show that ripple noise which will occur in sound vibrations will be less than the noise on voltage in oscilloscope screen.

2- Maybe some ripple noise which will exist in speaker volume will never be perceived by human beings except the factors reported above. As known, 100 kHz - 140 kHz carrier frequency which is suggested in catalog of TDA7482 and TDA7490 is in a place that human ear cannot hear. Any problem hasn't emerge when it's descended up to 60 kHz switching frequency in the thesis studies with this mentioned integrated circuits.

Usage fields of them have increased with proliferation of switched amplifiers. Wheeling ultrasonic elements, wheeling coils of magnetic resonance systems can be counted among these. It's clear in these last applications that switched amplifier noise will be more important.

In addition, capacitive speakers which have started to be seen again in sound applications recently may be more sensitive to switching noise than the classic ones.

The most suitable filtering techniques has been searched to decrease ripple noise of switched amplifiers in this study. “4395A Network/Spectrum/Impedance

Analyzer” device which support has been used very efficiently in the thesis. As input and output impedances are 50 Ohms, this device requires additional accessories to obtain Bode graphics (voltage or current is out of 50 Ohms). Instead of buying this expensive accessories, measurement amplifiers have been verified with a differential amplifier integrated circuit which has switching capacitor. Prototype measurement amplifiers have been verified with AD815 integrated circuit of “Analog Devices” firm and used in experiments. Oscillator output of “Network Analyzer” device has driven this amplifier over DC separation capacitor circuit and a resistance. An important protection has been provided for such a sensitive and expensive device. In addition, impedance has been driven with a small source by connecting filter circuits, which will be tested, to output of this amplifier. It has been studied on different filter topologies during the thesis work.

Especially simulation studies have been made on filter circuits with transmission line in the beginning months of the thesis work. It has been seen in the following experimental studies that this type filters require filter physical dimensions which are impractical in amplifiers whose switching frequency is around 100 kHz. The reason of it has been tried to be explained like that: when an inductance element is tried to be verified and leakage flux is ignored, it's proportional with square of winding number. Inductance of a transmission line changes with the length of the line. It can be reached to the inductance value, which is wanted for this reason, with more physical dimensions.

The second factor is to enable magnetic core winding number which will be benefited as lumped during inductance element verification to be less. It has been observed that ferrite core makes filter get away from transmission line filter when it's wanted to take notch characteristic of filter to lower frequencies with rod-shaped ferrite cores in transmission line filter which is tried to be verified with solenoid coils in the thesis studies. For this reason, it has been continued to work with transmission line filters in the last period of the thesis and a notch filter topology verified with lumped elements. It has been observed through simulations and experiments that suggested notch filter is quite successful beside classic LC- filter which will be

verified with the same elements. Notch filter can provide a good performance also in switched power supplies which are more common than switched amplifiers in application. Although high-value electrolytic capacitors can be used as different from amplifier application in the filter of switched sources, this type of capacitors don't have a good performance because of their resistances and leakage inductance at high frequencies.

For this reason, notch filter on which again an electrolytic capacitor is connected can provide a good performance for switched sources.

As known, duty- cycle doesn't need to be changed much in switched amplifiers. It's changed just a little bit by feedback circuit for the purpose of regulation. For this reason, notch filter may be very successful for a source whose duty - cycle changes a little around 50%.

It's seen that attenuation over enough f_o notch frequency from Vo/V_i transfer function of notch filter will increase 20 dB/decades with frequency and attenuation will increase 40 dB/decades with frequency after corner frequency for the known LC- filter. Even if it seems to be a weakness of this notch filter, it shouldn't be forgotten that classic filter will verify the least attenuation for f_o which will exist as the component which has the biggest amplitude in PWM. For this reason, choosing notch filter may be a good choice among many designs.

Notch attenuation of the filter suggested in the thesis work is strictly connected to r resistance which represents the losses of L_r and C_r elements. For this reason, it should be paid attention to the verification and choice of these elements to decrease the losses of L_r and C_r

While L_r element is verified, Q value can be assumed to be essential for high core and usage of Litz wire for a good filter performance. In addition, choosing C_r from a species whose losses are less for example from ceramic capacitor group may increase the performance.

f_s frequency is chosen as fixed in almost all of switched amplifiers. Recently, a kind of amplifier whose power levels are a few Watts and which is named as Spread Spectrum has started to take its place in the products of semiconductor firms. f_s value is randomly modulated around a chosen working point in this kind of amplifiers. Switching frequency has a relationship with the thesis concept as it's modulated. But this method is followed to provide Electromagnetic Compatibility conditions more easily and it differs from thesis amplifier with this aspect. Although there isn't a comprehensive study about whether it will be effective on ripple voltages which occur during switching moments of amplifiers with spread spectrum, measurement and investigations have been made. The subject has been asked also to manufacturers and the received responses have been given in Appendix 3 in this report. It has been seen that spread spectrum won't be effective on sudden ripple voltages but it will decrease amplitudes of peaks at spectrum by spreading energy spectrum which will occur at f_s around f_s. The subject can be discussed with such an example. Let a PWM signal be applied to a LC - filter which is mentioned in this report. When looked at spectrum which is formed on filter output load, it's seen that this spectrum gives an average information about formed ripple voltage of this spectrum. On the other hand, ripple amplitudes may be less at big peaks in the time interval in which PWM signal is close to square wave. A simple Amplitude spectrum won't provide any information about this subject.

7.1 Future Work

In this study, the concept of Notch Filter is evaluated (both theoretically and simulated) with resistive amplifier loads. As an extended work the proposed filter topology could be evaluated with inductive and capacitive loads.

With inductive or capacitive loads, filter performance may change more or less and then taking account load parameters in designing Notch Filter should be a necessity.

REFERENCES

Aggbossou K., Dion J.-L., Carignan S., Aldelkrim M., Cheriti A., Class-D Amplifier For A Power Piezoelectric Load, *IEEE Transactions On Ultrasonics, Ferroelectrics, And Frequency Control*, 47, 4, 1036-1041, (2000).

Baker D., A Reference-Cancelling Phase/Frequency Detector, *RF Design*, 35-40, (1989).

Balog R., Krein, P.T., Automatic Tuning Of Coupled Inductor Filters, Power Electronics Specialists Conference, (2002) Pp: 591-596.

Black H.S., *Modulation Theory*, Van Nostrand, Princeton N.J., 1953, Sayfa:263-281.

Brandt R.L., Orthogonal-Field Electrically Variable Magnetic Device, *United States Patent*, Appl. No: 281949, Filed: July 28, (1994).

Esram T., Kimball J.W., Krein P.T., Chapman P.L., Midya P., Dynamic Maximum Power Point Tracking Of Photovoltaic Arrays Using Ripple Correlation Control, *IEEE Transactions Power Electronics,* 21, 1282-1291, (2006).

Johns D., Martin K., "Analog Integrated Circuit Design", Wiley, (1996).

Karaca H., D Sınıfı Yükselteçlerde Aktif Bir Süzgeç Ile Harmoniklerin Azaltılması, Elektrik Mühendisliği 2. Ulusal Kongresi, Ankara, (1987) Pp: 813-815.

Karaca H., Paralel Tip Evirgeçler Için Bir Frekans Denetim Dizgesi, Elektrik Mühendisliği 4. Ulusal Kongresi, İzmir, (1991) Pp: 113-116.

Karaca H., PLL IC Forms Simple Digital Phase Shifter, *EDN (Electronic Design News)*, 106-107, (1996).

Karaca H., Equivalent Circuit For Class-D Half Bridge Amplifiers, *PCIM Power Conversion Inteligent Motion, Intertec International Publication*, 20-30, (1997).

Karaca H., Şenol Y., Aktif Ve Pasif Entegratör Devrelerinin Uygulamaya Yönelik Bir Karşılaştırması, Endüstri & Otomasyon, 23, (1999) Pp: 18-21.

Karaca H., A Malfunction Problem And Its Solution In Load Resonant Inverters, *International Journal Of Electronics*, 88, 3, 371-381, (2001).

Karaca H., Dijital PLL Kontrollü Sistemlerde Gürültü Ile Tetiklenen Hatalı Çalışma Modu, TUBİTAK Alt Yapı Projesi Sonuç Raporu, 30 Sayfa, (2005).

Koroglu M.H., Allen P.E., LC Notch Filter For Image-Reject Applications Using On-Chip Inductors, *Electronics Letters*, 37 5, 267-268, (2001).

Lymar D.S., Neugebauer T.C., Perreault D.J., Coupled-Magnetic Filters With Adaptive Inductance Cancellation, *IEEE Transactions On Power Electronics*, 21, 6, 1529-1540, (2006).

PE Magnetics, WEB Site:
http://www.Pe-Coils.com/index.htm

Phinney J.W., *Filters With Active Tuning For Power Applications*, (S.M. Thesis, Yüksek Lisans Tezi), Dept. Of Elect. Comput. Eng., Mass. Inst. Of Technol., Lab. Electromagn. Electron. Syst., Cambridge, MA, (2001).

Phinney J., Multi-Resonant Passive Components For Power Conversion," (Ph.D. Dissertation, Doktora Tezi), Dept. Elect. Eng. Comp. Sci., Lab. Electromagn. Electron. Syst., Mass. Instit. Technol., Cambridge, MA, (2005).

Polivka W.M., Cocconi A., Cuk S., Use Of Orthogonal Flux To Detect Impending Magnetic Saturation In Switching Converters, In "Advances In Switched-Mode

Power Conversion (S. Cuk, R.D. Middlebrook)", Volume III, Teslaco, USA, (1983). Pp. 119-149.

Rohde U.L., Digital PLL Frequency Synthesizers: Theory And Design, Prentice Hall, (1982).

Sabate J., Schutten M., Steigerwald R., Li Q.; Wirth W.F., Ripple Cancellation Filter For Magnetic Resonance Imaging Gradient Amplifiers, Applied Power Electronics Conference And Exposition (APEC '04), 2, (2004) Pp:792-796.

Sheen J.-W., A Compact Semi-Lumped Low-Pass Filter For Harmonics And Spurious Suppression, *IEEE Microwave And Guided Wave Letters*, 10, 3, 92-93, (2000).

Steigerwald R.L.,. Wirth W.F, High-Power, High-Performance Switching Amplifier For Driving Magnetic Resonance Imaging Gradient Coils, Power Electronics Specialists Conference (PESC '00), 2, (2000) Pp: 643-648.

Tan M.T., Chang J.S., Chua H.C., Gwee B.H., An Investigation Into The Parameters Affecting Total Harmonic Distortion In Low-Voltage Low-Power Class-D Amplifiers, *IEEE Transactions On Circuits And Systems-I: Fundamental Theory And Applications*, 50, 10, 1304-1315, (2003).

Van Der Zee R.A.R., Van Tuijl A.J.M., A Power-Efficient Audio Amplifier Combining Switching And Linear Techniques, *IEEE Journal Of Solid-State Circuits*, 34, 7, 985-991, (1999).

Walker G.R., A Class-B Switch-Mode Assisted Linear Amplifier, *IEEE Transactions On Power Electronics*, 18, 6, 1278-1285, (2003).

Wells J.R., Nee B.M., Chapman, P.L., Krein, P.T., Selective Harmonic Control: A General Problem Formulation And Selected Solutions, *IEEE Transactions On Power Electronics,* 20, 1337-1345, (2005).

Yin J., Liang Z., Van Wyk J.D., High Temperature Embedded Sic Chip Module (ECM) For Power Electronics Applications, *IEEE Transactions On Power Electronics*, 22, 392-398, (2007)

Agilent Technologies *Impedance Measurement Handbook, July 2006,* http://www.Agilent.Ccom/literature/

AMIDONCORP ; WEB: http://www.Amidoncorp.com/

APPENDICES

APPENDIX A : MATLAB CODE OF COEFFICIENTS OF f_s, 2 f_s, 3 f_s, 4 f_s, 5f_s, 6f_s, 7f_s FREQUENCY COMPONENTS

```
X1=[];
X2=[];
nu=0;
B1=[];B2=[];
 M=0:.01:1;
for m=1:7
    Z=m*pi*M;
    %1.fonksiyon
    Y1=(2)*(1-(besselj(nu,Z)*cos(m*pi)))/(m*pi);
    B1=[B1;Y1];
    %2.fonksiyon
    Y2=4*(besselj(nu,Z/2)*sin((m*pi)/2))/(m*pi);
    B2=[B2; Y2];
end
%Y2=4*besselj(nu,(Z/2))/pi;
%X2=[X2 Y2];
%
figure,plot(M,B1(1,:),M,B1(2,:),M,B1(3,:),M,B1(4,:),M,B1(5,:),M,B1(6,:),M,B1(
7,:));
legend('m=1','m=2','m=3','m=4','m=5','m=6','m=7');
xlabel('M'),ylabel('(2)*(1-Jo(pi*M)cos(m*pi)/m*pi)')

figure,plot(M,B2(1,:),M,B2(2,:),M,B2(3,:),M,B2(4,:),M,B2(5,:),M,B2(6,:),M,B2(
7,:));
legend('m=1','m=2','m=3','m=4','m=5','m=6','m=7');
xlabel('M'),ylabel('4*Jo(m*pi*M/2)*sin(m*pi/2)/m*pi)')
```

APPENDIX B: BESSEL FUNCTION VALUES WHICH ARE NECESSARY TO CALCULATE SOME OF SIDEBAND AMPLITUDES THAT WILL BE AROUND HARMONICS AND OHMS IN PWM SPECTRUM (TABLE 3.1)

M	n	m	$J_n(m\pi M)/m\pi$	M	n	m	$J_n(m\pi M)/m\pi$
0	-3	1	0	0.5	0	3	-0.0282
0	-3	2	0	0.5	0	4	0.0175
0	-3	3	0	0.5	0	5	0.0130
0	-3	4	0	0.5	1	1	0.1804
0	-3	5	0	0.5	1	2	0.0453
0	-2	1	0	0.5	1	3	-0.0299
0	-2	2	0	0.5	1	4	-0.0169
0	-2	3	0	0.5	1	5	0.0134
0	-2	4	0	0.5	2	1	0.0795
0	-2	5	0	0.5	2	2	0.0773
0	-1	1	0	0.5	2	3	0.0155
0	-1	2	0	0.5	2	4	-0.0229
0	-1	3	0	0.5	2	5	-0.0096
0	-1	4	0	0.5	3	1	0.0220
0	-1	5	0	0.5	3	2	0.0531
0	0	1	0.3183	0.5	3	3	0.0431
0	0	2	0.1592	0.5	3	4	0.0023
0	0	3	0.1061	0.5	3	5	-0.0183
0	0	4	0.0796	1	-3	1	-0.1061
0	0	5	0.0637	1	-3	2	-0.0046
0	1	1	0	1	-3	3	0.0089
0	1	2	0	1	-3	4	-0.0077
0	1	3	0	1	-3	5	0.0063
0	1	4	0	1	-2	1	0.1545
0	1	5	0	1	-2	2	-0.0458

0	2	1	0	1	-2	3	0.0232
0	2	2	0	1	-2	4	-0.0145
0	2	3	0	1	-2	5	0.0101
0	2	4	0	1	-1	1	-0.0906
0	2	5	0	1	-1	2	0.0338
0	3	1	0	1	-1	3	-0.0188
0	3	2	0	1	-1	4	0.0123
0	3	3	0	1	-1	5	-0.0089
0	3	4	0	1	0	1	-0.0968
0	3	5	0	1	0	2	0.0351

			$J_n(m\pi M)/$				$J_n(m\pi M)/$
	n	m	mπ	M	n	m	mπ
0.5	-3	1	-0.0220	1	0	3	-0.0192
0.5	-3	2	-0.0531	1	0	4	0.0125
0.5	-3	3	-0.0431	1	0	5	-0.0090
0.5	-3	4	-0.0023	1	1	1	0.0906
0.5	-3	5	0.0183	1	1	2	-0.0338
0.5	-2	1	0.0795	1	1	3	0.0188
0.5	-2	2	0.0773	1	1	4	-0.0123
0.5	-2	3	0.0155	1	1	5	0.0089
0.5	-2	4	-0.0229	1	2	1	0.1545
0.5	-2	5	-0.0096	1	2	2	-0.0458
0.5	-1	1	-0.1804	1	2	3	0.0232
0.5	-1	2	-0.0453	1	2	4	-0.0145
0.5	-1	3	0.0299	1	2	5	0.0101
0.5	-1	4	0.0169	1	3	1	0.1061
0.5	-1	5	-0.0134	1	3	2	0.0046
0.5	0	1	0.1502	1	3	3	-0.0089
0.5	0	2	-0.0484	1	3	4	0.0077
				1	3	5	-0.0063

APPENDIX C: VIEWS OF PRINTED CIRCUIT OF MEASUREMENT AMPLIFIER USED IN EXPERIMENTAL WORK

1- SWITCHED AMPLIFIER PROTOTYPE REALIZED WITH TDA7482

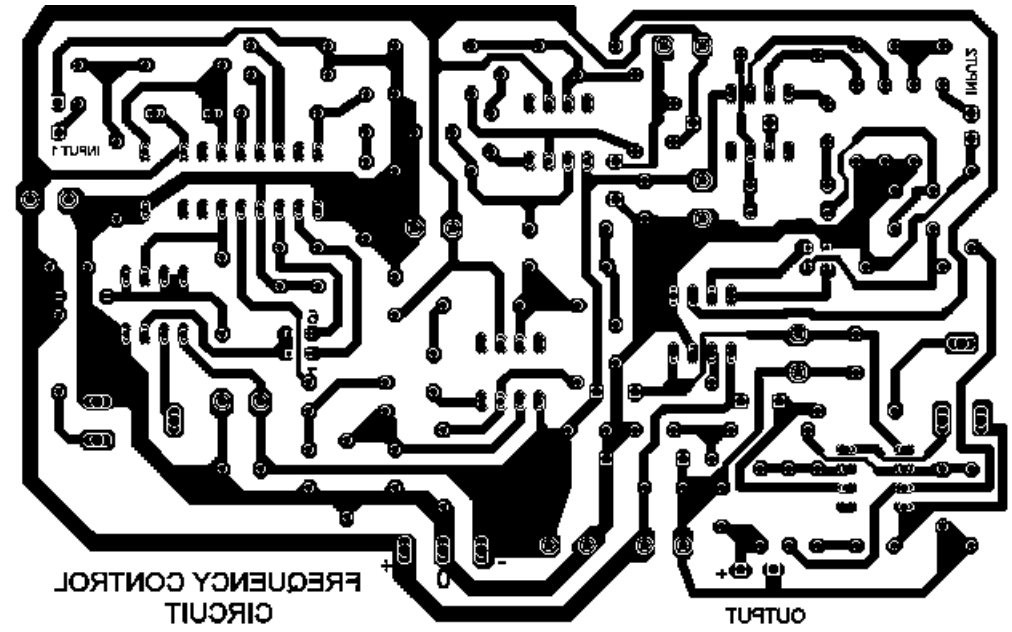

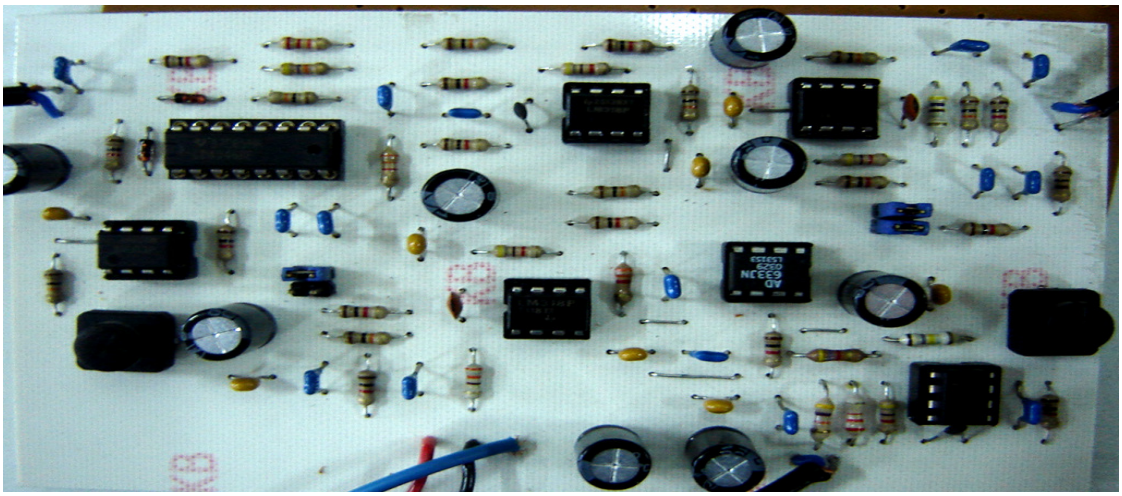

2- PROTOTYPE REALIZED WITH TDA7490 INTEGRATED CIRCUIT

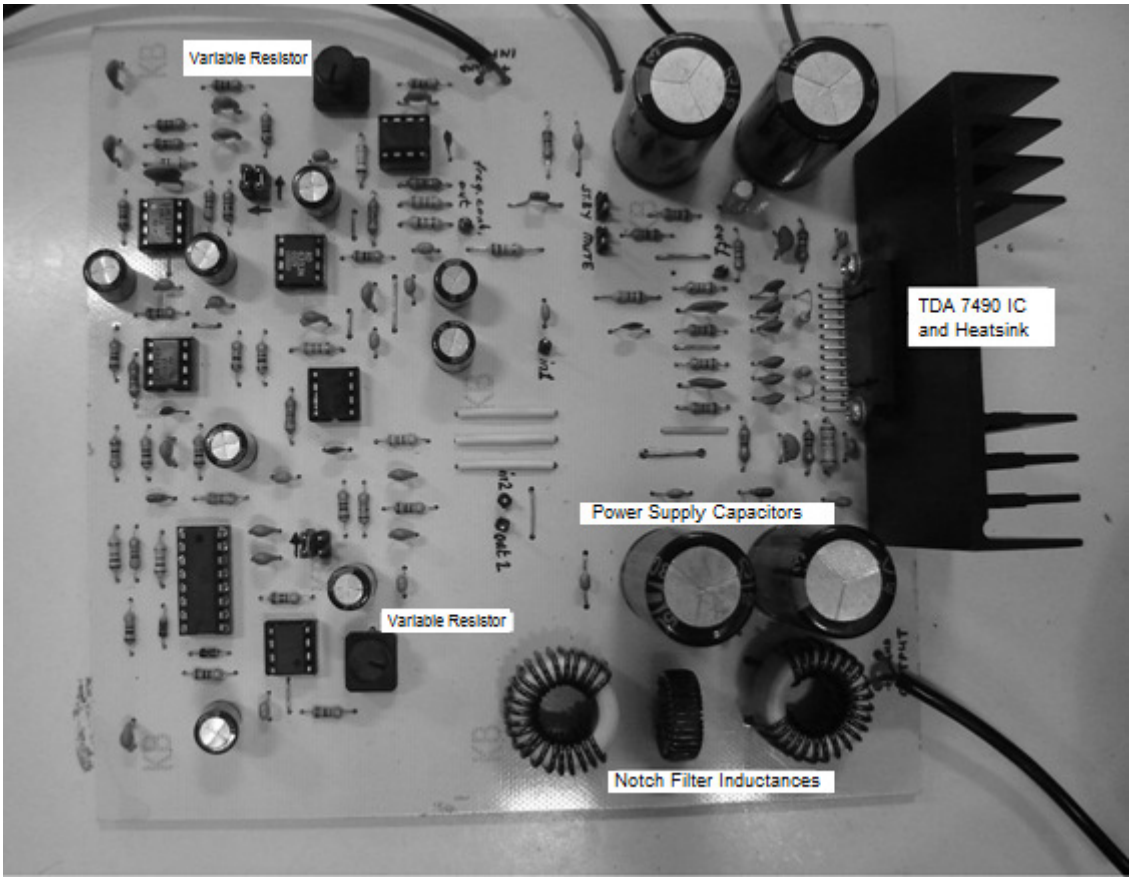

If it's thought that prototype verified with switched amplifier integrated circuit is separated with a line from the middle of seen figure, from upwards to downwards, left side is the verification of frequency control circuit and right side is the verification of suggested amplifier circuit in TDA7490 catalog. Notch filter exists at the right side.